Mechanism of Response and Resistance to CAR T Cell Therapies

Thesis by

Sharareh Gholamin

In Partial Fulfillment of the Requirements for
the Degree of
Doctor of Philosophy

CALIFORNIA INSTITUTE OF TECHNOLOGY
Pasadena, California

2023
(Defended June 9, 2023)

Sharareh Gholamin
ORCID:(0000-0001-7425-6074)

ACKNOWLEDGEMENTS

I must begin with appreciation for the incredible opportunity to undergo my graduate training at the California Institute of Technology. This institute along with City of Hope where I later developed my PhD thesis project provided me an unparalleled setting to grow as a physician scientist serving patients with cancer resistant to current treatment.

There have been many individuals who helped and supported me through my graduate studies. First and foremost, I would like to express my heartfelt gratitude to Drs. Stephen Forman and Christine Brown for their warm welcome and invaluable support during my graduate studies at City of Hope. Their mentorship and guidance have been instrumental in shaping my thesis project, which focuses on understanding the response and resistance mechanisms of hard-to-treat tumors, particularly brain tumors, to CAR T cell therapies.

I am immensely grateful to Dr. Brown for her exceptional knowledge in CAR T cell therapy for patients with glioblastoma and her remarkable leadership skills. She has been a constant source of inspiration to me, and I greatly admire her dedication and rapport with her mentees. As a pioneering figure in CAR T cell therapy, I have learned a great deal from her, especially as a woman leader in the field of cancer therapy. I owe a significant part of my growth and progress to her unwavering support.

Dr. Brown's insightful guidance and mentorship have played a pivotal role in my development as a researcher. Her expertise and compassionate approach have not only shaped my scientific endeavors but also instilled in me a sense of purpose to make a positive impact in the world. I am truly thankful for the opportunity to learn from her and for her continued support throughout my journey.

I would also like to extend my appreciation to Dr. Antony Ribas at UCLA for his generous support and the significant impact he has had on my project and career over the past few years. Collaborating with multiple fellows in his lab has been an incredible opportunity that has empowered me to develop a multidisciplinary approach and fostered the growth of new ideas within my project.

I am sincerely grateful to Dr. James Heath for his invaluable support, without which I would not have been able to commence my graduate studies at Caltech. In 2016, I became captivated by his pioneering research in cancer therapy and the exploration of neoantigens for treating cancer. Inspired by his groundbreaking work, I joined his lab to embark on my graduate journey. Regrettably, I was unable to accompany his team when he assumed the role of President at the Institute of Systems Biology in Seattle. I would also like to extend my special thanks to Dr. Marianne Bronner, Dr. David Baltimore, Dr. Mikhail Shapiro, and the other committee members who provided me with unwavering support throughout my pursuit of graduate studies and scientific discovery at Caltech.

I am also eternally very grateful for the support I received during my graduate work from Parker Institute in Cancer Immunotherapy. It was an unprecedented opportunity to meet and exchange ideas with the best minds in the field. I am thankful for the invaluable support from the Institute which gave me access to world-class resources and helped me to develop my research. I am confident that the

knowledge I gained from the Institute will benefit me throughout my career and result in breakthrough additions to the feild.

I would like to express my appreciation to all the collaborators and contributors involved in this project. Special thanks to the flowcore at UCLA and Dr. Begonya Comin-Anduix for their valuable support in mass cytometry analysis. I would also like to acknowledge the genomic center at City of Hope, especially Dr. Xiwei Wu Dr. Yuqi Zhao, for their contribution in sc-RNA analysis of mouse samples. Additionally, I extend my gratitude to the genomic center at TGen and Dr. Heini Natri for their insightful analysis on transcriptomic data from patient samples obtained during our trials at City of Hope.

Beyond the confines of the lab, I am humbled and profoundly grateful for my loving and supportive family. My dear departed mother dedicated her life to guiding and grounding me, while my father ignited my passion for science from an early age. Their unwavering dedication and support paved the way for my journey to the USA and subsequent success. Whenever I needed them, they were there.

But it is to my husband, Masoud Bitarafan, that I owe the greatest debt of gratitude. He has been my rock, providing unwavering strength throughout my entire journey. His unconditional love and unwavering support have given me the courage and determination to pursue my goals. I am forever grateful for his companionship and understanding during the countless hours I've devoted to my project, day and night.

There have been many people and organizations who have shaped me to grow as a scientist and become an impactful person and well-rounded individual. While I am very thankful of many of my friends who have supported me during my PhD studies, I should specifically thank my friend, Jilla Kashef, who brought hope

during the most challenging time in my life. She inspired me with her resilience, fighting 25 years with breast cancer, while simultaneously running one of the most successful charitable foundations helping thousands of children in Iran and Afghanistan suffering from lack of education. She has been challenged by cancer but has always remained hopeful and strong for her community. As I write this acknowledgement today, she has been struggling with a metastasized disease. Despite all the pain and suffering, she has kept a positive attitude and is a source of inspiration for everyone around her. Being a small part of the effort to save people like her motivates me to devote my career to fighting cancer.

ABSTRACT

While chimeric antigen T (CAR) T cell therapy has shown remarkable success in leukemia, lymphoma, and multiple myeloma, its effectiveness in solid tumors including glioblastoma (GBM) remains limited. It is crucial to understand mechanisms that reduce the efficacy of CAR T cell therapies and develop strategies to prevent tumor resistance. In this study, we conjectured that alterations in tumor cell-intrinsic interferon (IFN) signaling pathways contribute to establishment of immunosuppressive tumor microenvironment in solid tumors, leading to resistance of solid tumor cells to CAR T cell-mediated killing. We established syngeneic IFN signaling-deficient tumor models for murine IL-13Ra2 targeted CAR T cell therapy and showed that these models modulate the tumor microenvironment (TME), leading to resistance to CAR T cell therapy. We identified variations in gene expression associated with IFN signaling components and cytokines between IFN signaling-deficient tumor cells and wild type (WT) tumor cells after CAR T cell treatment. Furthermore, single-cell RNA sequencing and mass cytometry analysis of the tumor immune cell infiltrates in IFN-signaling deficient tumors compared to WT controls identified the immune-mediated causal components for the resistance of Janus Kinase1 knockout (JAK1/KO) tumors to CAR T cell therapy. CAR T cell-treated IFN signaling-deficient tumors presented decreased T-cell transcripts, with decreased frequency of CD8-early active, CD8-naive like T cells. Conversely, there were more regulatory and follicular T cells, exhausted endogenous T cells , and exhausted CAR T cells in treated IFN signaling-deficient tumors compared to treated WT tumors.

The analyses also showed the superior enrichment and crosstalk of genes that identified fibroblasts, neutrophils, and myeloid cells in IFN signaling-deficient tumors compared to those of WT tumors. Mass cytometry analysis on the immune cells infiltrates of JAK1/KO and WT tumors post CAR T cell treatment corroborated the results from gene expression analysis. The potential cause of immune suppressive crosstalk in IFN signaling-deficient tumor niches could be attributed to the varied enhancement of receptor-ligand interactions such as SPP1+ tumor-associated macrophages (TAMs) and CD44+ cancer-associated fibroblasts (CAFs), as well as SPP1+ TAMs and integrins present on other cell lineages. To overcome resistance to CAR T cell therapies, we employed two distinct actionable approaches: triggering the immune microenvironment and disrupting the extracellular matrix. Unconjugated interferon signaling gene-15 (ISG-15) enhanced CAR T cell efficacy in an INF-signaling deficient model, increasing the recruitment of endogenous T cells and reshaping the TME. Anti-SPP1 blocking antibody was used to prime the JAK1/KO tumors prior to the treatment with CAR T cell therapy potentially via enhancing the persistence and trafficking of CAR T cells in the TME.

We next identified immune signatures of 32 GBM patients who had progressive disease after CAR T cell treatment compared to those who had relatively stable disease or showed improvement. We identified the presence of fibroblasts and SPP1+ APOE+ C1QA+ C1QC+ myeloid cells in GBM signatures that are associated with immune suppression and resistance to therapy. Patients with GBM who exhibited a relatively stable response to treatment and increased T cell recruitment had differential expression of interferon regulatory factors (IRFs) and ISGs compared to patients with less response to the treatment. Our findings uncover a correlation between tumor-intrinsic driver mutations, the composition of the TME, and the responsiveness of solid tumors to CAR T cell

therapy, providing insights into potential approaches to address resistance in IFN non-responsive tumors.

PUBLISHED CONTENT AND CONTRIBUTIONS

Gholamin, S., Saravanakumar, S., Natri, Heini., Aftabizadeh, Comin-Anduix, B., Zhao, Y., Masia, C. Tong, Z., Starr, R., Aguilar, B., Reza, H., Under preparation for submission. Inactivation of Interferon signaling mediates resistance to CAR T cell therapy with establishment of immunosuppressive tumor niche.

S.G conceived the idea, designed and executed invitro and in vivo experiments, analyzed data, and interpreted the results. S.G and wrote the manuscript.

Gholamin, S., Saravanakumar, S., Wong, R., Maker, M., Aftabizadeh, Alizadeh, D., Starr, R., Aguilar, B. Under preparation for submission. overcoming the resistance of gliomas to combination therapies by tumor-dependent sequential delivery of anti-PD-1 and CAR T cell therapy.

S.G conceived the idea, designed and executed invitro and in vivo experiments, analyzed data, and interpreted the results.

Stern, L.A.*, **Gholamin, S.*,** Moraga, I.*, Yang, X., Saravanakumar, S., Cohen, J.R., Starr, R., Aguilar, B., Salvary, V., Hibbard, J.C. and Kalbasi, A., 2022. Engineered IL13 variants direct specificity of IL13Rα2-targeted CAR T cell therapy. Proceedings of the National Academy of Sciences, 119(33), p.e2112006119.

S.G executed experiments, analyzed data, interpreted the results, and contributed to revision of the manuscript.

*Contributed equally to this work

Brown, C.E., Alizadeh, D., Jonsson, V., Hibbard, J., Yahn, S., Wong, R.A., Yang, X., Ng, R., Dullerud, N., Maker, M. and **Gholamin, S.,** 2021. CAR T cell therapy reshapes the tumor microenvironment to promote host antitumor immune responses in glioblastoma. Cancer Research, 81(13_Supplement), pp.59-59.

S.G executed experiments, analyzed data, interpreted the results.

Alizadeh, D., Wong, R.A., **Gholamin, S.,** Maker, M., Aftabizadeh, M., Yang, X., Pecoraro, J.R., Jeppson, J.D., Wang, D., Aguilar, B. and Starr, R., 2021. IFNγ Is Critical for CAR T Cell–Mediated Myeloid Activation and Induction of Endogenous ImmunityCAR T Cells Induce Endogenous Immune Responses. Cancer discovery, 11(9), pp.2248-2265

S.G conceived the idea about the modulatory role of CAR T cells on human and mouse macrophages, designed and executed experiments testing the effect of CAR T cells on macrophages, analyzed data, and interpreted the results. S.G contributed in drafting and revising the manuscript.

TABLE OF CONTENTS

Chapter 1

INTRODUCTION

As an emperor of maladies, cancer has challenged mankind for centuries and researchers have worked tirelessly to find a cure. Despite some promising advancements, the battle against cancer is far from over and more investment in research on the pathogenesis of this disease and new therapeutic approaches is required to find a way to conquer this deadly disease. In recent years, discovery of chimeric antigen receptor (CAR) T cell therapies alongside immune checkpoint blockade therapies has shown notable advancements and promises in the fight against cancer [1,2].

CAR T cell therapy is an innovative approach and strategy for cancer treatment that utilizes the patient's own immune system to specifically target and destroy cancer cells. CAR T cells are T cells that have been genetically modified to express a chimeric antigen receptor on their surface to directly target and eradicate cancer cells by recognizing and binding to antigens on cancer cells' surfaces and initiating subsequent processes that lead to their destruction. In addition, they can act indirectly by activating or triggering the response of other immune cells against cancer cells [3–6].

In the last decade, CAR T cells have been heralded as a promising and effective approach in the treatment of hematological malignancies. Numerous CAR T-cell therapies have been FDA approved and/or reached clinical-stage studies by targeting CD19, CD20, CD22, and the B-cell maturation antigen [7–9]. The success of CAR T cells therapy is reflected as a considerable survival benefit in patients with B cell lymphomas, leukemias and multiple myelomas. However, there are still ongoing efforts to further optimize CAR T-cell systems for hematological malignancies by improving CAR structure design, transfection, and cell culture techniques. Many of these advancements have been successfully completed and have entered clinical validation trials [9–13].

Although CAR T cell therapies have made significant progress in treating blood malignancies, their application in solid tumor therapy presents difficulties due to existing limitations in CAR T cells and tumor-associated factors. The intrinsic profiles of CAR T cells, including their expansion, persistence, and cytotoxicity, are critical for the treatment's efficacy, and these factors may also be influenced by the TME [2,3,14–18]. Both tumor-intrinsic and tumor-extrinsic factors, such as host-related factors (gender, age, distribution of body fat, and gut microbiome), contribute to resistance against CAR T cell therapy [19–21]. Therefore, a comprehensive understanding of these factors is crucial to improve CAR T cell therapy efficacy against solid tumors.

Solid tumor-intrinsic factors driving resistance to immunotherapies, in particular CAR T cells therapy, are very complex and involve multiple aspects such as antigen loss, antigen heterogeneity, CAR T cell homing and infiltration within the tumor, and tumor-mediated suppressive microenvironment which largely hinder and protect solid tumors against CAR T cells [12,13,22–24].

Antigen escape

Antigen loss is a challenging limitation of CAR T cell therapy which usually results in antigen negative tumor recurrence. Recent trials have reported partial or complete loss of antigens in multiple relapsed blood malignancies. In solid tumors, there have been reports indicating the decreased expression of targeted antigen in the relapsed tumors, a phenomenon called antigen escape. As an example, the tumor relapse was linked to decreased expression of IL13Ra2 in a case report that introduced targeted IL13Ra2 in GBM. The mechanisms involved in tumor antigen escape are diverse and result from mutations, frameshifts, and insertions in exons encoding the targeted antigens. Lineage switching in cancer cells is

another proposed mechanism which was studied and reported in CD19-negative relapse in leukemia. Drug induced changes in cancer cells may result in emergence of sublineages with less expression of targeted antigen [11,12].

Accumulative body of studies also suggests occurrence of antigen positive relapses of cancer cells. CAR T cells exert antitumor effects that rely on the recognition of specific antigens and the induction of apoptosis in tumor cells. Signals mediating apoptosis in tumor cells include tumor necrosis factor (TNF)-related apoptosis-inducing ligand (TRAIL), Fas ligand (FasL), and cytokines such as interferon IFNγ. The mechanism of tumor antigen-positive resistance to CAR T-cell therapy is not fully uncovered but underlies changes in tumor cell survival, apoptosis and cancer cell-intrinsic parameters and subsequent changes in tumor immune milieu. Studies have shown that a TRAIL inhibitor can suppress the cytotoxic effect of normally functioning CD19 CAR T cells (as measured using the secretion of type I cytokines) when they cells are co-cultured with sensitive cells, indicating that a lack of TRAIL signaling in tumor cells can lead to tumor antigen-positive resistance to CAR T-cell therapy [25–27]. Surprisingly, the number of studies on deciphering the effect of solid tumor mutations on CAR T cell response has remained very limited [13,22,23,28,29]. Studying mutated tumors showing resistance to checkpoint blockade therapies may shed light on the mechanisms involved in resistance of tumors to immunotherapies other than antigen escape which can be further expanded to other immunomodulatory approaches like CAR T cell therapies. As an example, mutations in JAK1 and PTEN lead to lack of MHC-1 dependent antigen presentation and reduced tumor T cell infiltration and cytotoxicity, respectively [19–21,30,31].

Tumors with loss of function mutations in JAK1 and JAK2 have shown resistance to checkpoint blockade therapies and recent studies have shown that lack of IFNγ signaling pathway, including the abrogation of JAK/STAT pathways, results in limitation of adhesion molecules on cancer cells and reduced functional

cytotoxic synapsis between CAR T cells and cancer cells. However, further studies are warranted to investigate the immune regulatory role of mutated genes and pathways in cancer cells and their subsequent effect on sculpting the tumor immune landscape [13,22,23,29].

Another major obstacle in CAR T cell therapy of solid tumors is heterogeneity of antigens. Solid tumors can be composed of diverse arrays of cells, each with their own unique genetic and molecular characteristics. This can make it difficult to identify and target an appropriate antigen for CAR T cell therapy that is expressed consistently across all tumor cells [23,26].

Immunosuppressive tumor microenvironment

Solid tumors are not just masses of cancer cells, but rather complex ecosystems made up of a diverse array of different cell types, matrix proteins, and secreted factors. Understanding the immune characteristics of the TME is recognized as a crucial factor in predicting clinical outcomes for patients. It is classified as one of the ten fundamental tumor characteristics that significantly influence cancer progression. Recognizing the fundamental nature of the TME holds crucial implications for effectively combating solid tumors and developing effective CAR T cell therapies [12,27,32].

Among the prominent immune suppressor cells in the TME are regulatory T cells (Tregs), myeloid-derived suppressor cells (MDSCs), and M2 tumor-associated macrophages (TAMs). These cells, along with tumor cells, contribute to tumor growth by producing growth factors, local cytokines, and chemokines, such as VEGF, IL-4, IL-10, and TGFβ. Additionally, immune checkpoint molecules like CTLA-4 and PD-1/PDL1 reduce the antitumor immune response [16,32–36].

The presence of multiple cell types and inhibitory agents within the TME can limit the effectiveness of CAR T cell therapy. MDSCs have a detrimental effect on CAR T cells due to their potent immunosuppressive capabilities, directly targeting effector T cells. The suppression of CAR T cells by MDSCs is significant, and lower levels of MDSCs in individuals receiving CART19 therapy have been associated with positive responses in lymphoma and leukemia treatment. TAMs are the most abundant immune-infiltrating cells in the TME and they suppress T cell-mediated anti-tumor immunity through the secretion of cytokines and enzymes that deplete amino acids, such as arginase 1 or indoleamine 2,3-dioxygenase (IDO) [16,32,37,38]. Additionally, TAMs contribute to the increased recruitment of Treg cells, further suppressing the anti-tumor immune response [11,39,40].

In the TME, hyperactive cancer cells consume excessive amounts of glucose, which can limit the glycolytic capacity of T cells. This, in turn, hampers TCR/CAR signaling and impairs the effector responses of T cells. As a result, the efficacy of T cell therapy is reduced, as the tumor cells outcompete T cells for nutrients, overriding the antitumor immune response. This metabolic pressure within the TME poses a significant challenge in achieving optimal T cell function and highlights the importance of developing strategies to enhance the metabolic fitness of CAR T cells in order to improve their efficacy in nutrient-deprived environments. Despite the significant impact of nutrient deprivation in TME on CAR T cell efficacy, the underlying mechanisms are still poorly understood. Further research is needed to investigate the specific metabolic pathways that mediate the ineffectiveness of CAR T cells in the immunosuppressive TME [33,40–43].

Trafficking of CAR T cells into tumor tissue

The presence of a dense fibrogenic environment, facilitated by stromal cells like cancer-associated fibroblasts (CAFs), hinders the trafficking of CAR T cells within TME. When activated by multiple suppressive cytokines such a transforming growth factor β (TGF-β) and platelet derived growth factor (PDGF), CAFs stimulate the production of extracellular matrix (ECM) proteins, which create barriers that restrict the movement and trafficking of T cells. Moreover, TGF-β, functioning as a chemokine, directly inhibits T cell infiltration in solid tumors by suppressing the expression of chemokine receptors like CXCR3. Through complex mechanisms involving multiple growth factor associated cytokines and cell-to-cell contact, CAFs have been shown to impede the function of CAR T cells in preclinical models [44,45].

In hematological tumors, CAR-T cells have more contact with blood tumor cells as they circulate in the bloodstream and lymphatic system. However, in solid tumors, CAR-T cells often struggle to penetrate the tumor tissue through the vascular endothelium, preventing direct interaction with tumor cells [1,46]. Tumor tissues possess specific mechanisms that hinder CAR-T cell migration and infiltration. For example, the dysregulated vasculature in the TME of solid tumors plays a role in hindering T cell infiltration via downregulation of adhesion molecules that are necessary for T cell entry, such as vascular cell adhesion protein 1 (VCAM1) and intercellular adhesion molecule 1 (ICAM1) [22,23,29]. This downregulation amplifies the exclusion of T cells from the tumor site, further impairing immune surveillance and anti-tumor activity. In another study, Larson et al. demonstrated that IFNγR1/KO in solid tumors confers resistance to CAR T cell-induced killing, whereas this phenomenon is not observed in liquid tumor models. One of the key mechanisms underlying this distinction is related to the expression of cell-adhesion molecules. Following exposure to CAR T cells, IFNγR1/KO tumor cells exhibit reduced expression of ICAM-1,

impairing the formation of the immunological synapse between CAR T cells and tumor cells [13,22,29]. However, the importance of the ICAM-1/LFA-1 interaction for inducing tumor cell killing appears to be less significant in liquid tumors, where CD2-CD58 interaction might play a more prominent role[47]. Furthermore, hypoxia in the TME of solid tumors plays a significant role in promoting the recruitment of immunosuppressive cells. This is achieved through the secretion of various chemokines. Moreover, hypoxia induces the upregulation of immunosuppressive molecules on specific cell types. Regulatory T (Treg) cells increase the expression of CTLA4 or lymphocyte activation gene 3 protein (LAG3), while MDSCs, TAMs, and tumor cells upregulate programmed cell death 1 (PD-1) ligand 1 (PD-L1). These immunosuppressive molecules contribute to the suppression of the anti-tumor immune response [42,48,49].

Additionally, studies showed that the movement of CAR-T cells within solid tumors relies on the presence of chemokines such as ligand-11 and 12 chemokines. Unfortunately, these chemokines are typically expressed at lower levels in tumor tissue [50]. Consequently, the reduced expression of these crucial chemokines and the presence of dense fibrotic matrices, secreted largely by CAFs, in solid tumors impede the migration and invasion of CAR-T cells into tumor cells.

CAR T cell associated toxicities

The occurrence of toxicities and associated fatalities in CAR-T cell therapy further complicate the response of solid tumors to CAR T cell therapies. Several critical factors contribute to the incidence and severity of toxicities, including the design of the CAR, the specific target of the therapy, and the type of tumor being treated. The toxicities associated with CAR-T cell therapy have been extensively studied in patients receiving CD19-directed CAR T cells, however solid tumors are under investigation and future

efforts are required to better understand the toxicities to CAR T cells to improve the overall response to CAR T cell therapies [3,51–53].

The excessive systemic cytokine levels and immune cell cross-activation mediated by CAR T cells activity and proliferation lead to the following toxicities:

Cytokine-release syndrome (CRS): This condition is characterized by the overproduction of cytokines beyond normal physiological levels and the massive expansion of T cells in the body [3,53].

Hemophagocytic lymphohistiocytosis and/or macrophage activation syndrome (MAS): These are severe hyperinflammatory syndromes that manifest as a combination of CRS symptoms and elevated serum ferritin levels, hemophagocytosis, renal failure, liver enzyme abnormalities, splenomegaly, pulmonary edema, and the absence of natural killer (NK) cell activity [52,53].

Immune effector cell-associated neurotoxicity syndrome (ICANS): This syndrome is characterized by elevated cytokine levels in the cerebrospinal fluid, disruption of the blood-brain barrier, and associated neurological symptoms.

A recent study has identified a unique toxicity syndrome known as tumor inflammation-associated neurotoxicity (TIAN) in patients undergoing cell therapies for tumors in the central nervous system (CNS) [52–55].

CRS and ICANS, shedding light on the range of toxicities associated with CAR T cell therapy and their impact on treatment outcomes and highlighting the need for future strategies tuning the antigen density

and optimizing CAR T cell engineering to enhance the therapeutic response with minimal associated morbidity and mortality.

To address the challenges posed by solid tumors, researchers are actively exploring various strategies to enhance the efficacy of CAR T cell therapy. These include developing new CAR T cell constructs that are more capable of infiltrating the dense tumor microenvironment and targeting multiple antigens to increase the likelihood of targeting all tumor cells within the solid tumor. Additionally, combination therapies that target the immunosuppressive environment of solid tumors are being explored to improve the effectiveness of CAR T cell therapy. Among the ongoing effort to overcome the resistance of solid tumors to CAR T cell therapy, deeper understanding of association of cancer cell-intrinsic features and surrounding immune landscape, either through direct cell-to-cell contact, extracellular vesicles, nutrient availability, or the secretome, may direct future personalized immune intervention strategies for cancer treatment. To date, emerging studies introduce few pathways that have been extensively studied for their immunoregulatory properties, however, JAK1 mutated cancer cells and their immune regulatory effect on TME in the context of CAR T cell therapies are poorly studied[28]. Here we decipher the mechanism of resistance to CAR T cell therapies in JAK1/KO models which are largely mediated by JAK1/KO mediated suppressive microenvironment. We next found similarities and drew a connection between the JAK1/KO tumor associated microenvironment and the suppressive microenvironment found in GBM, one of the

hardest tumors yet to be cured. We highlighted the factors driving the suppressive environment in GBM tumors.

Chapter 2

INTERROGATING THE EFFICACY OF CAR T CELLS ON INTERFERON SIGNALING DEFICIENT TUMORS

The expression of interferon-γ (IFNγ) in the tumor microenvironment is crucial for an effective T cell response against tumor antigens. IFNγ activates the JAK-STAT signaling pathway, leading to the induction of PD-L1 expression and MHC class I molecules on tumor cells. However, disruptions in tumor cell responses to IFNγ signaling can result in a lack of PD-L1 and MHC class I molecules expression, compromising antigen presentation and rendering PD1-PD-L1 blockade therapies ineffective **(Figure 1)**. There is emerging data pointing to the loss-of-function mutations in JAK1 and JAK2 (from IFN signaling pathway) and B2M (from antigen presentation pathway) in patients who become resistant to immune checkpoint blockade therapy [30,31,56,57].

Following recognition of the significance of IFNγ signaling pathway in immune checkpoint blockade resistance, researchers have explored alternative approaches to overcome this resistance. These approaches aim to enhance antigen presentation and activate innate immune responses independently from the MHC pathway. Strategies include the use of Toll-like receptor (TLR) agonists, which can stimulate innate immune cells to enhance anti-tumor responses. Additionally, genetic or pharmacological interventions have been investigated to decouple MHC class I expression from interferon signaling, enabling improved antigen presentation even in the absence of IFNγ signaling pathway.

Cellular therapies utilizing NK cells have been explored as a strategy against MHC-deficient tumors. NK cells possess the ability to recognize and eliminate cells lacking MHC class I molecules, providing a potential therapeutic option to overcome the immune evasion mechanisms associated with MHC deficiency [19–21,30].

Furthermore, CAR T cell therapy was hypothetically introduced as another promising avenue which bypasses the requirement for MHC-dependent antigen presentation by directly targeting specific surface molecules on tumor cells, offering an alternative approach for effective tumor eradication [20,30].

A recent study conducted by Larson et al. revealed that the loss of genes in the IFNγ signaling pathway, such as IFNGR1, JAK1, or JAK2, led to increased resistance of solid tumors to CAR T cell-mediated killing, both in laboratory settings and in animal models [29,58,59]. Conversely, the loss of this pathway did not render leukemia or lymphoma cell lines insensitive to CAR T cells [22,29]. Through transcriptional profiling, the researchers observed that glioblastoma cells lacking IFNγR1 exhibited lower upregulation of cell-adhesion pathways following exposure to CAR T cells. It was discovered that the absence of IFNγR1 in glioblastoma cells resulted in reduced binding duration and avidity between CAR T cells and tumor cells which led to less effective cytotoxicity. This finding was unexpected, as CAR T cells do not rely on traditional antigen-presentation pathways. IFNγR signaling was found to be essential for promoting sufficient adhesion between CAR T cells and tumor cells to mediate effective cytotoxicity [13,22–24,29]. While previous studies have laid the foundation by demonstrating the effect of CAR T cells on JAK1 mutated tumors, the underlying mechanisms and the specific immunoregulatory role of JAK1 mutations in the context of CAR T cell therapy remain poorly understood. IL13Ra2-targeted CAR T cells have undergone trials for patients with GBM at City of Hope. While there has been a notable response in a few GBM patients, the overall efficacy of IL13R2-targeted CAR T cells in treating GBM remains poor [60,61]. In our laboratory, we have recently developed mouse IL13 (mIL13) CAR T cells [6], which will enable us to investigate the mechanism of response and resistance to mIL13 CAR T cells within the TME. This new mouse model will provide valuable insights into the potential mechanisms underlying the limited efficacy observed in GBM patients treated with IL13R2-targeted CAR T cells.The current study aims to fill the void in our understanding of the response of CAR T cells in JAK1-mutated tumors and shed light on the

immunoregulatory implications of these mutations in the context of CAR T cell therapy. By investigating the specific interactions and mechanisms involved, this research endeavors to provide crucial insights into how JAK1 mutations influence the effectiveness of CAR T cell therapy and the overall immunoregulatory landscape within the tumor microenvironment.

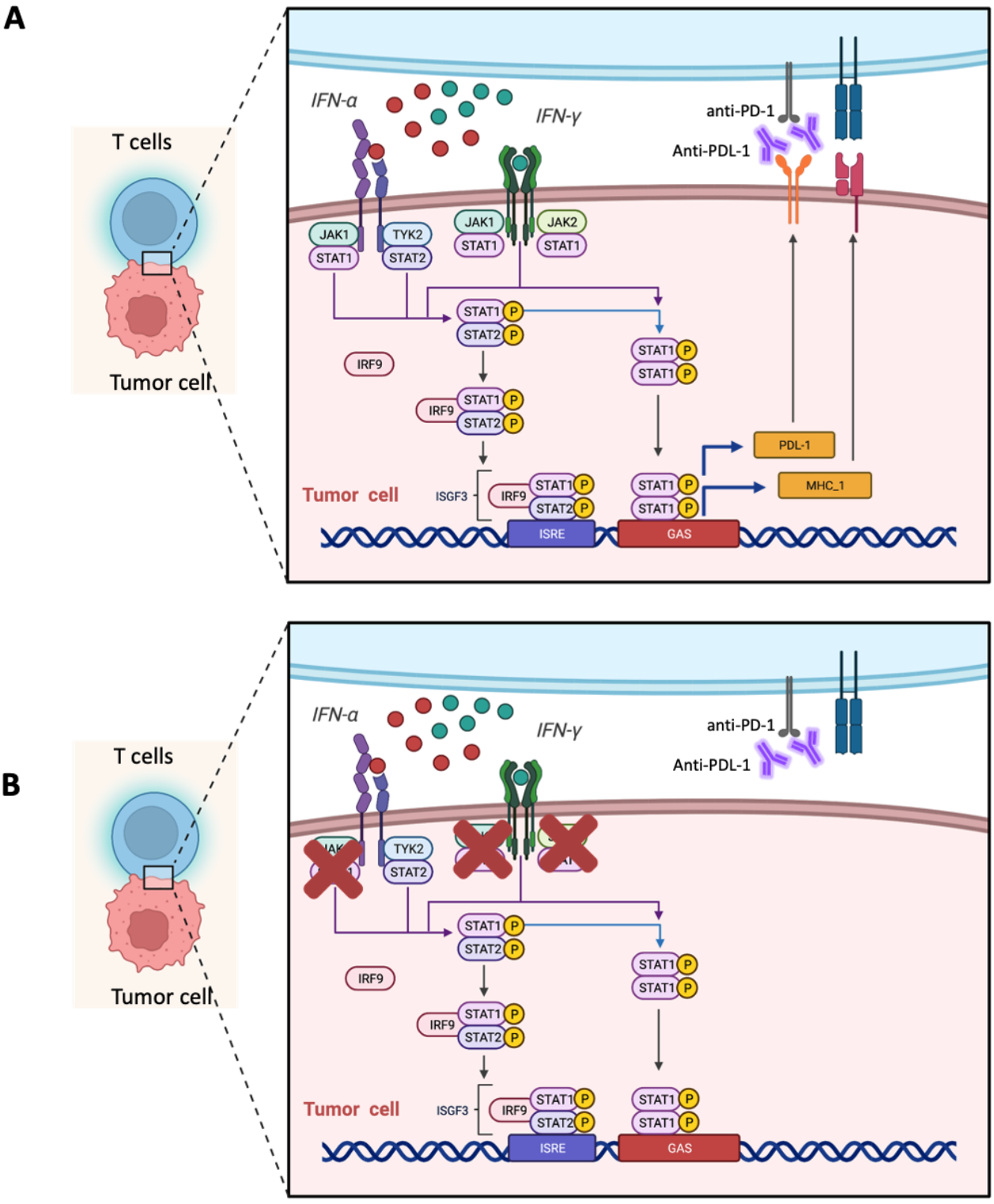
A
T cells
Tumor cell
IFN-α
IFN-γ
anti-PD-1
Anti-PDL-1
JAK1
TYK2
JAK2
STAT1
STAT2
P
IRF9
ISGF3
PDL-1
MHC_1
Tumor cell
ISRE
GAS
B
T cells
Tumor cell
IFN-α
IFN-γ
anti-PD-1
Anti-PDL-1
TYK2
STAT2
IRF9
ISGF3
Tumor cell
ISRE
GAS

Figure 1. A. Schematic figure illustrating the known mechanism of IFN signaling pathway mediating antigen presentation and response to checkpoint blockade therapies. **B.** Schematic figure illustrating how aborgated IFN signaling pathway confers resistance against the PD-1/PDL-1 blockade therapies.

In order to establish a comprehensive and representative model for murine IL-13 targeted CAR T cell therapy, we successfully generated JAK1/KO murine melanoma (YUMM 2.1) **(Figure 2.A)** and JAK1/KO colon adenocarcinoma (MC38) cell lines expressing IL13Ra2. This syngeneic model allows us to closely modulate the immune setting and investigate the changes occurring within TME in the absence of a functional IFN signaling pathway. To ensure reliability and consistency, we carefully selected clones from each JAK1KO subline and verified their comparable growth rates. This step ensures that any observed differences in the TME is not influenced by variations in cell proliferation rates between the JAK1/KO and WT counterparts **(Figure 2.B)**. We next characterized the expression of MHC-1 and PDL-1 upon exposure to IFNγ in both JAK1/KO and WT tumors (shown in replicates) **(Figure 2.C)**.
By utilizing both the JAK1/KO and WT tumor models, we can precisely decipher the alterations within the TME under conditions of fully functional immune responses. This approach offers a valuable platform for studying the impact of JAK1 deficiency on the TME and assessing the efficacy of IL-13 targeted CAR T cell therapy in the context of IFN signaling pathway impairment.

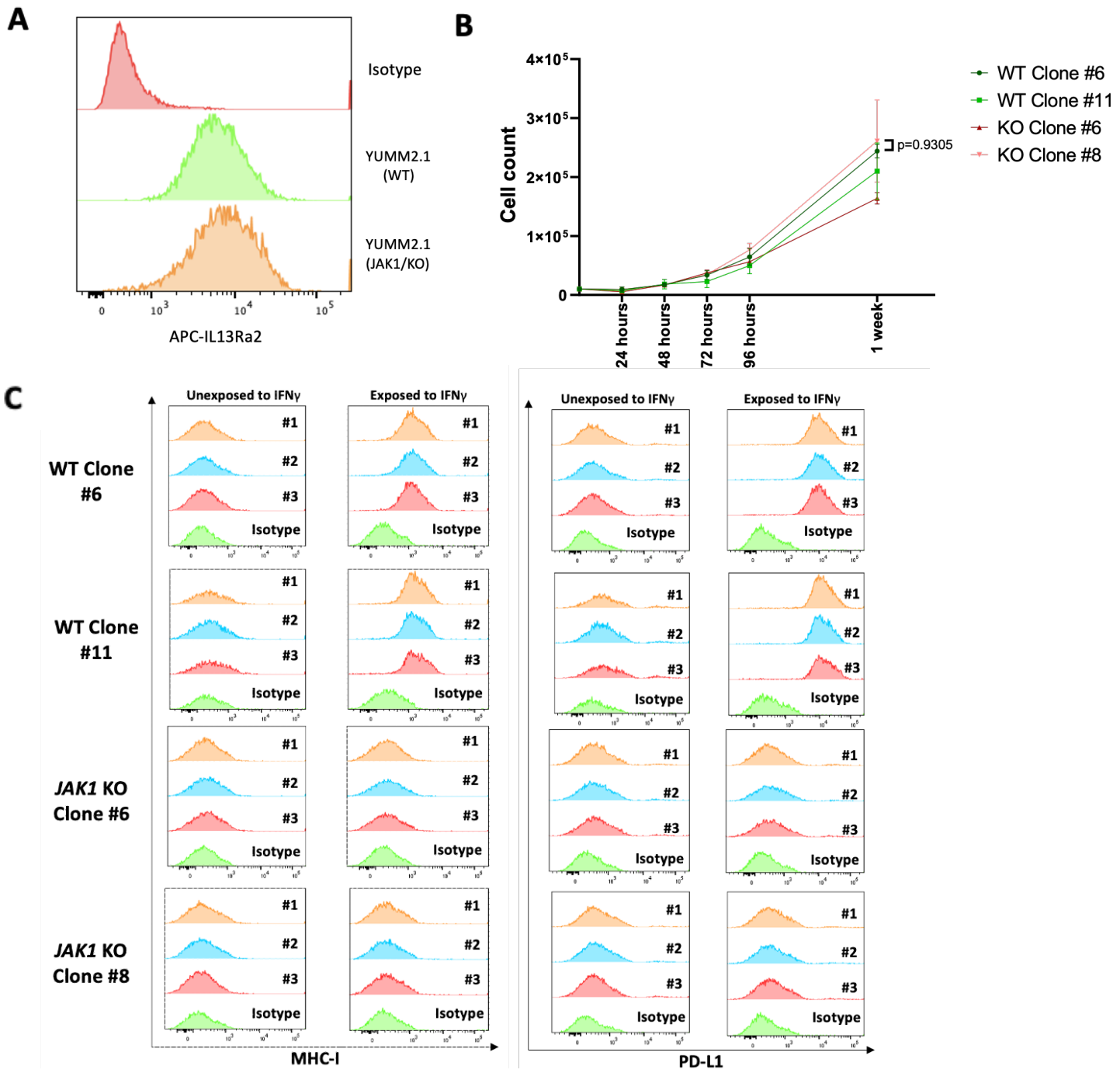

Figure 2. A. Flow analysis showing the expression of IL13Ra2 on YUMM2.1 WT and JAK1/KO tumors. **B.** growth dynamics of single clones of YUMM2.1 WT and JAK1/KO tumors expressing IL13Ra2. **C.** Flow analysis showing differential expression of PDL-1 and MHC-1 in YUMM2.1 WT and JAK1/KO tumor lines 18 hours post IFNγ exposure.

To evaluate the persistence of expression of MHC-I and PDL-1, IFNγ was introduced to the lines for 18 hours and subsequently removed. At 72 hrs, MHC-I and PDL-1expression were assessed using flow cytometry. Flow analysis revealed differential expression of MHC-I and PDL-1 was detected in YUMM JAK1/KO versus YUMM WT tumors **(Figure 3)**.

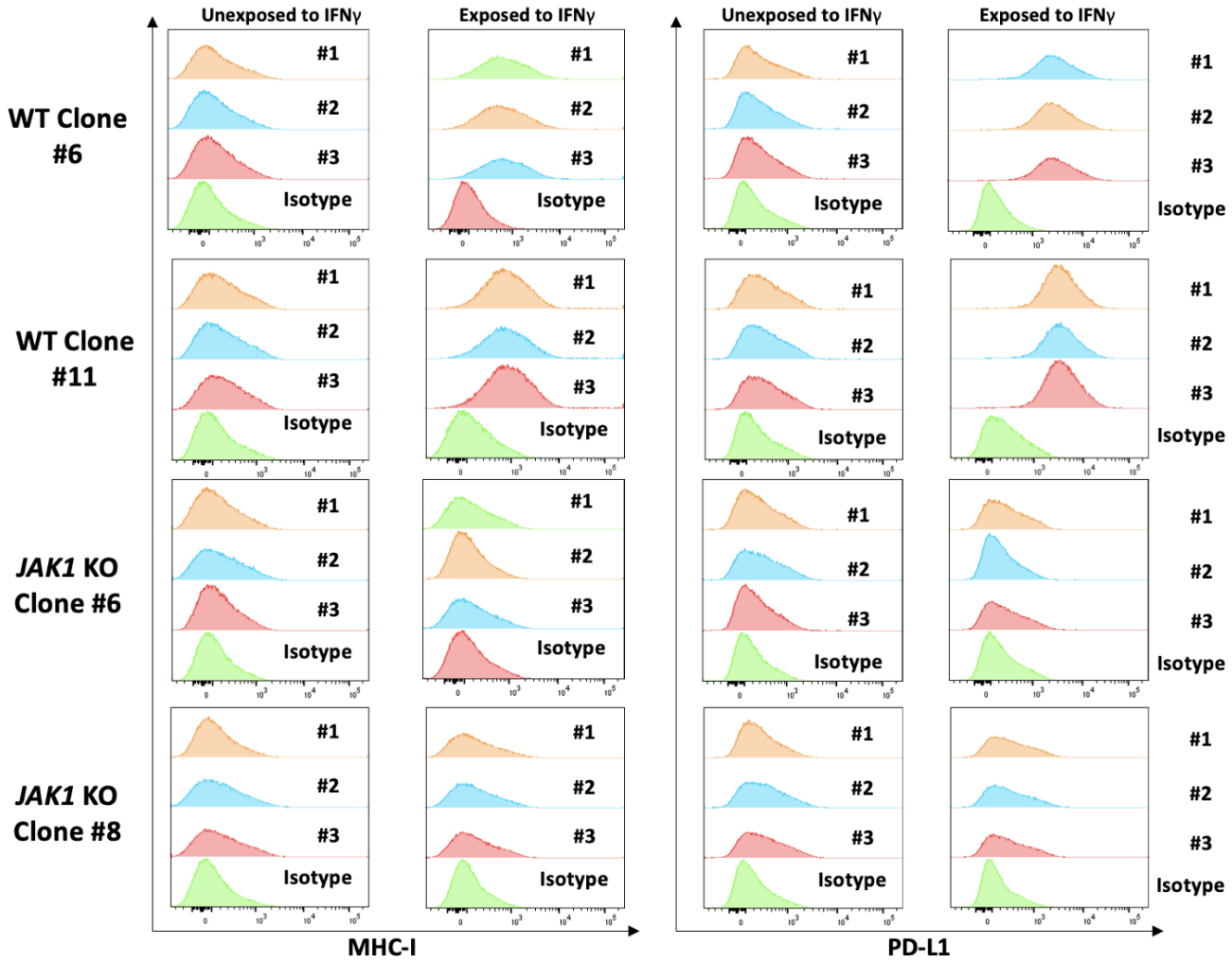

Figure 3. Differential expression of MHC-I and PD-L1 in YUMM 2.1 WT and JAK1/KO sublines at 72 hours following IFNγ exposure and removal after 18 hours.

To comprehensively investigate the differential gene expression induced by IFNγ, both YUMM JAK1/KO and YUMM WT cell lines were exposed to supernatants derived from CAR T cells coculture with WT tumors. Subsequently, the cells were subjected to bulk RNA-sequencing for detailed transcriptional analysis **(Figure 4. A).**

Our analysis revealed significant differences in the expression levels of PD-L1, MHC class I, and IFN signaling intermediates between YUMM JAK1/KO and YUMM2.1 WT tumor cells **(Figure 4. B).** Notably, the observed differences were more pronounced in the CAR T cell-induced condition as compared to the IFNγ-induced condition. Importantly, these differences were not limited to genes directly regulated by interferon signaling pathways. The transcriptional analysis unveiled alteration in additional genes associated with diverse biological functions, highlighting the multifaceted impact of JAK1 knockout on the inherent tumor cell transcriptome and modulation of CAR T cell-mediated cytotoxicity **(Figure 4. C)**. In both IFN-induced and CAR T cell-induced conditions, we observed minimal differences in ICAM-1 expression profile between the YUMM JAK1/KO and WT tumors. This suggests that ICAM-1 expression is negligibly affected by the JAK1 status. Conversely, significant differential expression of VCAM-1 was observed between the two tumor types in these conditions **(Figure 4. D)**. We next verified the expression of ICAM-1 and VCAM-1 on protein level using flow cytometry **(Figure 4. E)**. The contrasting expression patterns of ICAM-1 and VCAM-1 in YUMM JAK1/KO and WT tumors shed light on the complex mechanisms involved in the immunoregulatory role of abrogated IFN signaling pathway and their potential implications for tumor immune responses.

A

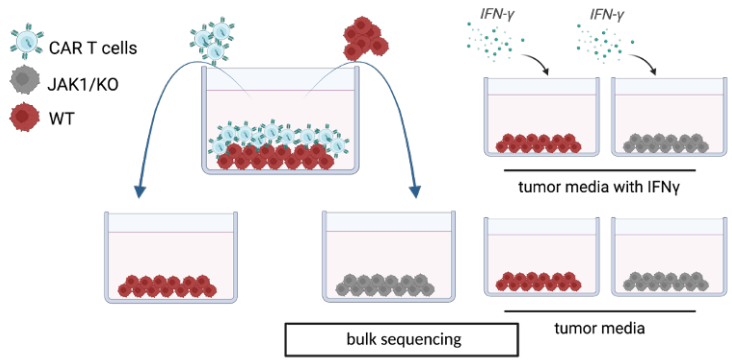
CAR T cells
JAK1/KO
WT
IFN-γ
IFN-γ
tumor media with IFNγ
bulk sequencing
tumor media

B

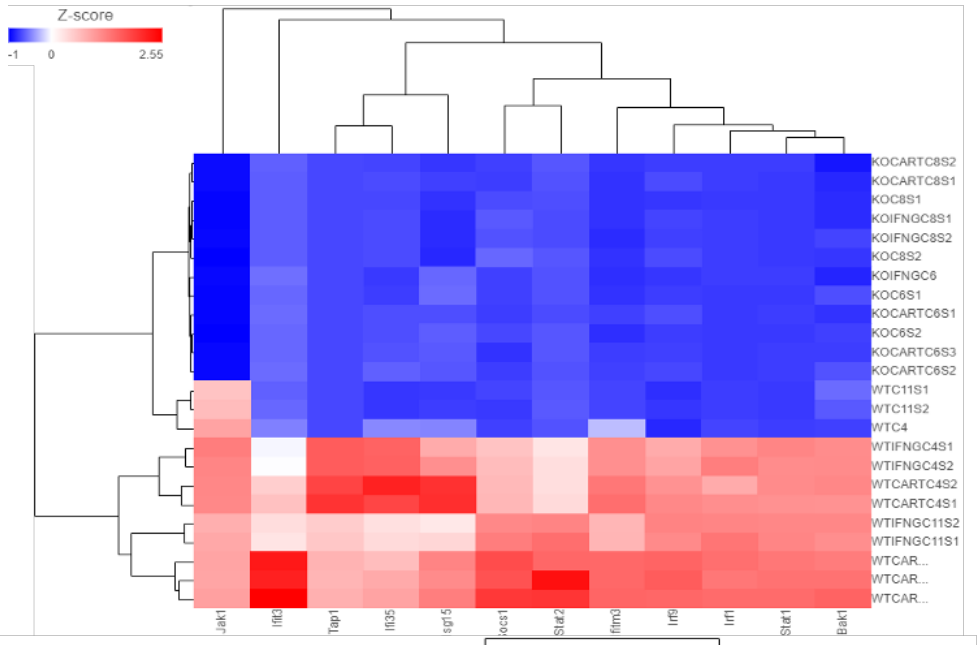
Z-score
-1
0
2.55
KOCARTC8S2
KOCARTC8S1
KOC8S1
KOIFNGC8S1
KOIFNGC8S2
KOC8S2
KOIFNGC6
KOC6S1
KOCARTC6S1
KOC6S2
KOCARTC6S3
KOCARTC6S2
WTC11S1
WTC11S2
WTC4
WTIFNGC4S1
WTIFNGC4S2
WTCARTC4S2
WTCARTC4S1
WTIFNGC11S2
WTIFNGC11S1
WTCAR...
WTCAR...
WTCAR...
Jak1
Ifit3
Tap1
Ifi35
Isg15
Socs1
Stat2
Ifitm3
Irf9
Irf1
Stat1
Bak1

C

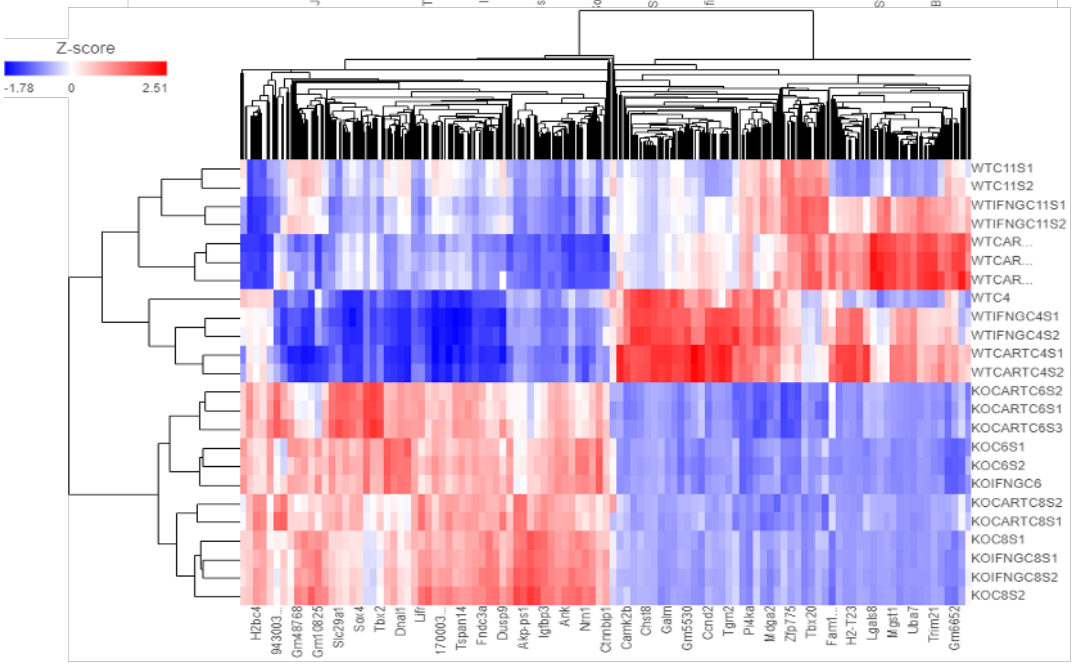
Z-score
-1.78
0
2.51
WTC11S1
WTC11S2
WTIFNGC11S1
WTIFNGC11S2
WTCAR...
WTCAR...
WTCAR...
WTC4
WTIFNGC4S1
WTIFNGC4S2
WTCARTC4S1
WTCARTC4S2
KOCARTC6S2
KOCARTC6S1
KOCARTC6S3
KOC6S1
KOC6S2
KOIFNGC6
KOCARTC8S2
KOCARTC8S1
KOC8S1
KOIFNGC8S1
KOIFNGC8S2
KOC8S2
H2bc4
943003...
Gm48768
Gm10825
Slc29a1
Sox4
Tbx2
Dnah1
Lif
170003...
Tspan14
Fndc3a
Dusp9
Alkp-ps1
Igfbp3
Ank
Nm1
Ctnnbip1
Camk2b
Chst8
Galm
Gm5530
Ccnd2
Tgm2
Pi4ka
Mgea2
Zfp775
Tbx20
Fam1...
H2-T23
Lgals8
Mgat1
Uba7
Trim21
Gm6652

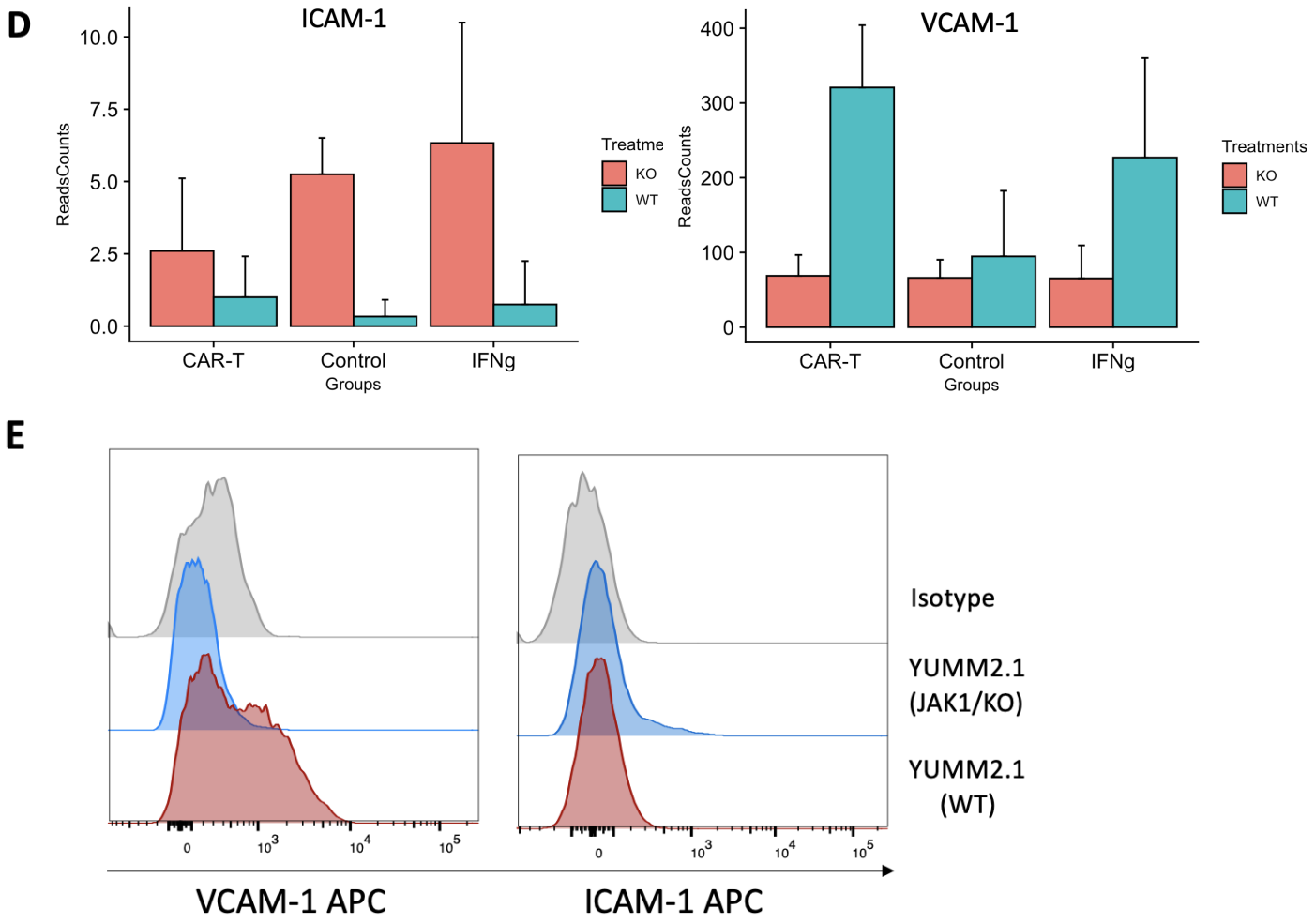

Figure 4. A. Schematic illustration describing the conditions introduced to YUMM JAK1/KO and WT tumors. YUMM JAK1/KO and WT tumors were exposed to supernatants from CAR T cells cocultured with WT tumors. Associated positive (IFNγ) and negative (tumor media) controls were included in the study. **B.** Differential expression of IFN signaling associated genes in JAK1/KO and WT sublines (the experiment was run in replicates for each condition). **C.** Transcriptome heatmap depicting global gene expression alterations in CAR T cell-induced, IFNγ-induced and control conditions. **D and E.** Comparison of VCAM-1 and ICAM-1 expression in JAK1/KO and WT tumors using RNA sequencing and flow cytometry analyses.

To assess the impact of IL13-CAR T cells on YUMM-JAK1/KO cells, we injected both YUMM-JAK1/KO and YUMM WT cells into the flank of C57BL/6 mice. After confirming successful tumor engraftment, murine IL13 (mIL13) CAR T cells were directly administered into the tumor site, and subsequent measurements of tumor size were recorded. The delivery of CAR T cells directly into the tumors aimed to minimize the potential confounding effects of CAR T cell trafficking to solid tumors. Our results clearly demonstrated that YUMM JAK1/KO tumors exhibited resistance to CAR T cell therapy, whereas YUMM-WT tumors showed significant regression in size following treatment with CAR T cells **(Figure 5. A-C)**.

To further validate the efficacy of mIL13-CAR T cell therapy, we utilize the same experimental approach using MC38 (colon cancer syngeneic model) JAK1/KO IL13Ra2+ cells and compare them to their MC38-WT IL13Ra2+ counterparts. Consistently, we observed a lack of response to mIL13-CAR T cell therapy in mice harboring MC38 JAK1/KO tumors, while MC38-WT tumors exhibited complete tumor eradication upon mIL13-CAR T cell treatment **(Figure 14. C and E)**. These findings highlight the critical role of JAK1 signaling pathway in mediating the therapeutic response of CAR T cells targeting IL13Ra2 and underscore the significance of JAK1 loss of function mutations in conferring resistance to this specific immunotherapy approach.

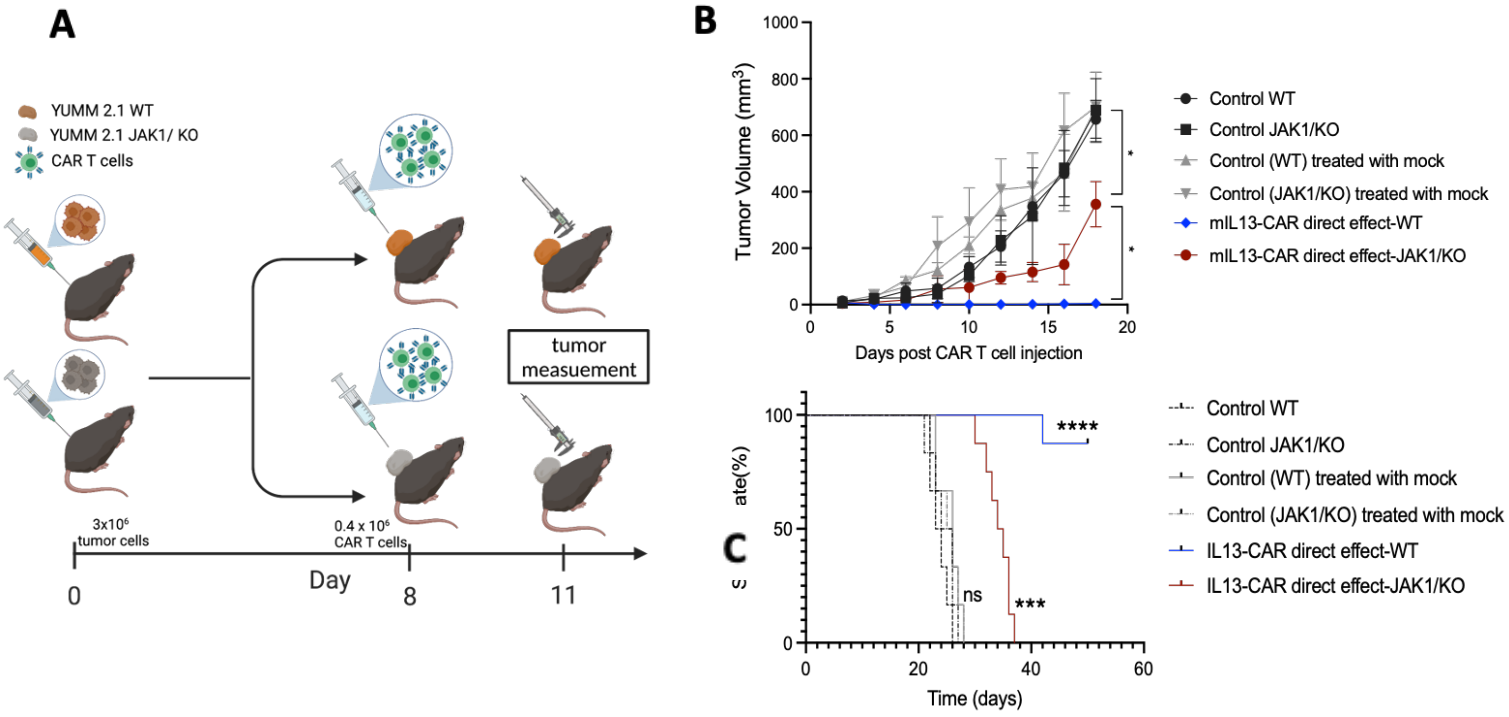

Figure 5. A. Schematic representation of the *in vivo* experiment design illustrating the effect of mIL13 CAR T cell against YUMM JAK1/KO and WT tumors. **B.** The analysis of tumor volumes of YUMM JAK1/KO versus YUMM WT tumors following mIL13 CAR T cell therapy. **C.** Representation of the tumor volume-associated survival analysis of YUMM JAK1/KO and YUMM WT tumors following mIL13 CAR T cell therapy.

To further validate our initial findings and assess the impact of systemic delivery of CAR T cells on YUMM JAK1/KO tumors, lymphodepleted C57BL/6 mice harboring both YUMM JAK1/KO and YUMM WT tumors were treated with IL13-CAR T cells via tail vein injection. To create a lymphodepleted model, mice were subjected to 5 Gray whole-body irradiation five days prior to the administration of CAR T cells. The lymphodepletion approach aimed to enhance the efficacy of CAR T cell therapy by reducing the competition and inhibitory effects of endogenous immune cells, allowing for better T cell expansion and tumor targeting. Our results showed that YUMM JAK1/KO tumors displayed resistance to CAR T cell therapy, whereas YUMM-WT tumors were effectively cured following treatment. Flow cytometric analysis of blood samples collected from the treated mice revealed a significant decrease in the total T cell and CAR T cell populations in YUMM JAK1/KO tumors compared to YUMM-WT counterparts **(Figure 6. A-D)**.

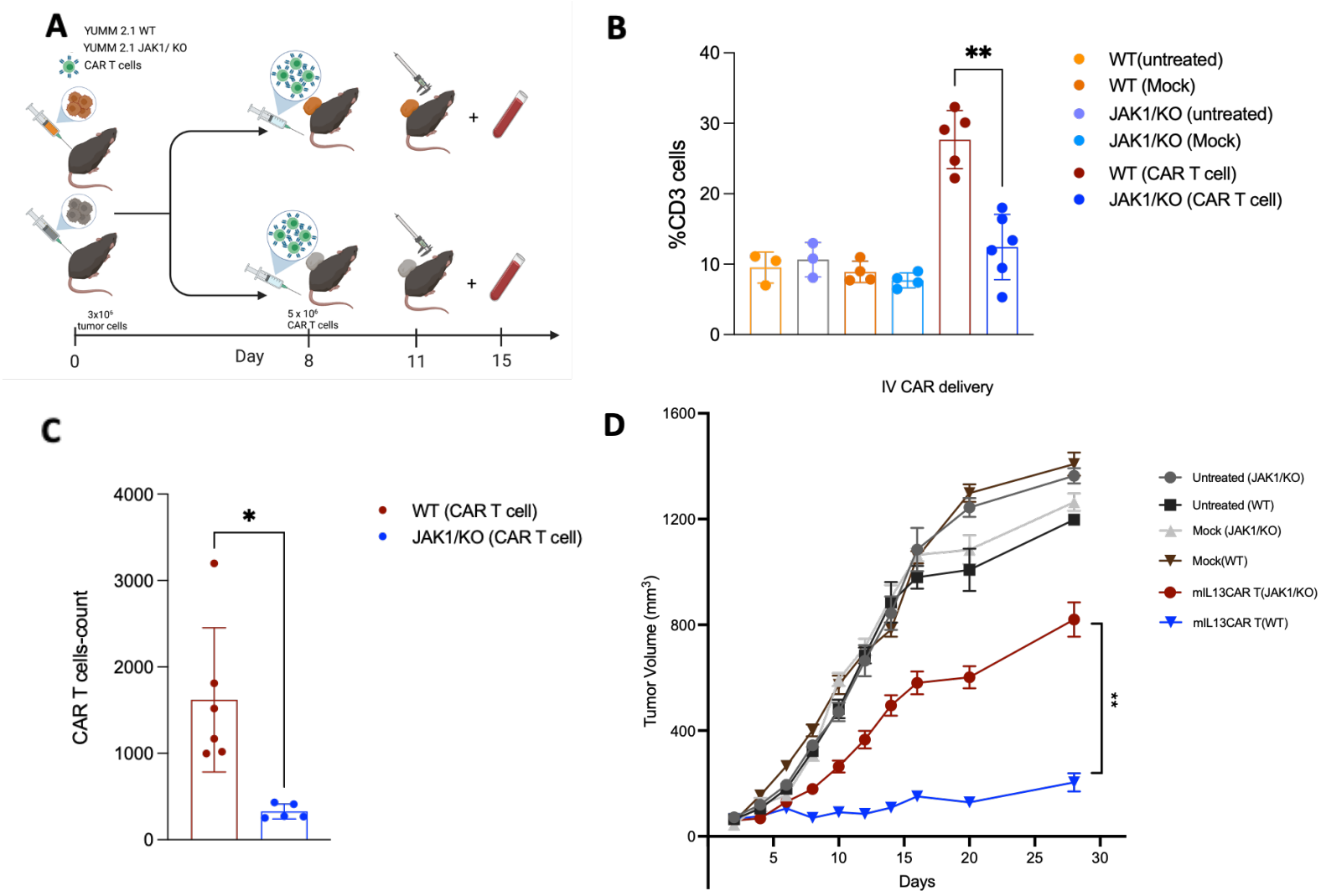

Figure 6. A. Schematic representation of the *in vivo* experiment design illustrating the effect of systemic mIL13 CAR T cell therapy on YUMM JAK1/KO and YUMM WT engrafted tumors. **B and C**. Flow cytometric analysis of T cells in the blood derived from mice bearing YUMM JAK1/KO and YUMM WT tumors, following treatment with mIL13 CAR T cells. **D.** The analysis of volumes of YUMM JAK1/KO versus YUMM WT tumors following mIL13 CAR T cell therapy.

To comprehensively analyze the tumor immune cell infiltrates and identify the underlying immune-related factors contributing to the resistance of YUMM JAK1/KO tumors to CAR T cell therapy, we dissociated size-matched YUMM JAK1/KO and YUMM WT tumors three days after CAR T cell treatment and enriched CD45+ cell population prior to single-cell RNA sequencing (sc-RNAseq) analysis **(Figure 7. A)**. This approach allowed us to transcriptionally characterize the immune cell populations and unravel the immunoregulatory role of JAK1 dysregulated signaling pathway and key molecular mechanisms associated with the observed therapeutic resistance.

Transcriptional analysis revealed distinct alterations in the immune cell composition of CAR T cell-treated YUMM-JAK1/KO tumors compared to YUMM WT counterparts **(Figure 7. B-C)**. YUMM JAK1/KO tumors exhibited decreased T-cell transcripts and increased presence of myeloid, neutrophil, and stromal cells. B cell signatures were significantly reduced in YUMM JAK1/KO tumors, suggesting a poor blood circulation and a hypoxic tumor microenvironment. Further analysis of T cell subclusters demonstrated reduced frequencies of CD8-early active and CD8-native like in CAR T cell-treated YUMM JAK1/KO tumors **(Figure 7. D-E)**. Conversely, higher proportions of follicular helper T cells, Treg cells, and exhausted T cells were observed in treated YUMM JAK1/KO tumors compared to treated YUMM-WT tumors. These findings highlight the immune cell dynamics and potential immunosuppressive cellular profile associated with JAK1 mutation in the context of CAR T cell therapy **(Figure 7)**. Next, using single-cell RNA sequencing, we profiled CAR T cells within the tumor microenvironment. mIL13 CAR T cells were engineered to express truncated CD19 which enabled us to successfully characterize mIL13 CAR T cells coexpressing CD19 (transduction marker) and CD3. Our analysis revealed an upregulated exhaustion profile in CAR T cells infiltrating YUMM JAK1/KO tumors compared to WT. These findings

provide further evidence that CAR T cells experience rapid exhaustion within the tumor microenvironment of JAK1/KO tumors compared to WT **(Figure 8. A-D)**

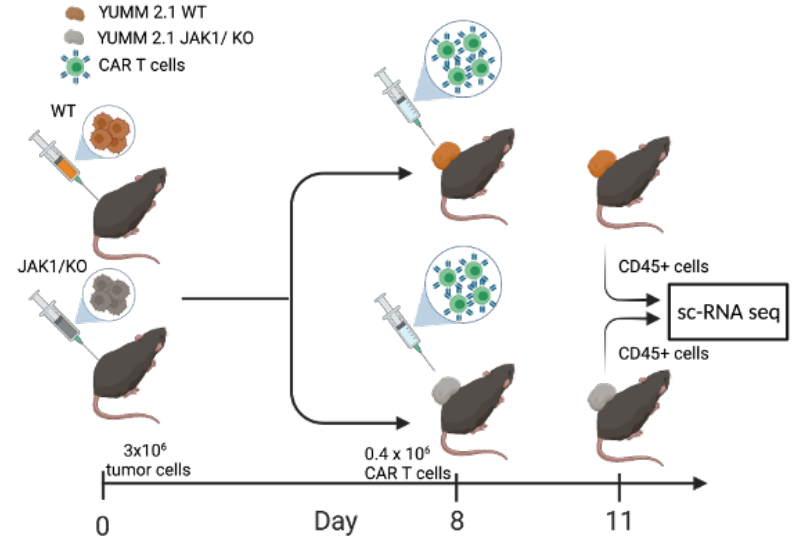

Figure 7. A. Schematic illustration depicting the experimental workflow for sc-RNA sequencing of size-matched YUMM-JAK1/KO and YUMM-WT tumors 72 hours post mIL13 CAR T cell therapy. **B and C**. UMAP profile of immune cell populations and the percentage of T cells within YUMM JAK1/KO and WT tumors following mIL13 CAR T cell therapy. **D and E.** UMAP analysis of T cell subtypes and their corresponding proportions in YUMM JAK1/KO and WT tumors following mIL13 CAR T cell therapy.

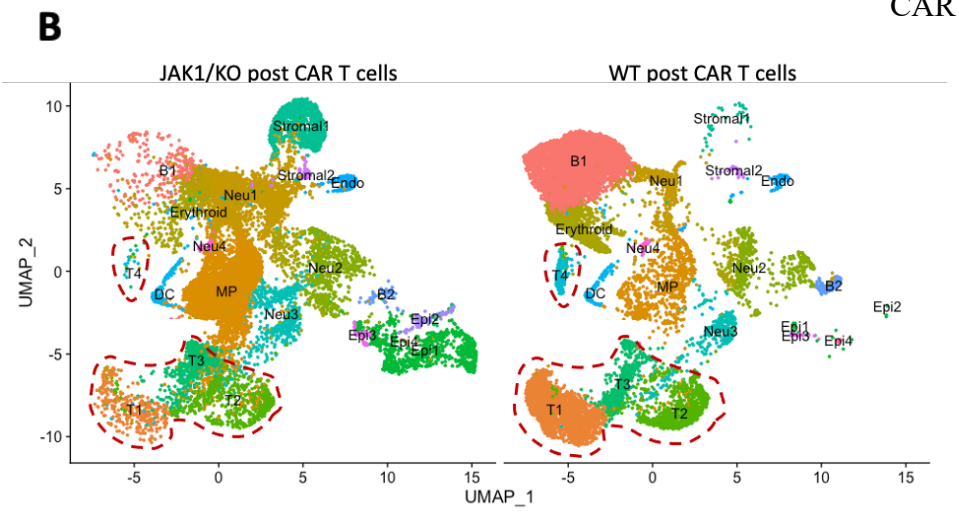

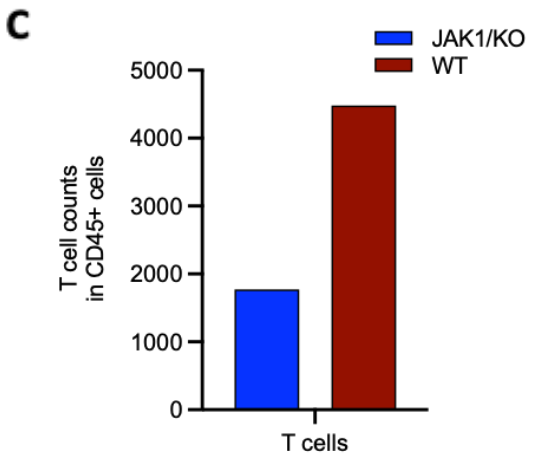

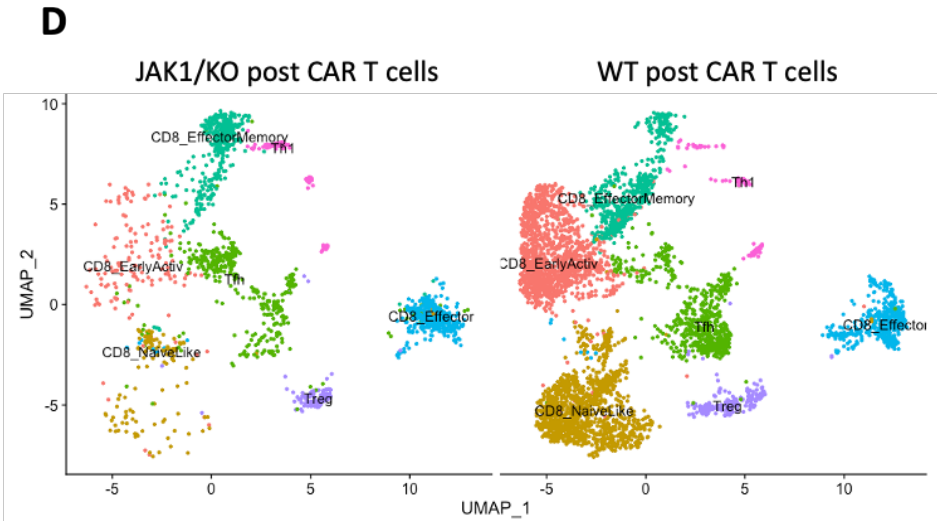

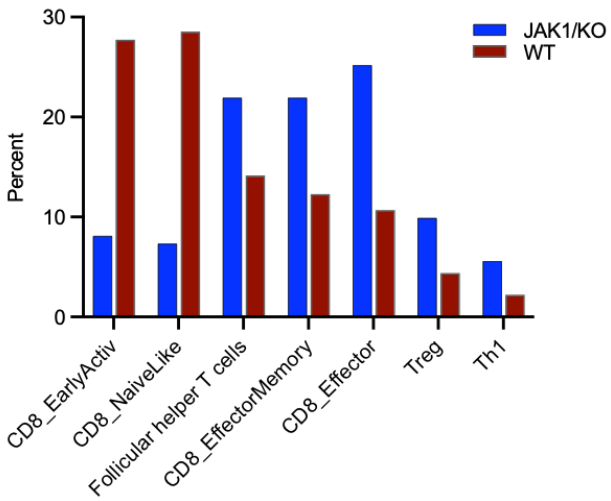

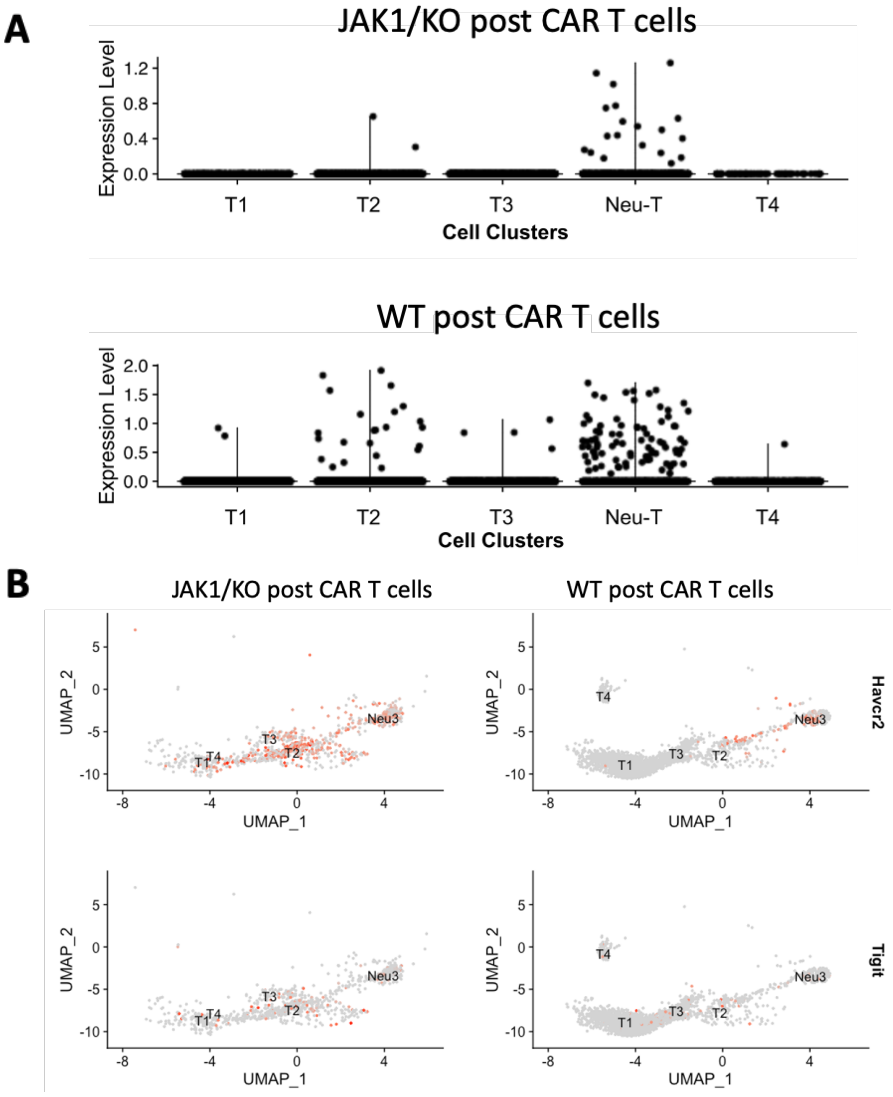

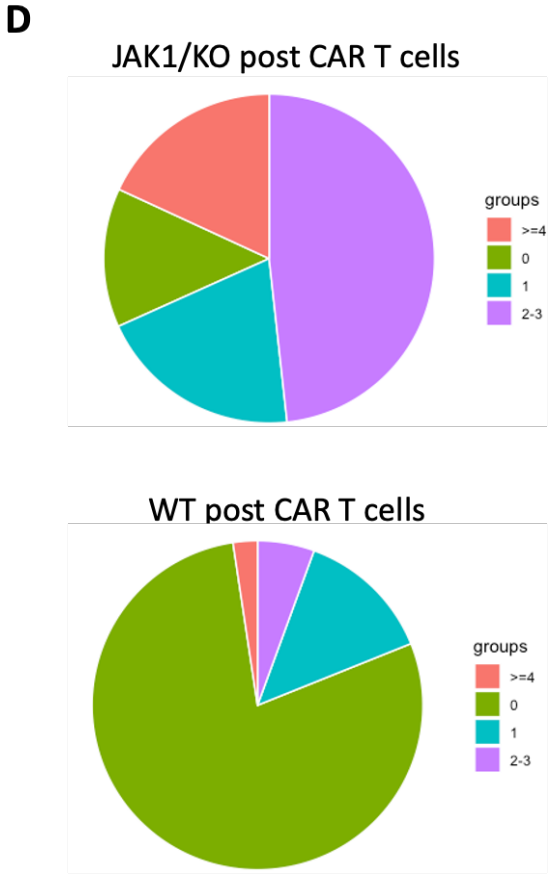

Figure 8. A. Dot plots illustrating mIL13 CAR T cells within YUMM JAK1/KO and WT tumors following mIL13 CAR T cell therapy. **B and C**. UMAP analysis of mIL13 CAR T cell exhaustion profile within YUMM JAK1/KO and WT tumors following mIL13 CAR T cell therapy. **D.** Pie charts illustrating the percentage of co-expression of exhaustion markers on CAR T cells within YUMM JAK1/KO and WT tumors following mIL13 CAR T cell therapy.

Pathway enrichment analysis of the sc-RNA seq data revealed notable differences in the pathway activities between JAK1/KO YUMM tumors and WT tumors following CAR T cell treatment. In JAK1/KO tumors, there was an upregulation of pathways associated with collagen degradation and ECM remodeling and degradation. Additionally, pathways related to chylomicron clearance and remodeling, lipid metabolism, IL10 signaling, and receptor-ligand interactions were found to be upregulated in JAK1/KO tumors compared to WT tumors. Conversely, WT tumors exhibited an upregulation of pathways involved in mRNA splicing, assembly, and antigen presentation. These findings suggest a potential regulatory role of JAK1 signaling in the tumor microenvironment and highlight the complex interplay between JAK1 signaling pathway, ECM remodeling, immune signaling, and metabolic pathways in response to CAR T cell therapy **(Figure 9)**.

The YUMM JAK1/KO tumor niche exhibited a significantly higher expression of CSF1-CSF1R in fibroblasts and CCL2-CCR2 in MDSCs, indicating an immune suppressive crosstalk within the tumor microenvironment. This finding suggests the involvement of these signaling pathways in promoting immune evasion and tumor progression in the JAK1 knockout model **(Figure 10)**.

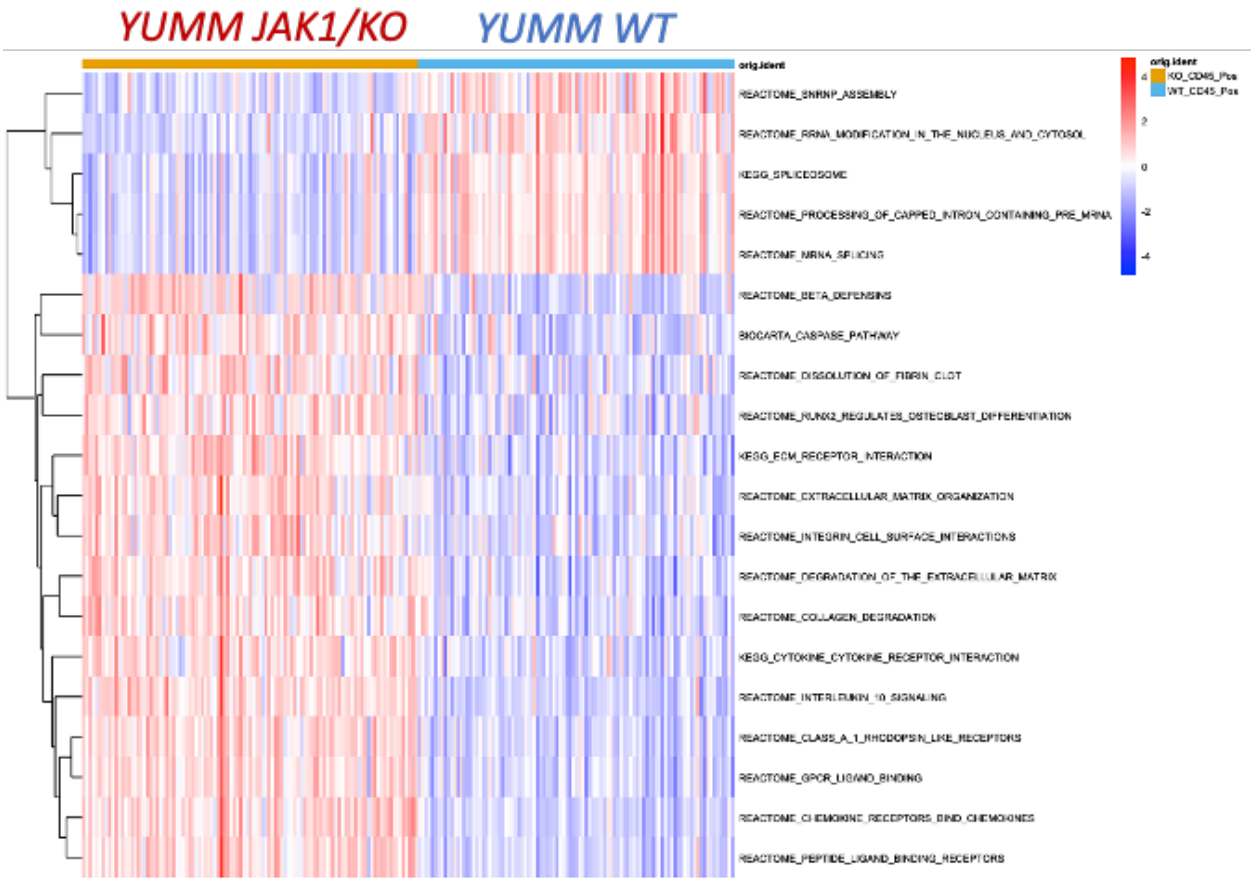

Figure 9. Pathway enrichment analysis of single-cell RNA sequencing (sc-RNA seq) data showing differential pathway activities between JAK1/KO melanoma tumors and WT tumors following CAR T cell treatment.

CellChat analysis was performed to systematically study cell-cell communication networks within the TME in YUMM JAK1/KO tumors. The analysis of receptor-ligand interactions revealed the upregulation of receptor ligands involved in laminin and collagen formation and remodeling **(Figure 11. A and B)**. Moreover, SPP1 upregulation was detected in the transcriptomic signature of suppressive immune cells of YUMM JAK1/KO tumors. SPP1+ TAMs were more likely to interact with CD44+ CAFs in the YUMM JAK1/KO tumor niche compared to WT tumor niche **(Figure 11. C-E)**. The study also identified differentially enhanced receptor-ligand interactions between fibroblasts and regulatory and exhausted T cells, mediated largely through the CCL2-CCR2 and CSF1-CSF1R axes **(Figure 11. F-G)**. This finding provided insights into the suppressive impact of fibroblasts on infiltrating T cells, promoting a regulatory and exhausted T cell phenotype in the TME of YUMM JAK1/KO tumors. Overall, the analysis revealed an increased number and strength of interactions among different cell populations, primarily driven by fibroblasts and myeloid suppressive cell (granulocyte- and myeloid-derived) populations, in the treated YUMM JAK1/KO tumors compared to treated YUMM-WT tumors.

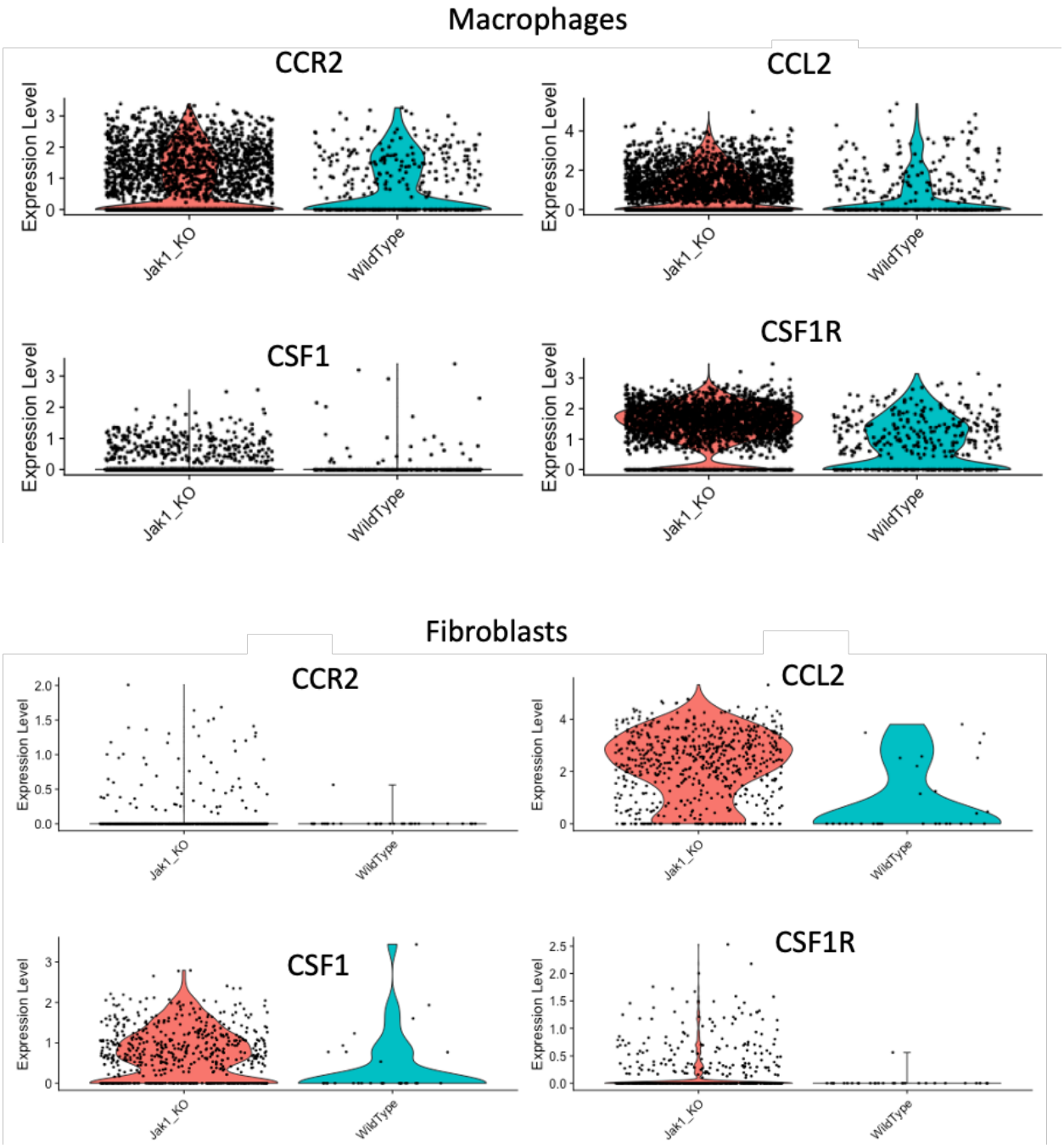

Figure 10. The expression of CSF1-CSF1R in fibroblasts and CCL2-CCR2 in MDSCs of YUMM JAK1/KO tumor compared to WT counterparts post mIL13 CAR T cell therapy.

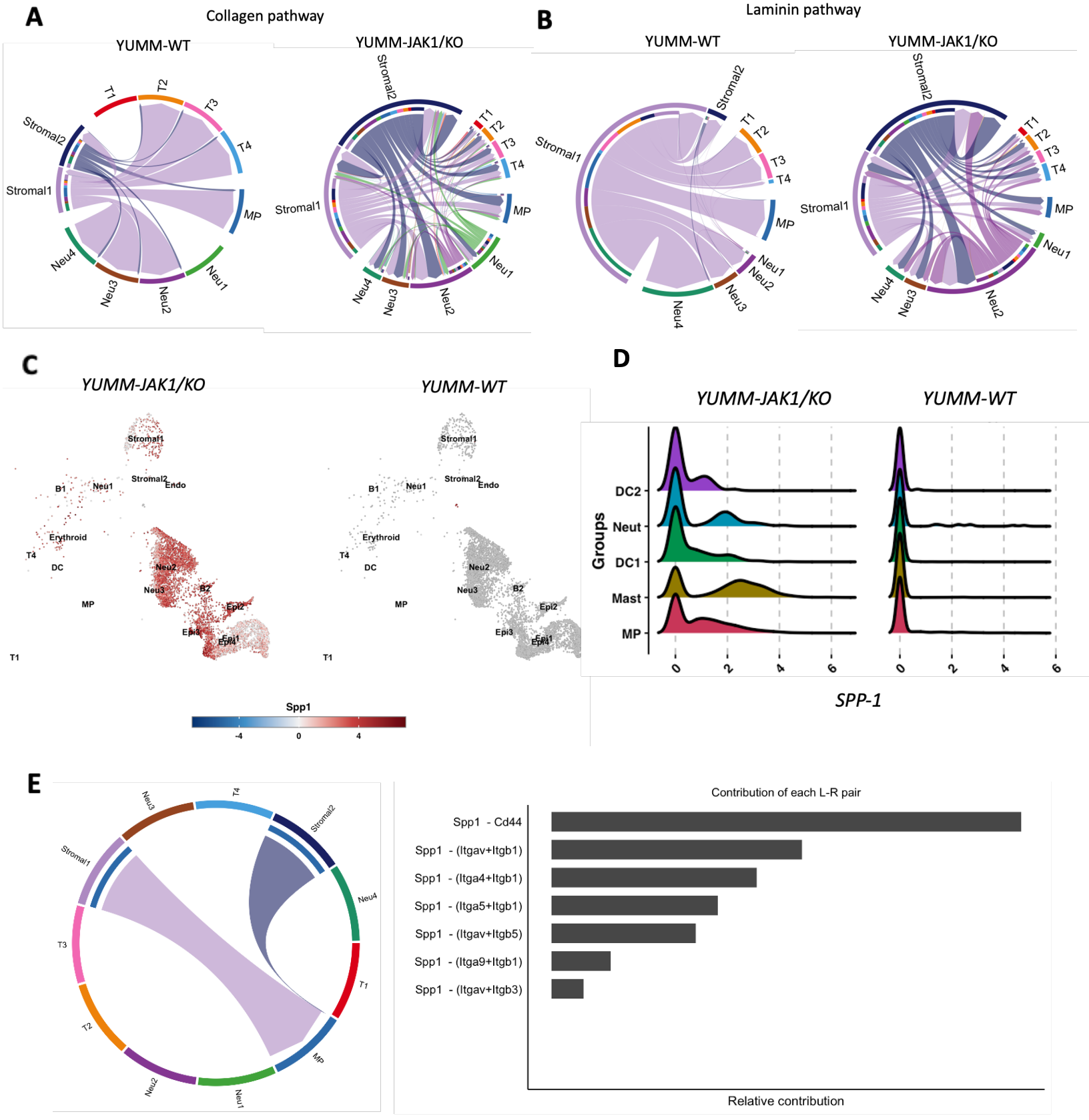
A
Collagen pathway
YUMM-WT
YUMM-JAK1/KO
B
Laminin pathway
YUMM-WT
YUMM-JAK1/KO
C
YUMM-JAK1/KO
YUMM-WT
Spp1
D
YUMM-JAK1/KO
YUMM-WT
Groups
DC2
Neut
DC1
Mast
MP
SPP-1
E
Contribution of each L-R pair
Spp1 - Cd44
Spp1 - (Itgav+Itgb1)
Spp1 - (Itga4+Itgb1)
Spp1 - (Itga5+Itgb1)
Spp1 - (Itgav+Itgb5)
Spp1 - (Itga9+Itgb1)
Spp1 - (Itgav+Itgb3)
Relative contribution

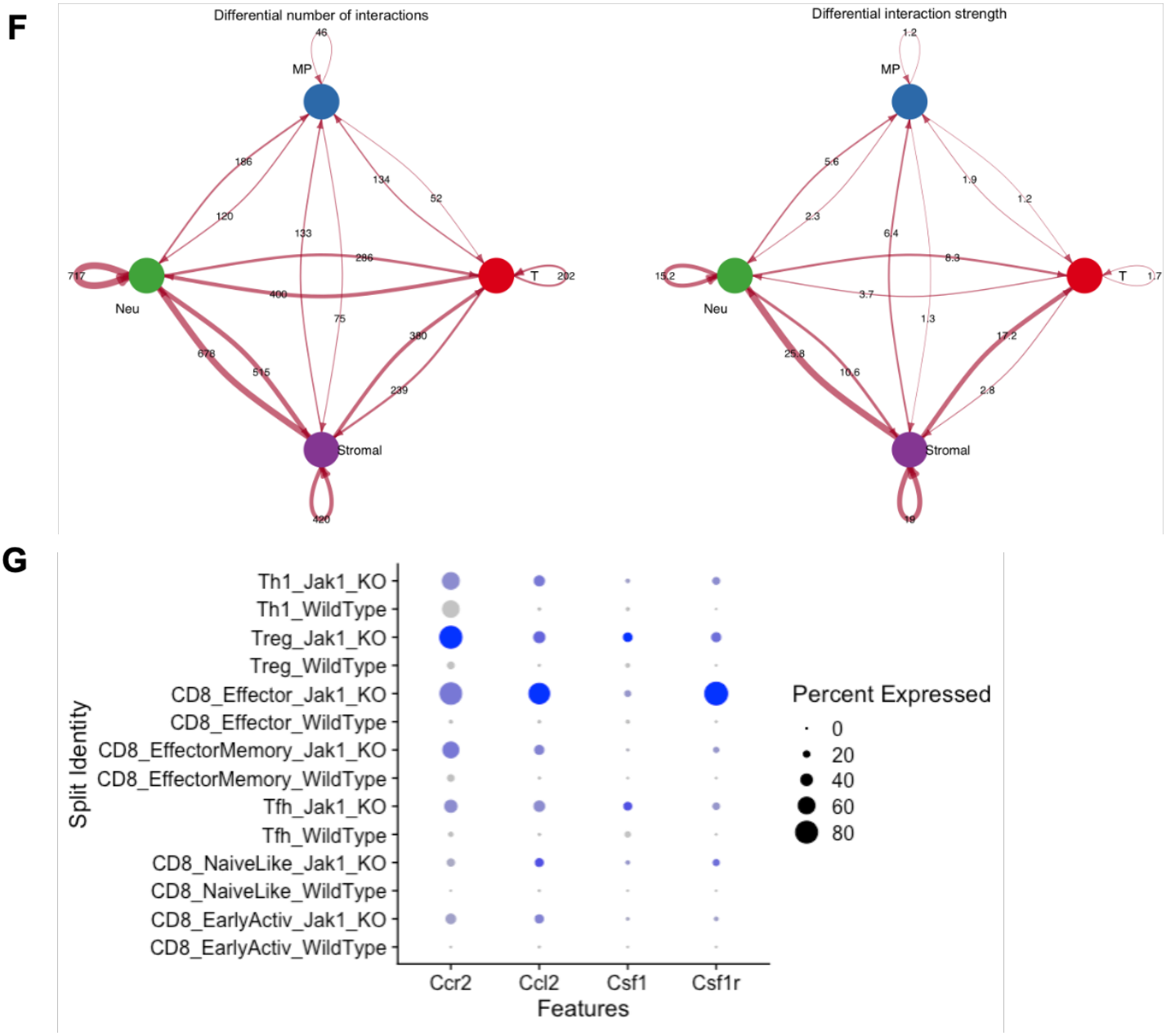

Figure 11. A and B. CellChat interaction likelihood analysis for laminin and collagen networks in the TME of YUMM-JAK1/KO tumors compared to YUMM-WT. Thickness of arrows represents interaction likelihood between populations. **C.** CellChat analysis of differential SPP-1 receptor-ligand interaction in YUMM JAK1/KO compared to YUMM WT post mIL13 CAR T cell therapy. **D and E.** Enhanced SPP-1 expression in YUMM JAK1/KO compared to YUMM WT post mIL13 CAR T cell therapy. **F and G.** Inferred enhanced receptor-ligand interactions between fibroblasts and regulatory and exhausted T cells in YUMM-JAK1/KO tumors compared to YUMM-WT.

To comprehensively analyze the protein-level phenotypes of tumor immune cell infiltrates and identify immune-related factors contributing to the resistance of JAK1/KO tumors to CAR T cell therapy, similar to the previous experiment, size-matched YUMM JAK1/KO and YUMM WT tumors were dissociated three days after CAR T cell treatment and were enriched for CD45+ cells and subjected to Cytometry by Time-of-flight analysis (CyTOF). All immune cell lineages were identified and characterized using a panel of 33 markers **(Figure 12. A-C)**. CyTOF analysis identified significantly decreased naïve, and early activate T cells in YUMM JAK1/KO tumors **(Figure 12. D and E)**. Further, YUMM JAK1/KO tumors revealed more exhausted T cells, regulatory T cells, myeloid derived MDSCs, and granulocyte derived MDSCs which, in total, were in favor of immune suppressive microenvironment in treated YUMM JAK1/KO tumors compared to YUMM-WT tumors **(Figure 12. F and G)**.

A

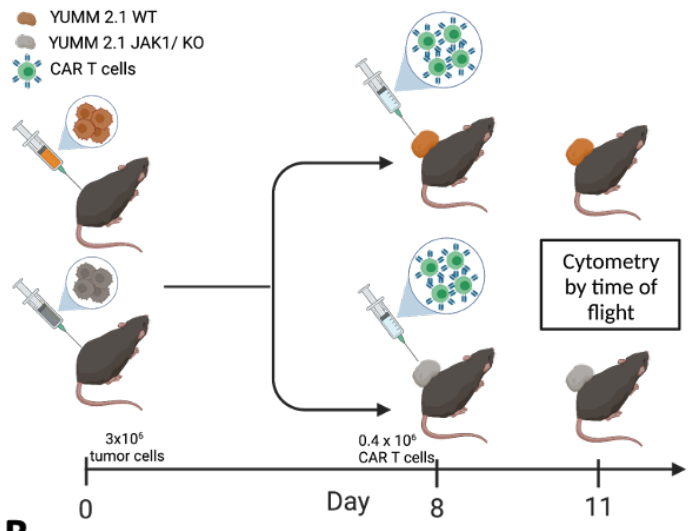
YUMM 2.1 WT
YUMM 2.1 JAK1/ KO
CAR T cells
Cytometry by time of flight
3x10⁵ tumor cells
0.4 x 10⁶ CAR T cells
0
Day
8
11

B

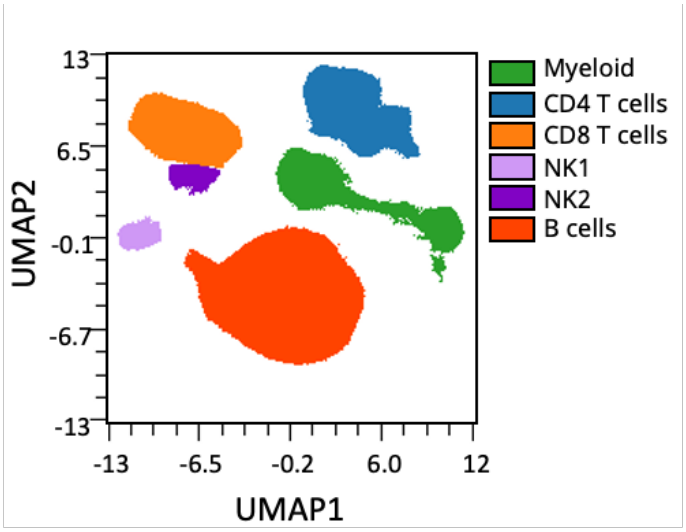
Myeloid
CD4 T cells
CD8 T cells
NK1
NK2
B cells
UMAP1
UMAP2
13
6.5
-0.1
-6.7
-13
-13
-6.5
-0.2
6.0
12

C

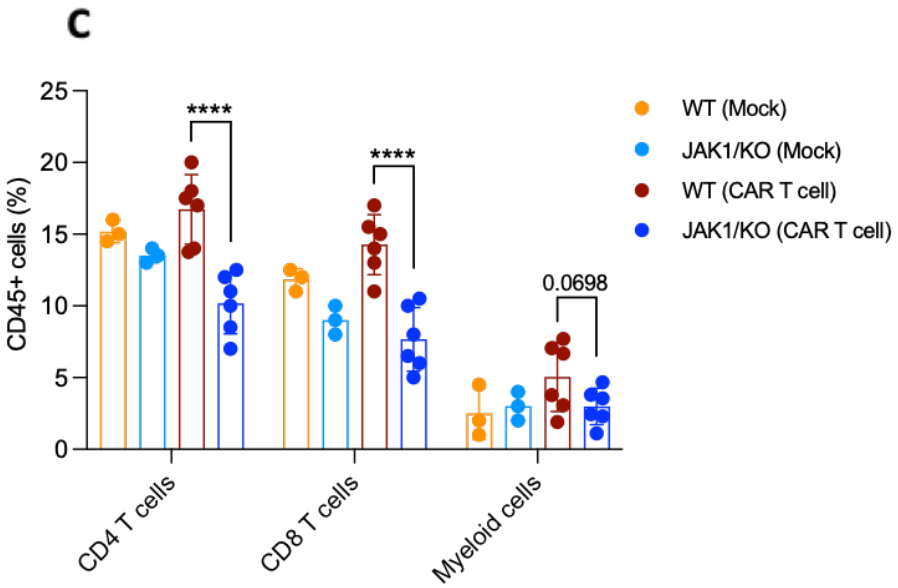
WT (Mock)
JAK1/KO (Mock)
WT (CAR T cell)
JAK1/KO (CAR T cell)
CD45+ cells (%)
25
20
15
10
5
0
****
****
0.0698
CD4 T cells
CD8 T cells
Myeloid cells

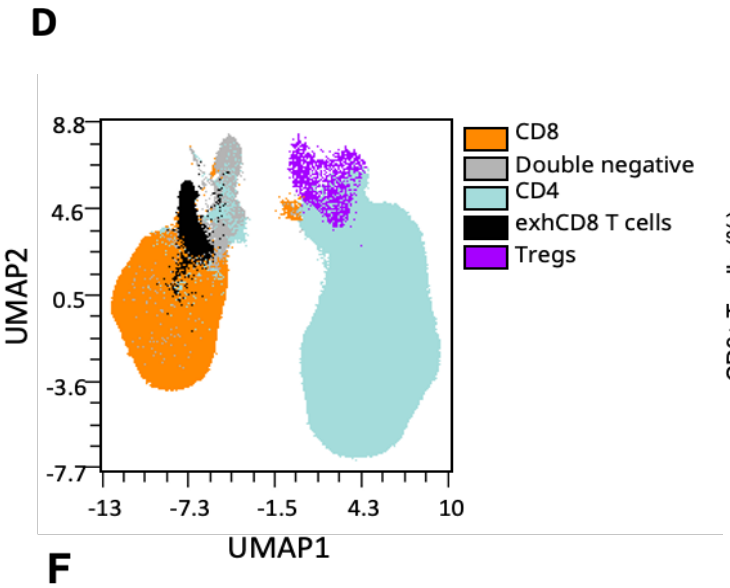

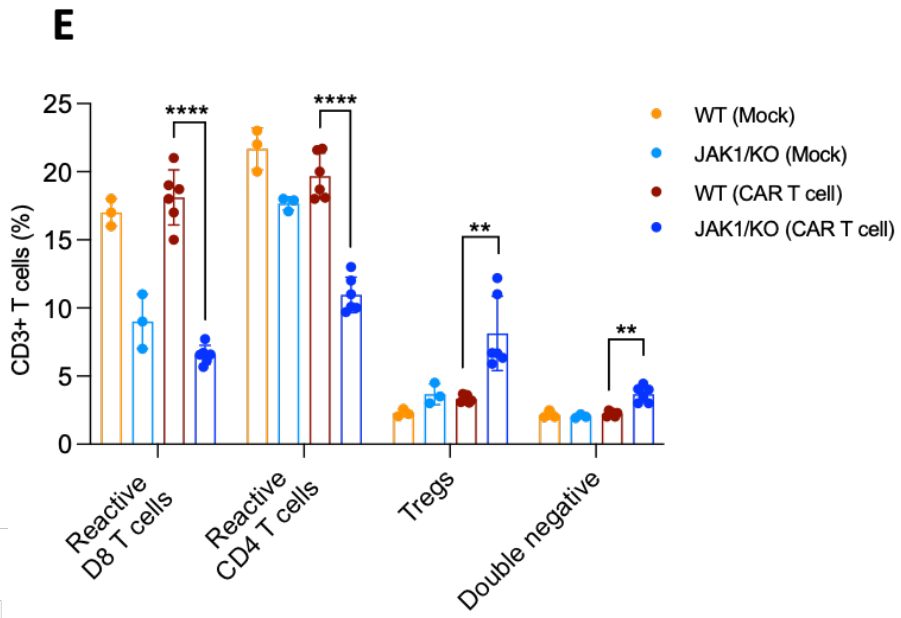

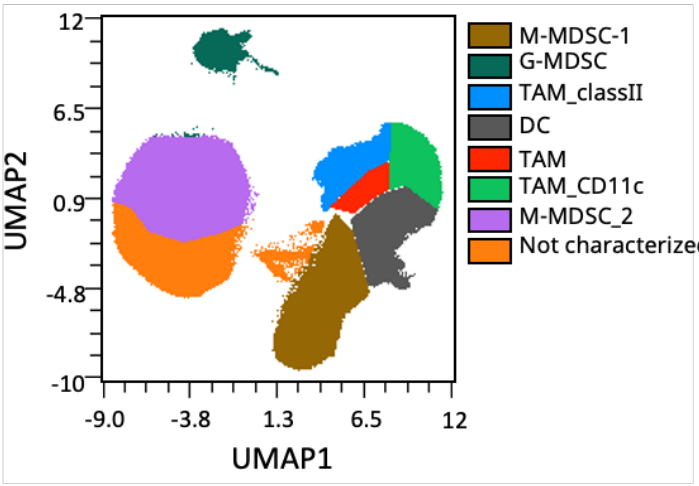

Figure 12. A. Illustrative scheme depicting the experimental procedure where dissociated tumors were enriched for CD45+ cells and subjected to CyTOF following mIL13 CAR T cell therapy. **B and C**. UMAP analysis of CD45+ cell subclusters. **D and E.** UMAP analysis of T cell subclusters in JAK1/KO and WT tumors post mIL13 CAR T cell therapy. **F-H.** UMAP analysis of myeloid cells subclusters in JAK1/KO and WT tumors post mIL13 CAR T cell therapy.

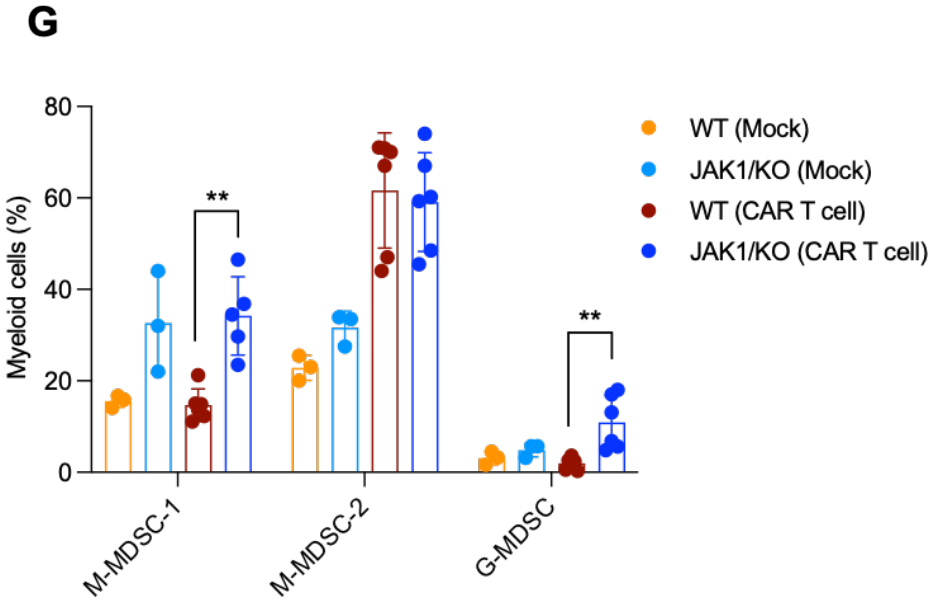

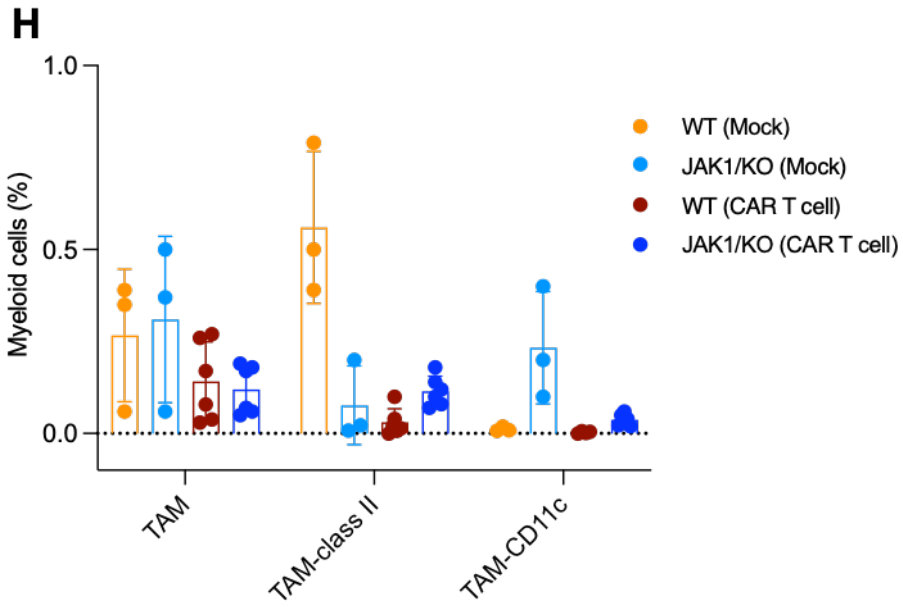

In order to assess the impact of ICAM-1 overexpression on the overall effectiveness of CAR T cell therapy in vivo, we created YUMM WT and JAK1/KO sublines with engineered ICAM-1 overexpression. These sublines were then injected into animal models and treated with mIL13CAR. Our findings indicate that there was no discernible difference in the response to CAR T cell therapy between the overexpressing and non-overexpressing cell lines. These results emphasize the immune regulatory effects of tumor intrinsic JAK1 signaling, which appears to outcompete the enhanced tumor cell-CAR T cell interaction, thereby contributing to resistance against CAR T cell therapy **(Figure 13. A-C)**.

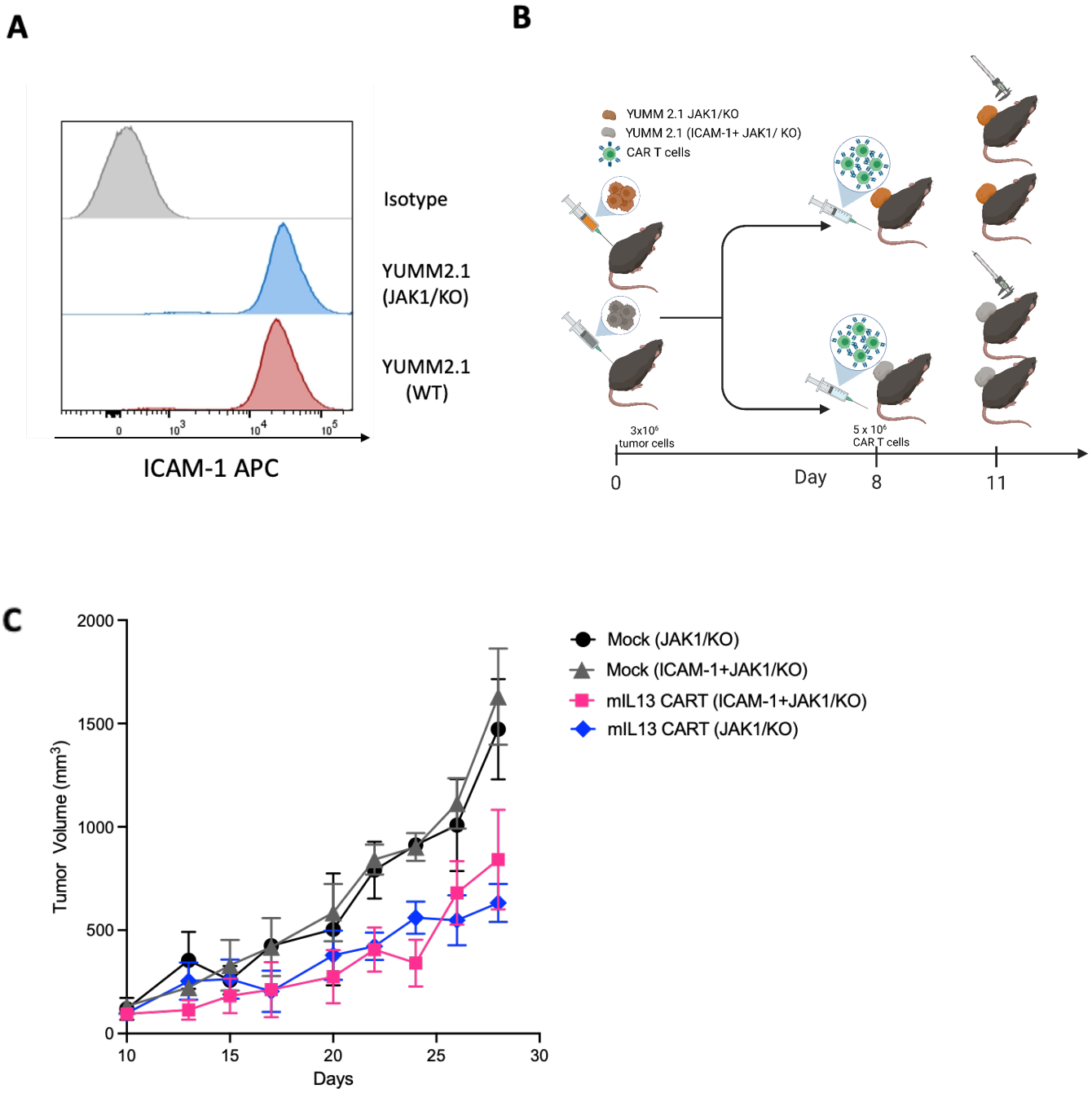

Figure 13. A. Overexpression of ICAM-1 in JAK1/KO and WT YUMM tumor cells verified by flow cytometry. **B.** Illustrative scheme representing the treatment of JAK1/KO and ICAM-1+JAK1/KO tumors with mIL13 CAR T cells. **C.** Survival analysis of ICAM-1 overexpressing YUMM JAK1/KO tumors compared to non overexpressing ICAM-1 YUMM JAK1/KO tumors in response to mIL13 CAR T cell therapy.

In our pursuit to gain a deeper understanding of the IFN-mediated resistance mechanism to CAR T cell therapies, we delved deeper into the IFN-associated differential gene expression in YUMM JAK1/KO cells compared to YUMM-WT cells treated with supernatants from CAR T cells cocultured with WT tumors **(Figure 4. A and B).** Our analysis revealed a notable down-regulation of IFN stimulating gene-15 (ISG-15) in YUMM JAK1/KO cells compared to YUMM-WT cells **(Figure 14. A)**. ISG-15 is known to be involved in propagating the effects of IFN stimulation and plays a role in antiviral immunity. However, the specific role of ISG-15, particularly unconjugated ISG-15, in theTME and its modulation of the response to CAR T cell therapy has not been well characterized.

In light of these findings, we investigated the combination of unconjugated ISG-15 with CAR T cell therapy in the treatment of YUMM and MC38 (WT and JAK1/KO) tumors. Our data revealed that the combination therapy resulted in a significant reduction in tumor size, whereas treatment with CAR T cells alone led to minimal changes in tumor size. This suggests that the addition of unconjugated ISG-15 enhances the therapeutic response of CAR T cells and overcomes the resistance observed in YUMM JAK1/KO tumors **(Figure 14. B-E)**. Next, we conducted flow cytometric analysis on unconjugated ISG-15 and mIL13 CAR T cell-treated tumors, comparing them to mIL13 CAR T cell-only treated tumors. Our analysis revealed an increased presence of T cells in the combination treatment group, demonstrating enhanced T cell infiltration compared to the control group **(Figure 14. F)**. In order to gain a deeper understanding of the immune modulatory effects of unconjugated ISG-15 on enhancing the efficacy of mIL13-CAR T cells against YUMM tumors, RNA extraction was performed on tumors treated with the combination therapy as well as tumors treated with each therapy individually. The extracted RNA samples will be analyzed and characterized to elucidate the underlying mechanisms and molecular changes associated with the combined treatment approach.

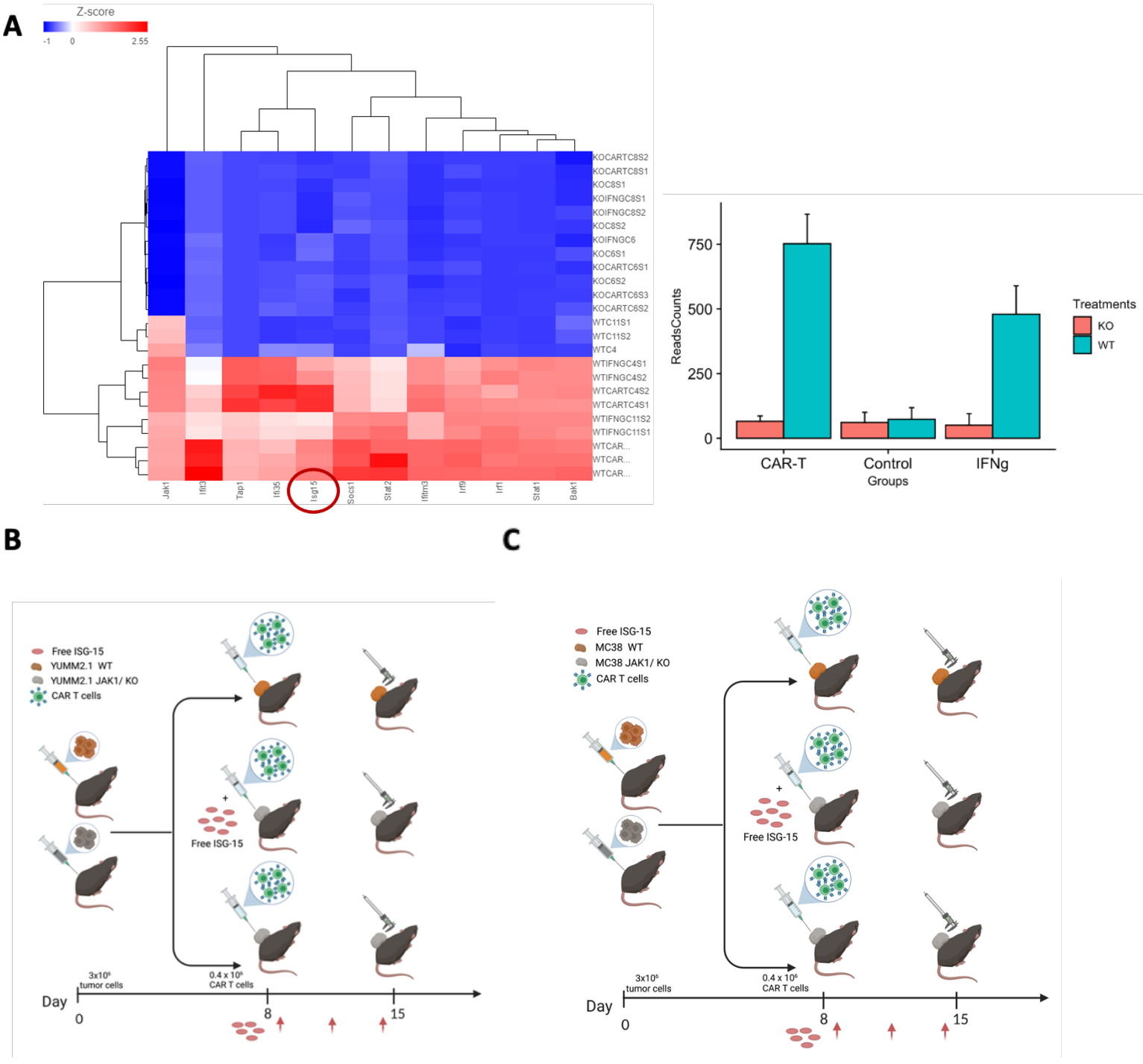
A
Z-score
-1
0
2.55
KOCARTC8S2
KOCARTC8S1
KOC8S1
KOIFNGC8S1
KOIFNGC8S2
KOC8S2
KOIFNGC6
KOC6S1
KOCARTC6S1
KOC6S2
KOCARTC6S3
KOCARTC6S2
WTC11S1
WTC11S2
WTC4
WTIFNGC4S1
WTIFNGC4S2
WTCARTC4S2
WTCARTC4S1
WTIFNGC11S2
WTIFNGC11S1
WTCAR...
WTCAR...
WTCAR...
Jak1
Ifit3
Tap1
Ifi35
Isgf15
Socs1
Stat2
Ifitm3
Irf9
Irf1
Stat1
Bak1
ReadsCounts
750
500
250
0
CAR-T
Control
IFNg
Groups
Treatments
KO
WT
B
Free ISG-15
YUMM2.1 WT
YUMM2.1 JAK1/ KO
CAR T cells
Free ISG-15
3x10⁶ tumor cells
0.4 x 10⁶ CAR T cells
Day
0
8
15
C
Free ISG-15
MC38 WT
MC38 JAK1/ KO
CAR T cells
Free ISG-15
3x10⁶ tumor cells
0.4 x 10⁶ CAR T cells
Day
0
8
15

D

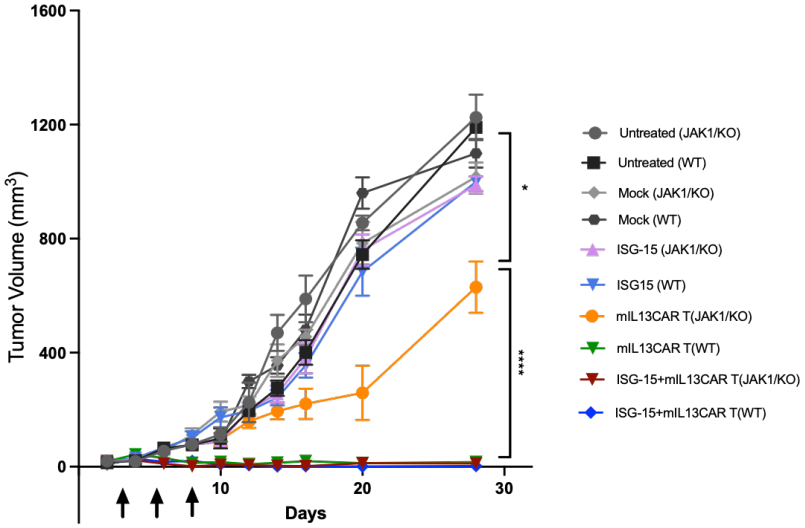
Tumor Volume (mm3)
1600
1200
800
400
0
10
20
30
Days
*
****
Untreated (JAK1/KO)
Untreated (WT)
Mock (JAK1/KO)
Mock (WT)
ISG-15 (JAK1/KO)
ISG15 (WT)
mIL13CAR T(JAK1/KO)
mIL13CAR T(WT)
ISG-15+mIL13CAR T(JAK1/KO)
ISG-15+mIL13CAR T(WT)

E

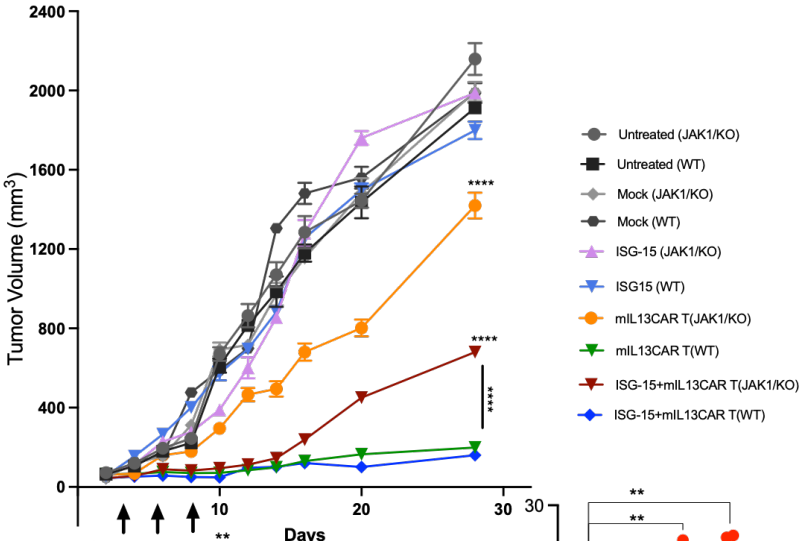
Tumor Volume (mm3)
2400
2000
1600
1200
800
400
0
10
20
30
Days
****
****
****
Untreated (JAK1/KO)
Untreated (WT)
Mock (JAK1/KO)
Mock (WT)
ISG-15 (JAK1/KO)
ISG15 (WT)
mIL13CAR T(JAK1/KO)
mIL13CAR T(WT)
ISG-15+mIL13CAR T(JAK1/KO)
ISG-15+mIL13CAR T(WT)

F

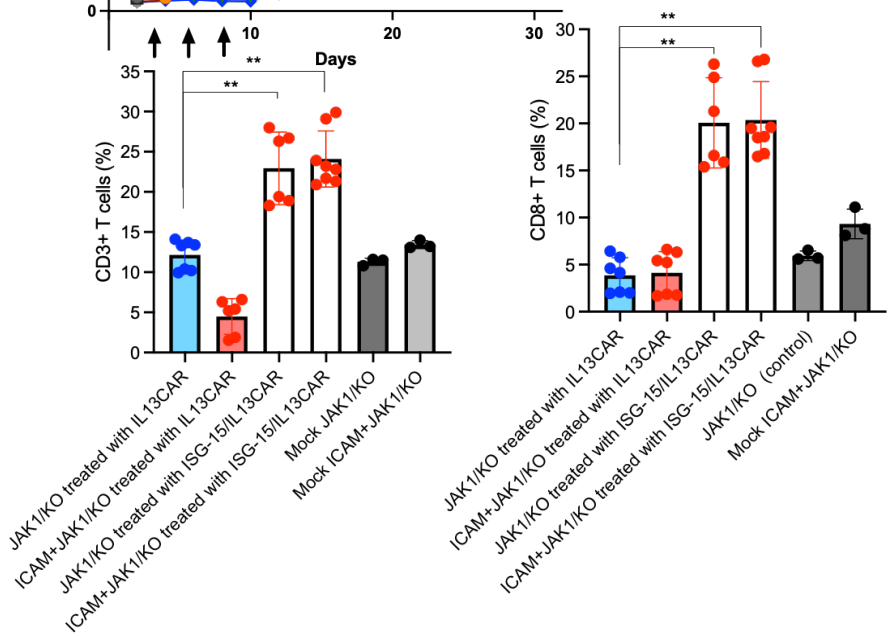
CD3+ T cells (%)
**
**
JAK1/KO treated with IL13CAR
ICAM+JAK1/KO treated with IL13CAR
JAK1/KO treated with ISG-15/IL13CAR
ICAM+JAK1/KO treated with ISG-15/IL13CAR
Mock JAK1/KO
Mock ICAM+JAK1/KO
CD8+ T cells (%)
**
**
JAK1/KO treated with IL13CAR
ICAM+JAK1/KO treated with IL13CAR
JAK1/KO treated with ISG-15/IL13CAR
ICAM+JAK1/KO treated with ISG-15/IL13CAR
JAK1/KO (control)
Mock ICAM+JAK1/KO

Figure 14. A. RNA sequencing analysis revealed the downregulation of ISG-15 in JAK1/KO tumor cells (blue) compared to WT cells (orange) following treatment with CAR T cell-mediated cytotoxicity supernatants. **B and C.** Illustrative scheme representing the combination therapy involving mIL13CAR and unconjugated ISG15 against YUMM and MC38 WT and associated JAK1/KO sublines. **D.** Survival analysis of combinatorial approach using mIL13CAR and unconjugated ISG15 compared to mIL13 CAR T cell and unconjugated ISG-15 treated arm against YUMM sublines. **E.** Survival analysis of combinatorial approach using mIL13CAR and unconjugated ISG15 compared to mIL13 CAR T cell and unconjugated ISG-15 treated arm against MC38 sublines. **F.** Flow cytometric analysis of CD3 and CD8 T cells recruited in tumors following treatment with a combination of mIL13CAR and unconjugated ISG15, in comparison to the arms treated with mIL13 CAR T cells and unconjugated ISG-15.

The existing literature, along with our recent findings **(Figure 11. A-G)**, emphasizes the significant role of osteopontin (OPN) (SPP1) expression in various cells within TME, contributing to its suppressive growth characteristics. In our study, we employed a monoclonal antibody against OPN (100D3 mAb, BioXCell) as a neoadjuvant approach prior to administering mIL13 CAR T cells to disrupt its binding to other immune components present in the TME . Our results highlight the potential of OPN neutralization monoclonal antibody as an effective strategy to target OPN and prime the TME of suppressive tumors, ultimately enhancing the efficacy of mIL13 CAR T cells **(Figure 15)**. To gain further insights into the underlying mechanisms of this therapeutic effect, we will run transcriptomics analysis on RNAs collected from treated samples with anti-OPN mAb alone, a combination of OPN mAb and mIL13 CAR T cells, as well as controls. This approach holds promise in alleviating the immunosuppressive TME environment and significantly improving therapeutic outcomes in resistant solid tumors with suppressive niche to CAR T cell therapies.

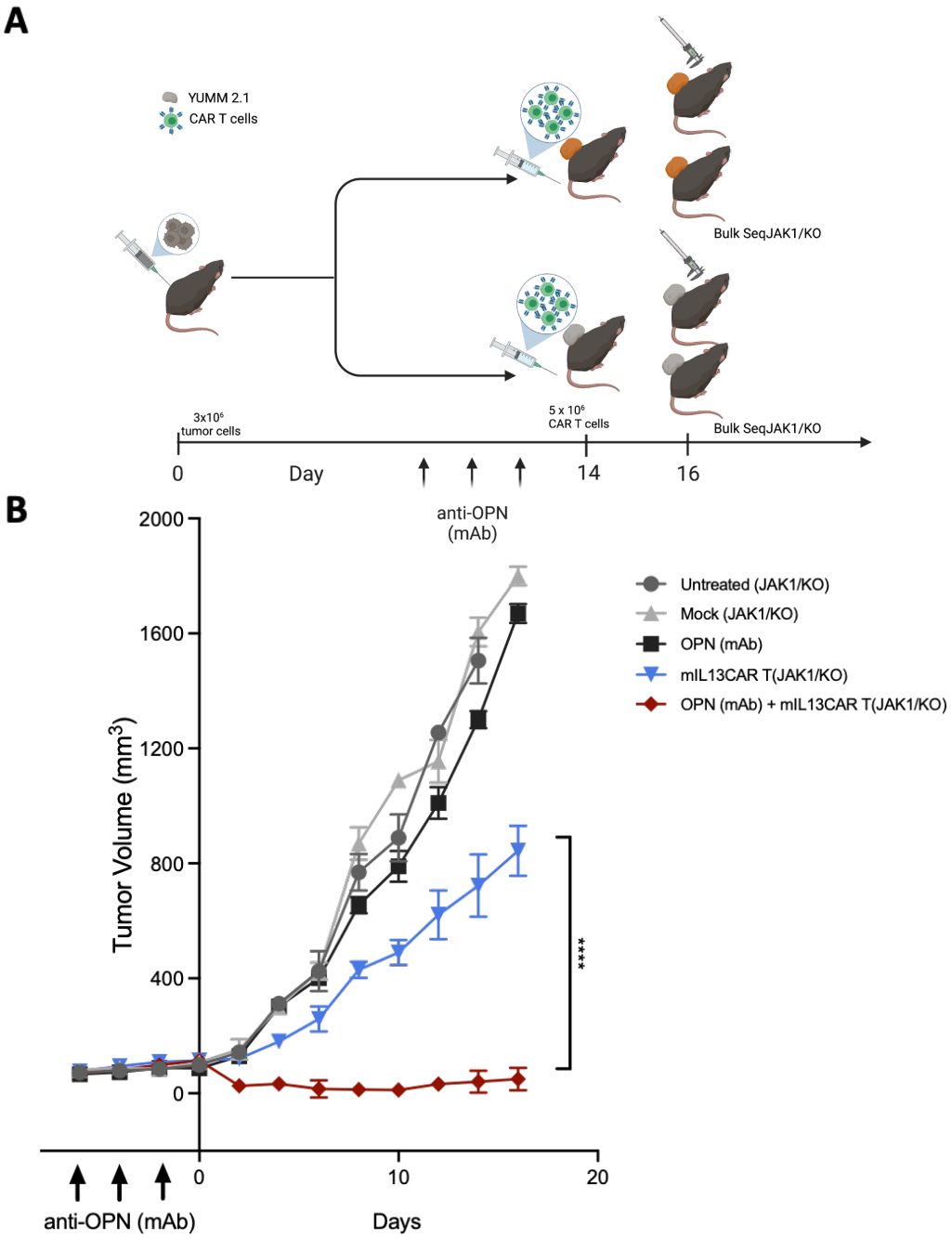

Figure 15. A. Illustrative scheme depicting the experimental design priming YUMM JAK1/KO tumors with anti-OPN mAb prior to administering mIL13-CAR T cells. **B.** Survival analysis of the efficacy of combination of anti-OPN mAb and mIL13-CAR T cells against YUMM JAK1/KO compared to individual treatments.

METHODS

Murine tumor lines preparation for in vitro and in vivo studies

The YUMM2.1, MC38, and associated JAK1/KO murine tumor sublines were initially established in the laboratory of Dr. Antoni Ribas. The YUMM2.1 and MC38 sublines, both WT and JAK1/KO, were transduced with lentivirus to generate sublines expressing murine IL13Rα2 (mIL13Rα2). These tumor cell lines were cultured in DMEM (Gibco) supplemented with 10% FBS (Hyclone Laboratories), 25 mmol/L HEPES (Irvine Scientific), and 2 mmol/L l-glutamine (Lonza). The expression of mIL13Rα2 on the cell surface was verified and confirmed by flow cytometry. These culture conditions were maintained to support optimal growth and viability of the cells. The cells were maintained under appropriate conditions and regularly tested for the absence of Mycoplasma contamination and were tested for authentication.

Surface Flow Cytometry Analysis of PD-L1 and MHC Class I

Murine tumor lines (YUMM2.1 sublines and MC38 sublines) were seeded into 6-well plates to reach 70%–80% confluence on the day of surface staining. On the following day, the culture media were replaced with fresh media containing IFNγ (100 ng/mL) for an 18-hour incubation. On day 3, after the incubation period, the cells were trypsinized and incubated at 37°C for 2 hours in media containing the same concentrations of IFNγ. The media were then removed by centrifugation, and the cells were resuspended in 100% FBS and stained with PE anti–PD-L1 and APC anti–MHC I for mouse cell lines.

The staining was performed on ice for 30 minutes. Subsequently, the cells were washed once with 3 mL PBS and resuspended in 300 μL of PBS. Each cell line was subjected to these experiments in multiple replicates and at least two separate experiments.

ICAM-1 engineering of the tumor cells

The plasmid containing the ICAM-1 gene and the packaging plasmids were provided by VectorBuilder. The lentiviral backbone was used for the construction of the expression vector. The cells were then incubated with the lentivirus following the protocol provided by Vectorbuilder. Neomycin (Geneticin) was used for positive selection of the transduced cells. The overexpression of ICAM-1 was confirmed using flow cytometry analysis.

Murine IL13 CAR T cells

The murine IL13Rα2 CAR construct was generated using a MSCV retroviral backbone (Addgene), incorporating the extracellular murine IL13 and murine CD8 hinge, transmembrane domain, and intracellular murine 4-1BB costimulatory and CD3ζ signaling domains. A truncated murine CD19 was included as a transduction marker using a T2A ribosomal skip sequence. The resulting plasmid was transfected into PlatE cells (gift from Dr. Zuoming Sun's lab) using Fugene (Promega), and after 48 hours, the supernatant was collected, filtered, and stored until transduction.

Generation of murine CAR T cells

Murine T cells were isolated from naïve C57BL/6J mice using the EasySep Mouse T cell Isolation Kit (STEMCELL Technologies) and stimulated with Dynabead Mouse T-Activator CD3/CD28 beads (Gibco) at a 1:1 ratio. Transduction of T cells was performed on RetroNectin-coated plates (Takara Bio) using the retrovirus-containing supernatants described above. The transduced cells were then expanded for 4 days in RPMI 1640 medium (Lonza) supplemented with 10% FBS (Hyclone Laboratories), 55 mmol/L 2-mercaptoethanol (Gibco), 50 U/mL recombinant human IL2 (Novartis), and 10 ng/mL recombinant murine IL7 (PeproTech). Prior to in vitro and in vivo experiments, the beads were magnetically separated from the T cells, and CAR expression was assessed by flow cytometry.

Mass Cytometry (CyTOF) Analysis

YUMM JAK1/KO and WT tumor cells (0.3 × 10^6) were implanted into the flanks of C57BL/6 mice. On day 8 post-inoculation, tumors were harvested from mice at predefined treatment time points. Tumors were digested using the Tumor Dissociation Kit Mouse (Miltenyi Biotec). Immune cells were isolated using the CD45+ isolation kit (EasySep™ Mouse CD45 Positive Selection Kit, STEMCELL Technologies). A panel of 35 immune markers was used for analysis. Samples were analyzed using the Fluidigm Helios Mass Cytometry System at the UCLA Flow Cytometry core. Manual gating was performed using FlowJo software (version 10.4.2) to identify cells, singlets, and viable CD45+ populations. Data files were analyzed using OMIQ software. Cluster median data were normalized, and a threshold of >0.5 was used to define positive immune markers for cluster identification and annotation.

Mice and in vivo studies

C57BL/6/J mice were obtained from The Jackson Laboratory, while NSG mice were bred at City of Hope in Duarte, CA. All experimental procedures involving mice were conducted in compliance with the guidelines and regulations set by the City of Hope Institutional Animal Care and Use Committee (IACUC).

Subcutaneous tumors were established by injecting 0.3 × 106 WT or established JAK1/KO cells of YUMM and MC38 sublines expressing mIL13Ra2 into the flanks of C57BL/6 mice. Tumor growth was monitored, and when tumors became palpable (day 8 for YUMM2.1 and day 5 or 6 for MC38), 5 x 105 mIL13 CAR T cells were injected either directly into the tumor site or 5x106 mIL13 CAR T cells were administered intravenously via the tail vein after lymphodepletion with 5 Gray total body irradiation. Tumor measurements were taken using calipers two or three times per week, and tumor volume was calculated using the formula: tumor volume = [(width)2 × length]/2. The mean and standard error (SE) of tumor volumes were calculated for each group.

In vivo studies using monoclonal anti-mouse osteopontin (OPN mAb)

On the eighth day after the inoculation of YUMM WT and JAK1/KO tumors inC57BL/6 mice, the tumor-bearing mice were administered OPN mAbs (BioXCell) intraperitoneally (at a dose of 200 μg per mouse) either as a standalone treatment or in combination with mIL13-CAR T cell therapies, with injections repeated every three days.

RNA Isolation and RNA-seq analysis

For in vitro experiments, melanoma cell lines were seeded of 1.5 × 105 cells per 6-well plate for treatment. After 24 hours, the culture media were replaced with fresh media containing IFNγ (BD Pharmingen, catalog no. 554616) or supernatant of mIL13 CAR T cells with YUMM2.1 WT tumors. Cells were harvested 8 hours after treatment. The cell pellets were lysed in TRIzol reagent (Invitrogen, catalog no. 15596018) and stored at -80°C until RNA extraction.

For in vivo experiments, engrafted tumors treated with or without mIL13, mIL13-ISG15, or mIL13-mutISG15 CAR T cells were harvested and dissociated into single cells and stored at -80°C prior to RNA extraction.

Total RNA was extracted from mouse tissues using TRIzol™ Reagent (Life Technologies) for transcriptome analyses. RNA integrity, purity, and concentration were evaluated using an Agilent 2100 Bioanalyzer (Agilent Technologies). Nanodrop and Qubit 3.0. RNA-seq libraries were constructed using KAPA mRNA HyperPrep Kit. RNA-seq was performed in the Illumina HiSeq2000 System using 51 bp single-end sequencing. High-quality reads were obtained by trimming the raw reads using fastp (v0.23.3) 1 and by carrying out FastQC (v0.11.9) for the quality control assessment. The clean reads were aligned to the mouse reference genome GRCm38 with HISAT-STRINGTIE analytic pipeline 2. The DESeq2 (v.1.26.0) framework 3 was adopted for differential expression analysis.

scRNA-seq Analysis

Raw base call files of scRNA-seq data were analyzed using CellRanger (version 5.0). The “mkfastq” command was used to generate FASTQ files and the “count” command was used to generate raw gene-barcode matrices aligned to the 10X Genomics GRCm38 reference genome (mm10). The data from all samples were combined in R (4.0.4) using the Read10X() function from the Seurat package (version

4.0.3)4 and an aggregate Seurat object was generated. Filtering was conducted by retaining cells that had unique molecular identifiers (UMIs) greater than 400, expressed 200 and 9000 genes inclusive, and had mitochondrial content less than 15 percent. No sample batch correction was performed. Data were normalized using the “LogNormalize" method and using a scale factor of 10,000. Using Seurat’s Scale.Data() function and “vars.to.regress” option UMI’s and percent mitochondrial content were used to regress out unwanted sources of variation. The number of variably expressed genes were calculated using the following criteria: normalized expression between 0.125 and 3, and a quantile-normalized variance exceeding 0.5. To reduce dimensionality of this dataset, the resulting variably expressed genes were summarized by principal component analysis (PCA), and the first 20 principle components further summarized using Uniform Manifold Approximation and Projection (UMAP) dimensionality reduction. Doublets were assessed using the DoubletFinder (version 2.0.2) 5 algorithm and few (<10%) doublets were observed outside of the cell population. Clustering was conducted with the FindClusters() function using 20 PCA components and a resolution parameter set to 0.3. Cell cycle analysis was conducted using the CellCycleScoring() in Seurat package with a list of cell cycle markers from Aviv Regev et al’s study.

a.Gene markers and pathway analysis

Differentially expressed genes among clusters and treatments were identified with logFC greater than 0.25 (adjusted $P < 0.05$) as determined in Wilcoxon rank-sum test from Seurat. The markers for different cell types were retrieved from the CellMarker database, which is a manually curated resource of cell markers in human and mouse. The pathway analysis was done using Gene Ontology and canonical pathways in enrichr 8, with adjusted $P < 0.05$ as the cutoff for statistically differential pathways.

b.Inference of cell-cell communication

Cell–cell interactions based on the expression of known ligand–receptor pairs in different cell types were inferred using CellChatDB67 (v.1.0.0). The total counts of interactions and interaction strengths were calculated using the compareInteractions function in CellChat. The differential edge list was passed through CircosDiff (a wrapper around the R package 'circlize') and netVisual_chord_gene in CellChat to filter receptor ligand edges and generate Circos plots.

scRNA-seq Analysis

Raw base call files of scRNA-seq data were analyzed using CellRanger (version 5.0). The "mkfastq" command was used to generate FASTQ files and the "count" command was used to generate raw gene-barcode matrices aligned to the 10X Genomics GRCm38 reference genome (mm10). The data from all samples were combined in R (4.0.4) using the Read10X() function from the Seurat package (version 4.0.3)1 and an aggregate Seurat object was generated. Filtering was conducted by retaining cells that had unique molecular identifiers (UMIs) greater than 400, expressed 200 and 9000 genes inclusive, and had mitochondrial content less than 15 percent. No sample batch correction was performed. Data were normalized using the "LogNormalize" method and using a scale factor of 10,000. Using Seurat's Scale.Data() function and "vars.to.regress" option UMI's and percent mitochondrial content were used to regress out unwanted sources of variation. The number of variably expressed genes were calculated using the following criteria: normalized expression between 0.125 and 3, and a quantile-normalized variance exceeding 0.5. To reduce dimensionality of this dataset, the resulting variably expressed genes were summarized by principal component analysis (PCA), and the first 20 principle components further summarized using Uniform Manifold Approximation and Projection (UMAP) dimensionality reduction. Doublets were assessed using the DoubletFinder (version 2.0.2) 2 algorithm and few (<10%) doublets were observed outside of the cell population. Clustering was conducted with the FindClusters() function

using 20 PCA components and a resolution parameter set to 0.3. Cell cycle analysis was conducted using the CellCycleScoring() in Seurat package with a list of cell cycle markers from Aviv Regev et al's study 3.

Gene markers and pathway analysis

Differentially expressed genes among clusters and treatments were identified with logFC greater than 0.25 (adjusted $P < 0.05$) as determined in Wilcoxon rank-sum test from Seurat. The markers for different cell types were retrieved from the CellMarker database, which is a manually curated resource of cell markers in human and mouse 4. The pathway analysis was done using Gene Ontology and canonical pathways in enrich 5, with adjusted $P < 0.05$ as the cutoff for statistically differential pathways.

Inference of cell-cell communication

Cell–cell interactions based on the expression of known ligand–receptor pairs in different cell types were inferred using CellChatDB67 (v.1.0.0) 6. The total counts of interactions and interaction strengths were calculated using the compareInteractions function in CellChat. The differential edge list was passed through CircosDiff (a wrapper around the R package 'circlize') and netVisual_chord_gene in CellChat to filter receptor ligand edges and generate Circos plots.

Statistical analysis

Statistical analysis was performed using GraphPad Prism software (v5). Student's t-test was used for two-group comparisons, while one-way ANOVA with a Bonferroni post hoc test was used for comparisons involving three or more groups. Kaplan-Meier survival curves were generated, and statistical significance

was assessed using the log-rank (Mantel-Cox) test. The significance levels were indicated as follows: *, P < 0.05; **, P < 0.01; ***, P < 0.001; ****, P < 0.0001.

Chapter 3

NAVIGATING THE COMPLEX TUMOR MICROENVIRONMENT OF GLIOBLASTOMA MULTIFORME: INSIGHTS FROM INTERFERON SIGNALING DEFICIENT TUMORS IN RESPONSE TO CAR T CELL THERAPIES

In our investigation, we initially focused on preclinical data from YUMM JAK1/KO tumors, which have demonstrated resistance to CAR T cell therapies. This observation prompted our study on patients with GBM who were undergoing CAR T cell therapy as part of an IL13Ra2 clinical trial. It is noteworthy that CAR T cell therapies have shown limited effectiveness in GBM, with only a small subset of patients experiencing improvements.

Analyzing the cells derived from the patient samples, we identified 13 distinct populations with a significant population of myeloid and fibroblast cells. These populations likely represent different cell types or functional states, and further investigations are necessary to characterize these populations more precisely. Fibroblasts are identified by COL1A1, PDGFRB, ACTA2, SPRY1, CALD1, and LRRC15 **(Figure 1)**. In our analysis, we identified several distinct populations of myeloid cells within the glioblastoma (GBM) samples. Intriguingly, we observed a consistent pattern of high expression for the genes SPP1, C1QA, C1QC, and APOE in the GBM samples, similar to what we observed in our JAK1/KO model. These findings imply a potential shared expression pattern for these genes across different tumor types, suggesting their involvement in the formation of suppressive microenvironments within tumors **(Figure 2).**

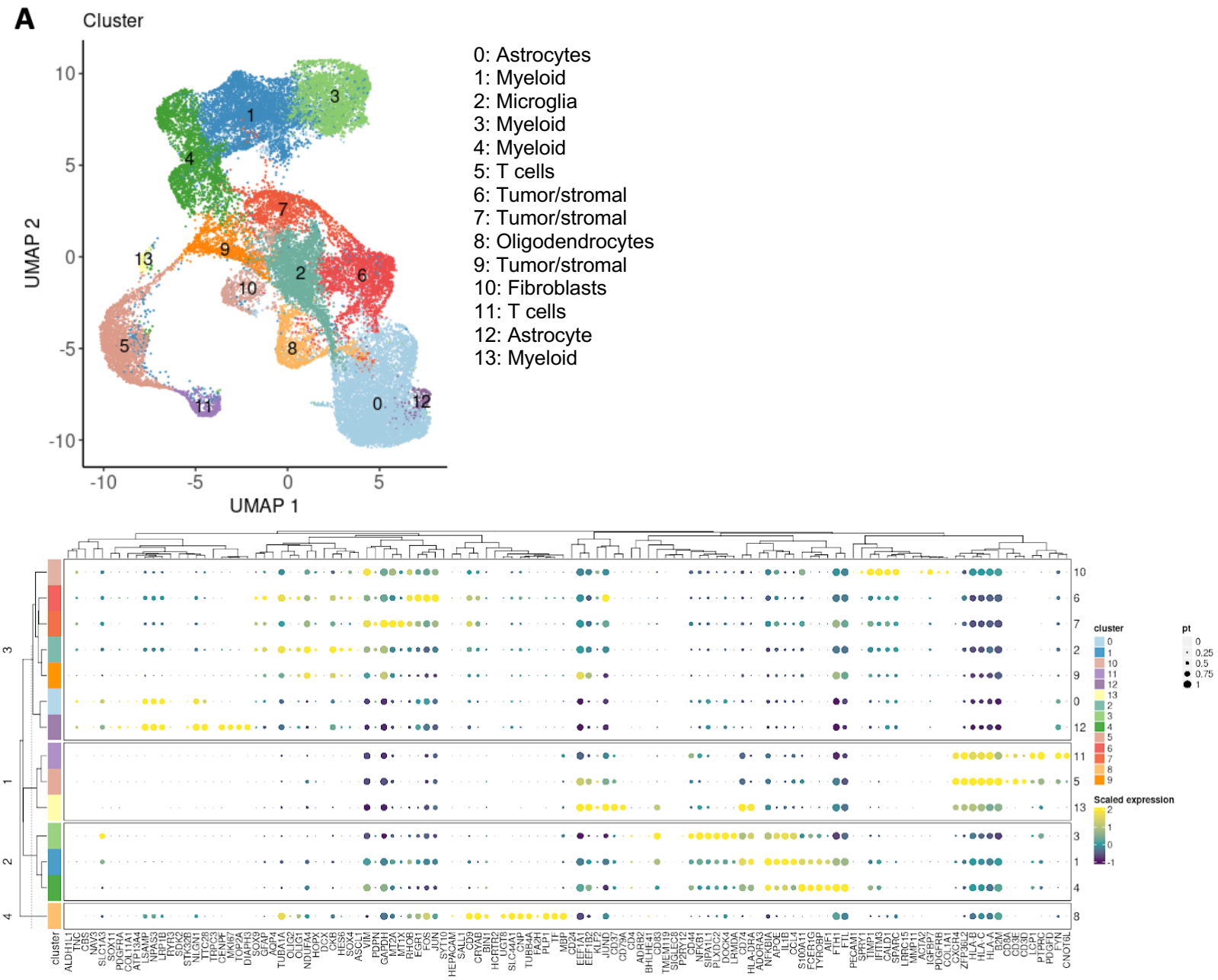

Figure 1. A. Representative UMAP analysis of 32 GBM patients recruited to IL13Ra2 CAR T cell therapy trial. Characterization of cells from patients revealed fibroblasts and multiple myeloid cell populations in the UMAP.

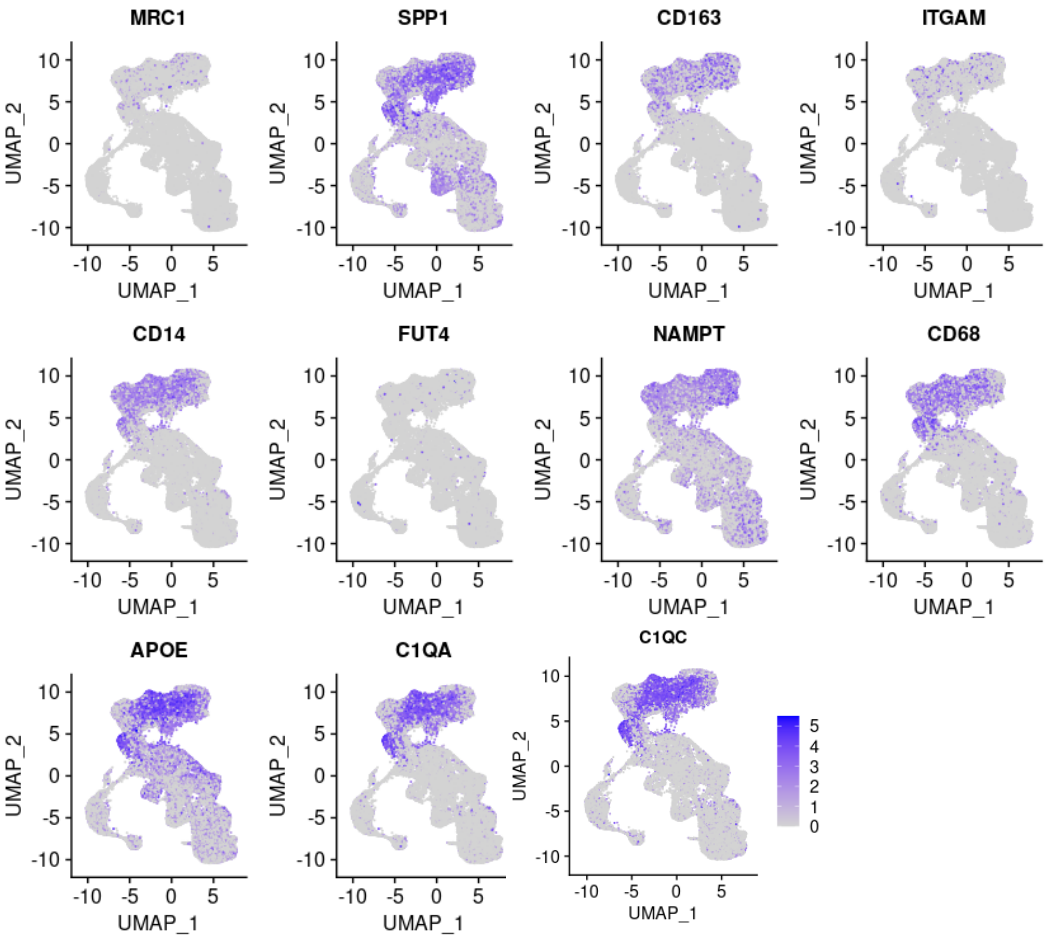

Figure 2. A. UMAP projection of myeloid cells in 32 GBM patients. Upregulation of SPP1, APOE, C1QA, and C1QC across myeloid subpopulations.

We further categorized the patients based on their response to CAR T cell therapy, distinguishing between progressive disease (PD), complete response (CR), and stable disease[62]. Additionally, we evaluated the presence of recruited T cells at the tumor site, stratifying them into two groups: CD3 high and CD3 low.

Continuing our analysis, we focused on assessing the IFN signaling-associated genes specifically in tumor cells from patients with PD compared to those with SD/CR. Interestingly, we observed a noticeable lower expression of IFN-associated genes in the tumor cells of PD patients when compared to those with CR, suggesting potential differences in the IFN signaling pathway between these disease states**(Figure 3)**.

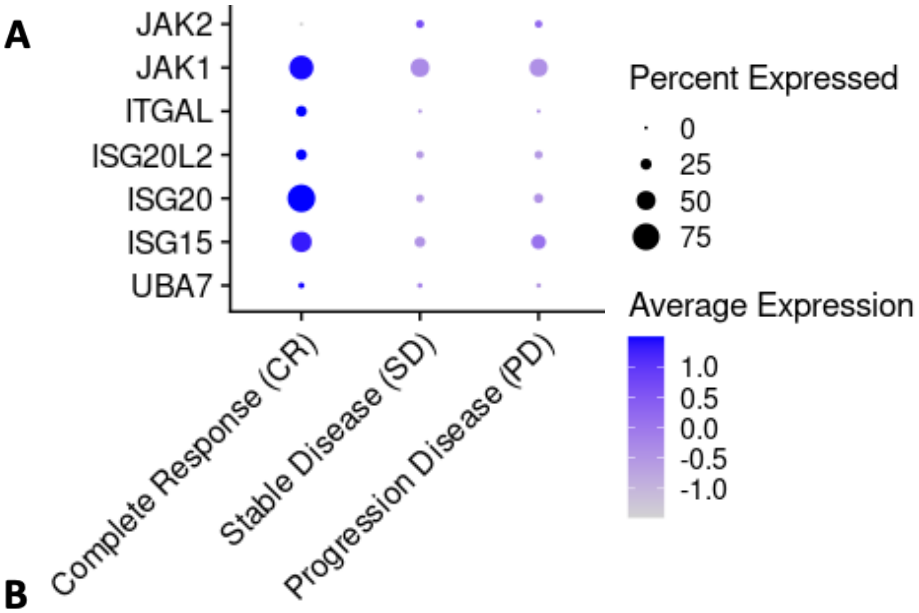
A
JAK2
JAK1
ITGAL
ISG20L2
ISG20
ISG15
UBA7
Complete Response (CR)
Stable Disease (SD)
Progression Disease (PD)
Percent Expressed
0
25
50
75
Average Expression
1.0
0.5
0.0
-0.5
-1.0

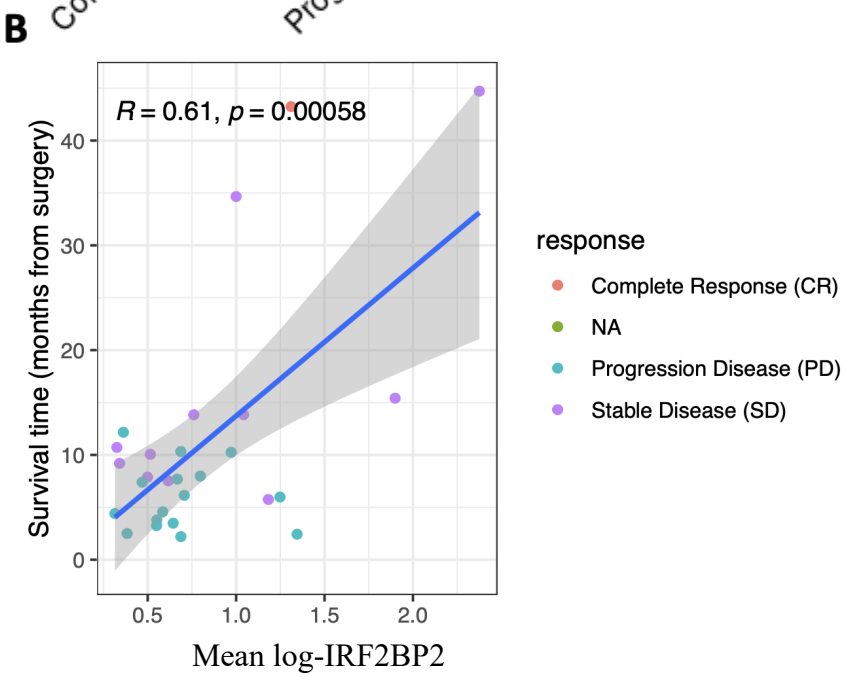
B
R = 0.61, p = 0.00058
Survival time (months from surgery)
0
10
20
30
40
0.5
1.0
1.5
2.0
Mean log-IRF2BP2
response
Complete Response (CR)
NA
Progression Disease (PD)
Stable Disease (SD)

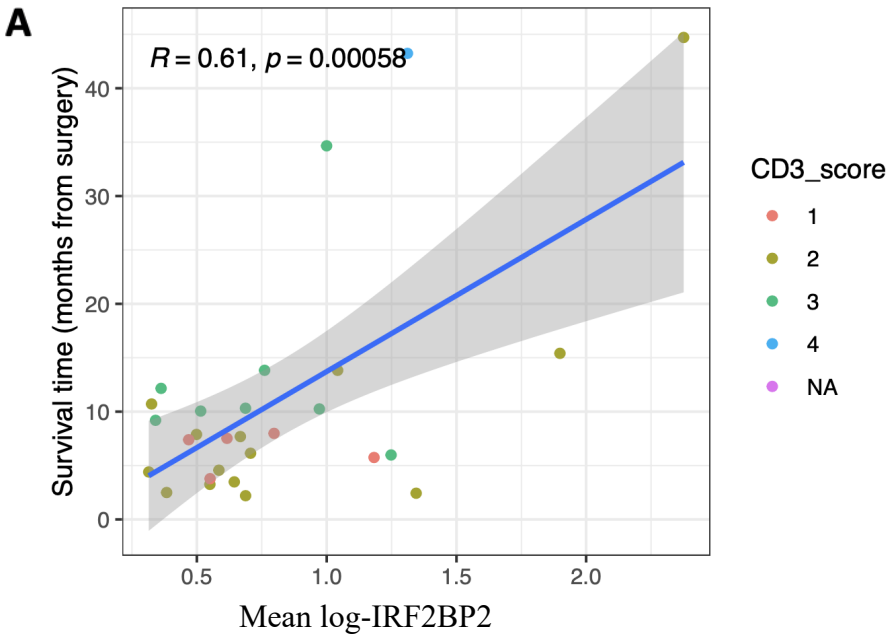

Figure 3. **A**.Expression pattern of IFN signaling associated genes in CR, SD and PD. Higher expression of JAK1, JAK2 and interferon associated genes are observed in the CR group. Direct correlation between IRF2BP2 expression and survival time and CD3 score in patients with GBM.

We employed CellChat analysis to investigate the outgoing and incoming signals within different cell populations in patients with CR/SD compared to those with PD. Additionally, we examined the signaling differences between CD3 high and CD3 low patients. Similar to our JAK1/KO model, Visfatin and SPP1 signaling is upregulated in the fibroblast population of the PD group compared to CR/SD **(Figure 4)**. Upregulated SPP-1 and associated receptors were observed in PD compared to CR/SD.

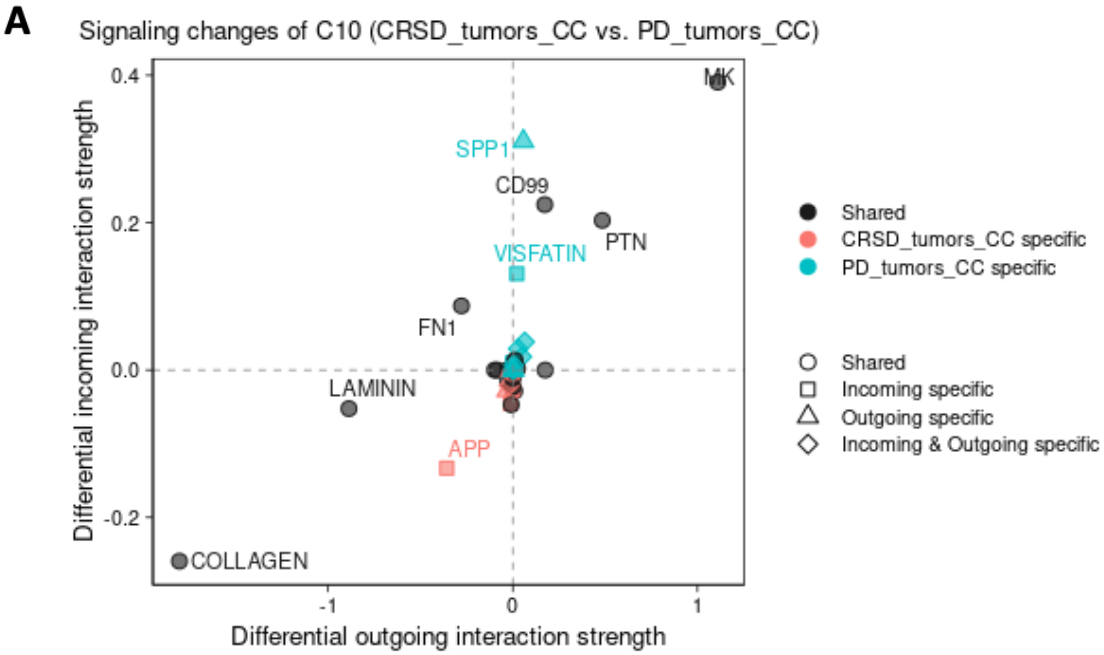

Figure 4. **A**. Inferred signaling analysis using CellChat reveals higher outgoing and incoming signals for SPP1 and visfatin in PD compared to CR/SD.

In order to examine the distribution of fibroblasts and SPP-1+ myeloid cells within the TME of GBM patients with PD compared to those withCR/SD, we performed immunofluorescence (IF) staining analysis. Specifically, we evaluated the expression of COL1A1, SPP1, and CD68 in a PD patient cohort in comparison to CR/SD patients.

Our analysis revealed a higher expression of COL1A1, which serves as a marker for the fibroblast population, in the PD group as compared to patients with a relatively better treatment response.

Additionally, we observed an increased expression of SPP1+ cells in close association with CD68+ myeloid cells in the PD group.

These findings provide insights into the differential distribution and expression of fibroblasts and SPP-1+ myeloid cells within the TME of GBM patients with progressive disease. Understanding the role of these cell populations in the context of treatment response may contribute to the development of more targeted therapeutic strategies for GBM patients.

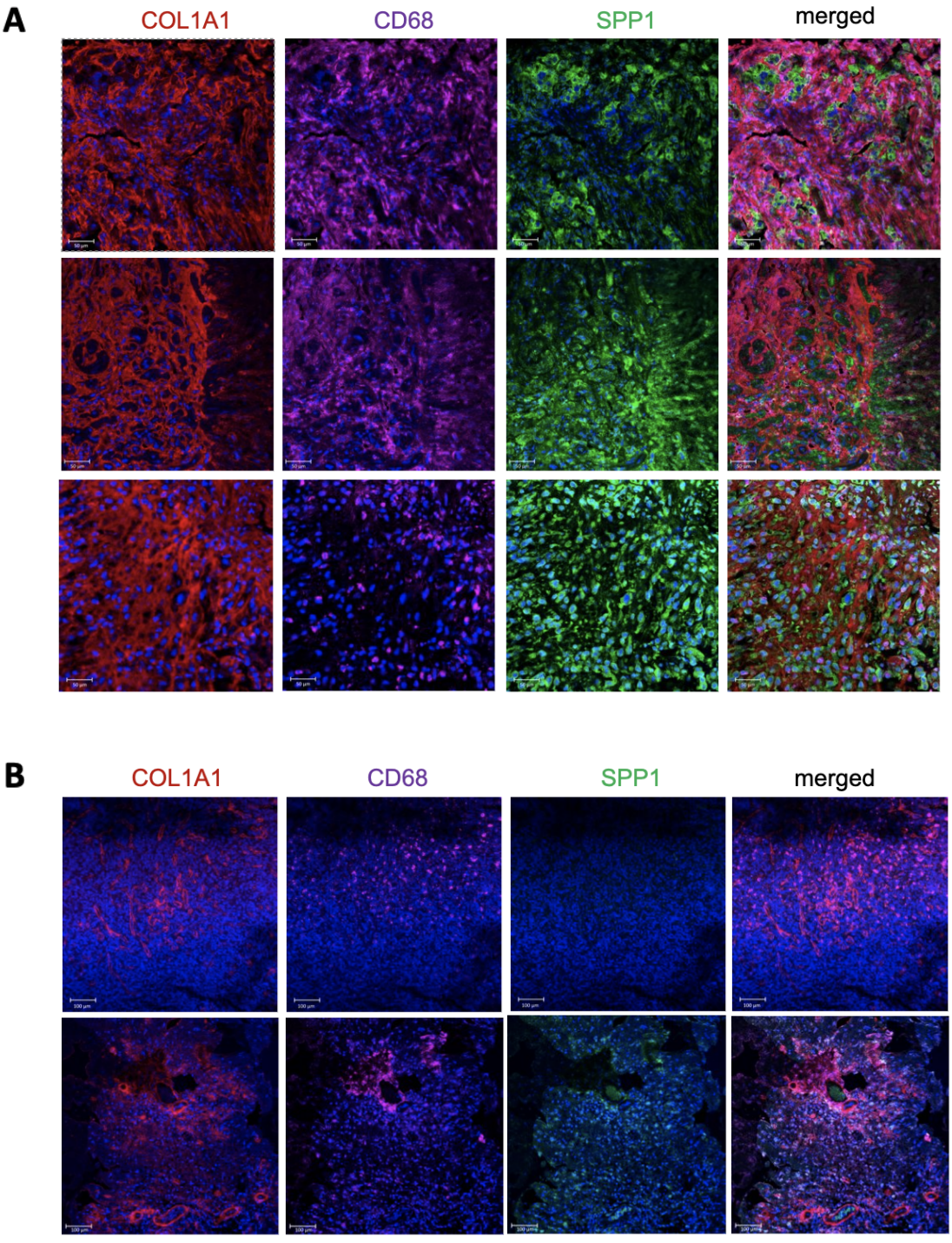

Figure 5. **A**. Representative of patients with higher expression of COL1A1, SPP1 and CD68. **B.** lower expression of COL1A1, SPP1 and CD68 are seen in better responsive patients.

Methods

Library preparation and single-cell sequencing

Single-cell sequencing of cryopreserved freshly dispersed tumor samples from 32 individuals was carried out using the 10x Chromium platform. For Batch 1, patient PBMC's exomes were collected via Illumina exome panel and sequenced at 20M read pairs per patient for sample deconvolution. For batches 2-6, Biolegend Total Seq-C hashtag antibodies were used to allow sample deconvolution after pooled processing, with 8 barcoded samples were sorted at equal proportions into a single collection tube. Samples in the remaining batches (21-28) were sequenced without pooling. 60,000 cells were loaded to a single Gel Bead-in-Emulsion (GEM) reaction onto the Chromium instrument. Sc-RNA-seq library preparation was performed according to manufacturer protocols and sequenced on Illumina Iseq100 for cell count validation and NovaSeq6000 at the recommended depth. Sequence data were processed using 10x Genomics Cell Ranger V5.0 and Ensemble 98.

Single-cell data processing and analysis

Single-cell sequencing data were analyzed using Seurat v4(Hao et al. 2021). CellRanger objects for each batch were imported to create a Seurat object for each of the 19 batches. For Batch 1, sample identities were deconvoluted and multiplets were identified using Demuxlet(Kang et al. 2018). Exome sequencing FASTQ reads were chunked to 40M reads, aligned to GRCh38 using BWA(Li and Durbin 2009), and processed with samtools fixmates and samtools(Li et al. 2009) sort. Individual chunks were merged and PCR and optical duplicates were marked with samtools. Genotypes were called with DeepVariant (https://github.com/google/deepvariant). The single-cell data were filtered to retain singlets with >500

unique RNA features detected, >1,000 RNA feature counts, and less than 10% of reads mapping to mitochondrial genes.

Gene expression data were normalized with SCT and samples were integrated using rPCA. The number of significant principal components (PCs) to be included in dimensionality reduction and unsupervised clustering was determined by calculating the difference between the proportion of variation associated with each PC and their subsequent PC and selecting the last point where the difference is more than 0.1%. Uniform Manifold Approximation and Projection (UMAP) was used for dimensionality reduction and 2D visualization of cell clusters.

Highly expressed marker features for each cluster were identified using the presto implementation of the Wilcoxon rank test (https://github.com/immunogenomics/presto). Clusters were annotated based on cell type marker expression. We tested for differences in cell type abundance between groups using the propeller function(Phipson et al. 2022) of the speckle R package (https://github.com/phipsonlab/speckle).

Ligand-receptor interaction analysis was carried out using CellChat (Jin et al. 2021) leveraging the CellChatDB human database which contains 1,939 validated molecular interactions, including 61.8% of paracrine/autocrine signaling interactions, 21.7% of extracellular matrix (ECM)-receptor interactions and 16.5% of cell-cell contact interactions. Expression data were preprocessed for the cell-cell communication analysis by identifying over-expressed ligands or receptors in one group and then identifying over-expressed ligand-receptor interactions. Then, gene expression data were projected onto the protein-protein interaction network using the function projectData(). Then, communication probabilities were computed using computeCommunProb(), and the results were filtered to retain instances with a minimum of ten cells

in each group. Cell-cell communication was inferred at a pathway level by summarizing the communication probabilities of all ligands-receptor interactions associated with each signaling pathway using computeCommunProbPathway(), and the aggregated communication network was calculated by counting the number of links and summarizing the communication probability using aggregateNet().

Immunofluorescence staining

Immunofluorescence staining was performed on tumor samples from glioblastoma (GBM) patients to investigate the expression of COL1A1, CD68, and SPP1. The antibodies were diluted in 1x plus amplification diluent (1:250) and incubated with the samples for 15 minutes at room temperature. After washing, the samples were incubated with a HRP polymer detection system, followed by incubation with secondary antibodies. Finally, the samples were washed again before imaging.

Chapter 4

CHALLENGES AND STRATEGIES TO OVERCOME THE RESISTANCE TO IMMUNOSUPPRESSIVE TUMORS

This study highlights the crucial role of cancer cell intrinsic features and their interaction with the immune system in cancer development, progression, and response to CAR T cell therapies. With the advent of multi-omics technologies, our understanding of cancer cell-immune cell crosstalk has expanded significantly in recent years [28,63].

The use of single cell RNA sequencing and cell-chat analysis on transcriptomics data from in vivo studies of JAK1 mutated melanoma tumors and glioblastoma (GBM) patient samples that exhibited resistance to CAR T cell therapies is a promising approach to gain insights into the complex interplay between cancer cells and the immune system.

Our investigation, here, has identified similarities between the composition of tumor stroma and extracellular matrix in the tumor microenvironments of both JAK1 mutated tumors and GBM patient samples resistant to CAR T cell therapies that infer possible underlying mechanisms of immune resistance in these tumor types.

We provided a high throughput analysis of the TME comparing the JAK1/KO YUMM tumor immune profile with its WT counterpart. The observation of reduced CD8+ T cell infiltration, increased follicular CD4 T cells, increased exhaustion properties of T cells, and increased T regulatory cells in JAK1/KO melanoma tumors is consistent with what was observed in GBM patients. These similarities suggest that there may be common underlying mechanisms deriving lack of response to CAR T cells in such tumors.

The increased exhaustion profile and reduced trafficking and persistence of CAR T cells in JAK1/KO YUMM tumor compared to WT counterpart underscores the importance of cancer cell-intrinsic mechanisms, specifically abrogated JAK1 cell signaling pathway, in regulating and suppressing CAR T

cell presence and functionality in the tumor microenvironment. One possible interpretation of this finding suggests a suppressive communication between cell components of the immune system and CAR T cells, as further inferred from cell-cell analysis. An alternative rationale is the absence of adequate access to nutrients and limited glycolytic capacity resulting from competition with tumor cells, which hampers CAR T cell function within the tumor TME [1,40,42].

Additionally, various aspects of the TME can induce a state of metabolic exhaustion in T cells which is characterized by impaired proliferation and function, increased expression of inhibitory receptors, and dysregulated glycolysis beyond what is necessary for effective T cell proliferation. Growing studies have revealed a significant upregulation of glycolytic genes and downregulation of T cell factor 7 (TCF7) gene signatures associated with T cell self-renewal in terminally exhausted T cells, compared to progenitor or effector T cell subsets [64–67]. The TME induces and accelerates exhaustion in CAR T cells by subjecting them to repetitive stimulation of their T cell receptors (TCR), resulting in bioenergetic stress on glycolytic and oxidative metabolism. This stress induces transcriptional and enzymatic alterations that define the dysfunctional exhausted state of CAR T cells, ultimately compromising their ability to mount an effective immune response against tumors [15,68].

To further understand the underlying mechanisms of these observations, further studies are needed. As a possible approach in future studies, by comparing the secretome of JAK1/KO melanoma tumors to their WT counterparts,we could identify secreted factors that may impair CAR T cell activity and function, such as cytokines and chemokines, and explore potential approaches to overcome these inhibitory signals. This information could also lead to the identification of novel targets for therapeutic intervention to

enhance CAR T cell therapy efficacy in JAK1/KO melanoma and other suppressive tumor microenvironments.

Unlike the WT YUMM tumor, The enrichment of myeloid suppressive cells, neutrophils, and fibroblasts in impaired JAK1 signaling tumors may indeed play a key role in shaping the tumor microenvironment in a way that promotes tumor growth and enhances resistance to CAR T cell therapies [2,36,39].

Myeloid suppressive cells are a heterogeneous population of immature myeloid cells that are generated in response to tumor-derived factors, such as cytokines, growth factors, and chemokines. Their abundance in the tumor microenvironment has been associated with poor prognosis and resistance to therapy. They are known to suppress the activity of T cells, NK cells, and other immune cells, thereby creating an immunosuppressive microenvironment that allows tumors to evade immune surveillance and continue to grow [16,39,69].

MDSCs can be divided into two main subtypes based on their morphology and surface marker expression: granulocytic MDSCs (G-MDSCs) and monocytic MDSCs (M-MDSCs). However, the distinction between these subtypes is not always clear-cut, and there is considerable overlap between them. Accumulative evidence over years has demonstrated that MDSCs produce a variety of immunosuppressive factors, such as arginase, reactive oxygen species ROS, and prostaglandin E2, that can inhibit the activity of T cells, NK cells, and other immune cells. They also promote the differentiation of Tregs and other immunosuppressive cells, which further contribute to the immunosuppressive microenvironment [70–72]. Our research, encompassing preclinical and clinical high throughput studies, as well as other emerging research findings, has unveiled the heterogeneous nature of MDSCs within the TME and their intricate

involvement in fostering resistance to immunotherapies. These observations emphasize the imperative of conducting additional investigations to comprehensively grasp the mechanisms that underlie their interactions with other cell types in the TME.

While it is known that MDSCs can interact with other immune and stromal cells in the TME through physical contact or secretion of suppressive cytokines, the precise mechanisms of these interactions are not yet fully understood. Compelling research studies underscore the critical significance of reciprocal interactions between suppressive macrophages and CAFs in both the progression of tumor cells and their resistance to immunotherapies. These interactions are facilitated through multiple receptor-ligand interactions across diverse tumor types, illuminating their crucial role in mediating these processes [44,48,73,74]. For example, in breast cancer, CAFs can express the receptor for hyaluronan-mediated motility (RHAMM), which can bind to hyaluronan produced by tumor cells, leading to the recruitment of MDSCs to the TME[75]. MDSCs in turn can secrete factors that can activate CAFs, promoting tumor growth and angiogenesis. In pancreatic cancer, CAFs can secrete the cytokine CXCL12, which can bind to the CXCR4 receptor on MDSCs, promoting their recruitment to the TME[76]. Similarly, MDSCs in turn can secrete factors that can promote the survival and proliferation of CAFs, leading to the formation of a fibrotic stroma that can shield the tumor from immune attack[77].
In melanoma, CAFs can express the receptor PDGFR-β, which can interact with its ligand PDGF-BB produced by tumor cells, leading to the recruitment of MDSCs and the suppression of T cell responses [44,78–81].

Predicted upregulated cross-talk between suppressive macrophages and CAFs involved multiple components in JAK1/KO melanoma tumors: SPP-1 (secreted phosphoprotein 1) and multiple integrin

subtypes, CSF1R (colony-stimulating factor 1 receptor) and CSF1 (colony-stimulating factor 1), CCR2 (C-C chemokine receptor type 2), and CCL2 (C-C motif chemokine ligand 2), collagen families and integrins[44,82–85]. These findings provide important insights into the mechanisms underlying resistance to CAR T cell therapies in JAK1/KO melanoma tumors.

Through pathway enrichment analysis on sc-RNA sequencing data, our findings have shed light on distinct molecular mechanisms that are activated or suppressed in the context of abrogated interferon signaling in YUMM JAK1/KO tumor cells compared to their WT counterparts. Notably, we observed significant upregulation of extracellular remodeling pathways, such as collagen and laminin, as well as receptor-ligand interactions, the interleukin 10 signaling pathway, and lipid metabolism in tumor-associated immune cells of JAK1/KO tumors. These differentially expressed genes within the TME of JAK1/KO-regulated tumors may contribute to a reduced sensitivity to CAR T cell therapies.

The ECM is an intricate blend of proteins that undergoes remodeling within the TME, exerting an influence on signal transmission and tumor progression. This remodeling process involves alterations in the composition of proteins, such as increased synthesis of collagen, as well as changes in the activity of enzymes like matrix metalloproteinases (MMPs). Altered expression of MMPs has been linked to tumor progression and active ECM remodeling across different types of cancer. The interactions between cells in the TME shape the ECM and contribute to the creation of an immunosuppressive environment, impeding the immune cell-mediated eradication of tumors. However, it is worth noting that ECM remodeling also presents potential targets for therapeutic interventions [80,82,86–8889].

In the JAK1/KO model, laminin and collagen are upregulated, indicating ECM remodeling that contributes to tumor progression and possible immune evasion by hindering effective trafficking of immune cells. Additionally, the interaction between SPP1 and CD44, observed in this model, suggests their involvement in promoting tumor cell survival and immune evasion. SPP1, a matricellular protein, is associated with tumor progression and interacts with CD44, involved in cell adhesion and migration. Understanding the interplay between ECM remodeling and these upregulated molecules provides insights into tumor progression and therapeutic resistance [90–93]. Targeting these interactions and associated ECM components may offer novel therapeutic strategies to disrupt tumor-stromal communication and enhance anti-tumor immune responses.

The observation of higher spliceosome, a large RNA-protein complex that is responsible for the splicing of pre-mRNA transcripts into mature mRNA molecules, and small nuclear ribonucleoproteins (snRNP) assembly in WT tumors compared to JAK1/KO tumors suggests that there are differences in the alternative RNA splicing patterns between these two types of tumors which might be due to more effective antigen presentation in the WT tumor and subsequent stronger immune response against WT tumors compared to JAK1/KO tumors.

However, it is important to note that alternative splicing is a complex process, and the functional implications of specific alternative splicing events can be difficult to predict. Therefore, further research will be necessary to fully understand the functional implications of the observed differences in alternative RNA splicing patterns between WT and JAK1/KO tumors.

The upregulation of lipid metabolism-associated pathways in the TME of JAK1/KO tumors may have significant implications for the immune response to CAR T cell therapy, as it represents another way that

tumors attempt to evade immunotherapies. This upregulation may lead to increased lipid accumulation and altered lipid profiles in the TME, which can impact the function of immune cells involved in antitumor responses, such as T cells, natural killer cells and dendritic cells. The altered lipid profile in the TME of JAK1/KO tumor can have a negative impact on the function of CAR T cells, potentially reducing their efficacy in eliminating cancer cells. Furthermore, this metabolic reprogramming may contribute to the immunosuppressive phenotype of certain immune cells, such as MDSCs, which can further impair the efficacy of CAR T cell therapy. CAFs and MDSCs may transfer lipids to the TME, leading to lipid accumulation in the tumor that further modulates the immune response. Growing evidence suggests that MDSCs, Tregs and tumor associated neutrophils (TANs) benefit from increased lipid availability and upregulated fatty acid oxidation (FAO) which support their immunosuppressive and pro-tumoral functions. Further studies to better understand the reprogramming of lipid metabolism in the TME of interferon abrogated tumor are critical for developing strategies to improve the efficacy of CAR T cell therapy and overcome tumor immune evasion mechanisms [94–98].

The presence of fibroblasts and suppressive myeloid cells with high expression of SPP1, C1QC, C1QA, and APOE in GBM samples suggests their role in creating an immunosuppressive environment, similar to what is observed in the JAK1/KO model. Additionally, the upregulation of ECM pathways, including laminin, collagen, and visfatin, further supports the immunosuppressive nature of the TME in GBM.

The similarities between the immune landscape in the JAK1/KO model and GBM patients highlight the need to investigate the underlying mechanisms responsible for the limited response to CAR T cell therapy. While dysregulation of the JAK1 signaling pathway may be one contributing factor, it is essential to

explore other pathways that may also play a role in modulating the TME and influencing the effectiveness of immunotherapies.

In contrast to earlier studies focusing on blocking the IFNγR1 pathway and its effect on CAR T cell functionality, our research goes beyond and delves into the intricate influence of the immunosuppressive TME on CAR T cell response, specifically in the context of IFN signaling deficiency. Interestingly, our study revealed that simply overexpressing ICAM-1 and improving the T cell synapse with tumor cells did not successfully address the problem of CAR T cell unresponsiveness in vivo. This suggests that augmenting ICAM-1 expression alone and enhancing the interaction between CAR T cells and tumor cells are insufficient to overcome the challenges imposed by the immunosuppressive TME. The suppressive nature of the TME, with its direct and indirect impact on the persistence and activation profile of CAR T cells, presents a significant obstacle to the therapeutic efficacy of CAR T cell therapy.

Our research sheds light on the immunoregulatory role of intracellular pathways within tumors. We discovered that IFN signaling deficiency not only disrupts the expression of interferon stimulatory genes involved in immune cell trafficking but also leads to the recruitment of immunosuppressive cells such as MDSCs, CAFs, and other suppressive immunoregulatory components. Building upon recent findings, we explored the introduction of unconjugated ISG-15 as a chemoattractant for active T cells [99–103]. Excitingly, we observed a therapeutic response in JAK1/KO tumors treated with a combination of IL13 CAR T cells and unconjugated ISG-15. This emphasizes the critical role of intratumoral active interferon signaling in triggering neighboring antitumor immune responses within solid tumors. Furthermore, our investigation unveiled the upregulation of IRF-9 and the downregulation of IFN2BP2 in the JAK1/KO model and GBM patients, demonstrating its possible correlation with downregulation of PDL-1 and regulation of

endogenous T cells in GBM patients. This discovery provides supporting evidence for the involvement of tumor-intrinsic IFN signaling-associated proteins in the immune regulation within the TME. Additionally, we explored an alternative approach by targeting the SPP-1/CD44 interaction within JAK1/KO tumors as a combination therapy with CAR T cells to enhance efficacy. The favorable outcome of this study supports the potential of targeted therapies aimed at the ECM to improve the therapeutic response of CAR T cells. This finding has significant translational implications for future studies, particularly in the case of GBM, where SPP-1 is markedly upregulated across various tissues, enabling a more robust response to CAR T cells in GBM patients.

Overall, our findings underscore the complex relationship between the TME and CAR T cell efficacy, necessitating further exploration of the underlying mechanisms driving immunosuppression. It is evident that additional factors within the TME contribute to the inadequate response of CAR T cells, emphasizing the multifaceted nature of immunosuppression in the tumor context.

Chapter 5

SUMMARY AND FUTURE DIRECTIONS

This study focuses on advancing CAR T cell therapies within the immunosuppressive environment of interferon signaling deficient cancer cells. The research highlights the challenges of CAR T cell therapies in solid tumors and the importance of understanding tumor-suppressive mechanisms and developing strategies to overcome resistance. The study uses JAK1 knockout murine tumor models expressing IL13Ra2 to investigate the impact of IFN signaling deficiency on the TME and CAR T cell therapy response. The findings demonstrate that IFN signaling deficient tumors modulate the TME, leading to resistance to CAR T cell therapy. The study also identifies the downregulation of ISG-15, a gene involved in IFN stimulation, in the deficient tumors. Combining unconjugated ISG-15 with CAR T cell therapy shows promising results in reducing tumor size. Additionally, analysis of patient samples treated with IL-13 CAR T cells reveals the correlation between IFN signaling pathway activity, fibroblast gene expression, and therapy response. Overall, this research provides insights into the immunosuppressive TME and potential strategies to enhance CAR T cell therapy efficacy in IFN signaling deficient tumors.

As part of our future research, we aim to delve deeper into the spatial positioning of cells within the GBM tumor microenvironment and uncover the local variations in cell compositions. By employing tissue multiplex staining and spatial transcriptomics, we will closely examine the spatial organization of diverse cell types, including fibroblasts, MDSCs, and other immune cells, in relation to specific regions within the tumor.

Through this comprehensive spatial analysis, we anticipate gaining valuable insights into the intricate interactions and communication occurring between these cells within the GBM tumor microenvironment. Understanding how different cell types are spatially arranged and how they influence each other's

behavior and functions will provide crucial information for developing more effective CAR T cell-targeted therapies.

In addition to studying spatial positioning, we will investigate the correlation between cell localization patterns and the metabolic profiles of GBM tissues obtained from patients. This analysis will shed light on the spatial heterogeneity of the tumor microenvironment, illustrating how variations in cell compositions and their metabolic activities contribute to the response or resistance to CAR T cell therapies.

By integrating this spatial information with detailed cell compositions and metabolic profiles, we aim to achieve a comprehensive understanding of the complex cellular interactions and local variations within the GBM tumor microenvironment. This knowledge will be instrumental in guiding the development of novel strategies to enhance the efficacy of CAR T cell therapies.

Furthermore, we will implement various strategies to enhance CAR T cell therapeutics. One approach involves engineering highly persistent and efficacious CAR T cells that are capable of sustained activity within the tumor microenvironment. Additionally, we will explore techniques to disrupt the extracellular matrix, which can impede the trafficking and persistence of CAR T cells within the GBM tumor microenvironment. Overcoming the tumor's intrinsic immunoregulatory characteristics, which often suppress immune responses, will be another important focus of our research.

By addressing these challenges and combining the insights gained from spatial analysis with targeted therapeutic approaches, we are optimistic about improving the overall efficacy of CAR T cell therapies in

the treatment of GBM. This research endeavor holds promise for advancing the field and ultimately providing more effective treatment options for patients with this devastating disease.

References:

1. Fonkoua, L. A. K., Sirpilla, O., Sakemura, R., Siegler, E. L. & Kenderian, S. S. CAR T cell therapy and the tumor microenvironment: Current challenges and opportunities. *Mol Ther - Oncolytics* **25**, 69–77 (2022).

2. Sterner, R. C. & Sterner, R. M. CAR-T cell therapy: current limitations and potential strategies. *Blood Cancer J* **11**, 69 (2021).

3. Yan, T., Zhu, L. & Chen, J. Current advances and challenges in CAR T-*Cell* therapy for solid tumors: tumor-associated antigens and the tumor microenvironment. *Exp Hematology Oncol* **12**, 14 (2023).

4. Boulch, M. *et al.* A cross-talk between CAR T cell subsets and the tumor microenvironment is essential for sustained cytotoxic activity. *Sci Immunol* **6**, eabd4344 (2021).

5. Stern, L. A. et al. Engineered IL13 variants direct specificity of IL13Rα2-targeted CAR T cell therapy. *Proc National Acad Sci* **119**, e2112006119 (2022).

6. Alizadeh, D. et al. IFNg is Critical for CAR T *Cell* Mediated Myeloid Activation and Induction of Endogenous *Immunity*. *Cancer Discov* candisc.1661.2020 (2021) doi:**10**.**11**58/2159-8290.cd-20-1661.

7. Martyniszyn, A., Krahl, A.-C., André, M. C., Hombach, A. A. & Abken, H. CD20-CD19 Bispecific CAR T Cells for the Treatment of B-Cell Malignancies. *Hum Gene Ther* **28**, 1147–1157 (2017).

8. Fousek, K. et al. CAR T-cells that target acute B-lineage leukemia irrespective of CD19 expression. *Leukemia* **35**, 75–89 (2021).

9. Domizi, P. et al. Prediction of Patients at Risk of CD19Neg Relapse Following CD19-Directed CAR T Cell Therapy in B Cell Precursor Acute Lymphoblastic Leukemia. *Blood* **134**, 749–749 (2019).

10. Brown, C. E. & Mackall, C. L. CAR T cell therapy: inroads to response and resistance. *Nat Rev Immunol* **19**, 73–74 (**20**19).

11. Rejeski, K., Jain, M. D. & Smith, E. L. Mechanisms of resistance and treatment of relapse after CAR T-cell therapy for large B-cell lymphoma and multiple myeloma. *Transplant Cell Ther* (2023) doi:10.1016/j.jtct.2023.04.007.

12. Lesch, S. et al. Determinants of response and resistance to CAR T cell therapy. *Semin Cancer Biol* **65**, 80–90 (2020).

13. Hagel, K. R. et al. Systematic Interrogation of Tumor Cell Resistance to Chimeric Antigen Receptor T-cell Therapy in Pancreatic Cancer. *Cancer Res* **83**, 613–625 (2023).

14. Kantari-Mimoun, C. et al. CAR T-cell entry into tumor islets is a two-step process dependent on IFNγ and ICAM-1. *Cancer Immunol Res* **9**, 142**5**–1438 (2021).

15. Gumber, D. & Wang, L. D. Improving CAR-T immunotherapy: Overcoming the challenges of T cell exhaustion. *Ebiomedicine* **77**, **10**3941 (2022).

16. Nalawade, S. A. et al. Overcoming the breast tumor microenvironment by targeting MDSCs through CAR-T cell therapy. *J Clin Oncol* **39**, 1032–1032 (2021).
17. Hamieh, M., Mansilla-Soto, J., Rivière, I. & Sadelain, M. Programming CAR T Cell Tumor Recognition: Tuned Antigen Sensing and Logic Gating. Cancer Discov 13, OF1–OF15 (2023).

18. Tian, Y. et al. CXCL9-modified CAR T cells improve immune cell infiltration and antitumor efficacy. *Cancer Immunol Immunother* **71**, 2663–2675 (2022).

19. Torrejon, D. Y. et al. Overcoming Genetically Based Resistance Mechanisms to PD-1 Blockade. Cancer Discov 10, 1140–1157 (2020).

20. Kalbasi, A. & Ribas, A. Tumour-intrinsic resistance to immune checkpoint blockade. Nat Rev Immunol 20, 25–39 (2020).

21. Kalbasi, A. et al. Uncoupling interferon signaling and antigen presentation to overcome immunotherapy resistance due to JAK1 loss in melanoma. *Sci Transl Med* **12**, eabb0152 (2020).

22. Bailey, S. R. et al. Blockade or deletion of IFNg reduces macrophage activation without compromising CAR-T function in hematologic malignancies. *Blood Cancer Discov* bloodcandisc.BCD-21-0**181**-E.2021 (2021) doi:10.1158/2643-3230.bcd-21-0181.

23. Salas-Benito, D., Berger, T. R. & Maus, M. V. Stalled CARs: Mechanisms of Resistance to CAR T Cell Therapies. *Annu Rev Cancer Biology* **7**, 23–42 (2023).

24. Weber, E. W., Maus, M. V. & Mackall, C. L. The Emerging Landscape of Immune Cell Therapies. Cell 181, 4**6**–62 (2020).

25. Cheng, J. et al. Understanding the Mechanisms of Resistance to CAR T-Cell Therapy in Malignancies. *Frontiers Oncol* **9**, **1237** (2019).
26. Song, M.-K., Park, B.-B. & Uhm, J.-E. Resistance Mechanisms to CAR T-Cell Therapy and Overcoming Strategy in B-Cell Hematologic Malignancies. *Int J Mol Sci* **20**, 5010 (20**19**).

27. Zeng, W. & Zhang, P. Resistance and recurrence of malignancies after CAR-T cell therapy. *Exp Cell Res* **410**, **11**2971 (2022).

28. Weverwijk, A. van & Visser, K. E. de. Mechanisms driving the immunoregulatory function of cancer cells. *Nat Rev Cancer* **23**, 193–**21**5 (2023).

29. Larson, R. C. et al. CAR T cell killing requires the IFNγR pathway in solid but not liquid tumours. *Nature* **604**, 563–570 (2022).

30. Paschen, A., Melero, I. & Ribas, A. Central Role of the Antigen-Presentation and Interferon-γ Pathways in Resistance to Immune Checkpoint Blockade. Annu Rev Cancer Biology 6, 1–18 (2021).

31. Zaretsky, J. M. et al. Mutations Associated with Acquired Resistance to PD-1 Blockade in Melanoma. *New Engl J Medicine* **375**, 819–**82**9 (2016).

32. Andrea, A. E. et al. Advances in CAR-T Cell Genetic Engineering Strategies to Overcome Hurdles

in Solid Tumors Treatment. *Front Immunol* **13**, 830292 (2022).

33. McGee, H. M. et al. Targeting the Tumor Microenvironment in Radiation Oncology: Proceedings from the 2018 ASTRO-AACR Research Workshop. *Clin Cancer Res* **25**, clincanres.3**78**1.2018 (20**19**).

34. Zhang, H. et al. Targeting PARP**11** to avert immunosuppression and improve CAR T therapy in solid tumors. *Nat Cancer* **3**, **80**8–820 (2022).

35. Rodriguez-Garcia, A. et al. CAR-T cell-mediated depletion of immunosuppressive tumor-associated macrophages promotes endogenous antitumor immunity and augments adoptive immunotherapy. *Nat Commun* **12**, 877 (2021).

36. Wieboldt, R. et al. Abstract 1259: Disturbing the Siglec-Sialoglycan axis to target myeloid- derived suppressor cells in the tumor microenvironment. Cancer Res 83, 1259–1259 (2023).

37. Nandre, R. et al. IDO-vaccine ablates immune-suppressive myeloid populations and enhances anti-tumor effects independent of tumor cell IDO statusIDO vaccine-mediated ablation of suppressive myeloid cells. Cancer Immunol Res 10, 571–580 (2022).

38. Miar, A. et al. Hypoxia Induces Transcriptional and Translational Downregulation of the Type I IFN Pathway in Multiple Cancer Cell Types. Cancer Res 80, 5245–5256 (2020).

39. Rivas, C. H., Cole, A., Rooney, C. M. & Parihar, R. Abstract 4734: Suppressive myeloid cells of the solid tumor microenvironment enhance regulatory T cell function and differentially affect CAR-T cell function. Cancer Res 78, 4734–4734 (2018).

40. Noman, M. Z. et al. Hypoxia: a key player in antitumor immune response. A Review in the Theme: Cellular Responses to Hypoxia. *Am J Physiol-cell Ph* **309**, C569–C579 (2015).

41. Aria, H., Ghaedrahmati, F. & Ganjalikhani-Hakemi, M. Cutting edge: Metabolic immune reprogramming, reactive oxygen species, and cancer. *J. Cell. Physiol.* **236**, 6168–6189 (2021).

42. Renauer, P. et al. Immunogenetic metabolomics revealed key enzymes that modulate CAR-T metabolism and function. *Biorxiv* 2023.03.**14**.532663 (2023) doi:10.1101/2023.03.14.532663.

43. Li, Y., Wan, Y. Y. & Zhu, B. Immune Metabolism in Health and Tumor. *Advances in Experimental Medicine and Biology* **1011**, 163–196 (2017).

44. Buechler, M. B., Fu, W. & Turley, S. J. Fibroblast-macrophage reciprocal interactions in health, fibrosis, and cancer. Immunity **54**, 903–915 (2021).

45. Pernot, S., Evrard, S. & Khatib, A.-M. The Give-and-Take Interaction Between the Tumor Microenvironment and Immune Cells Regulating Tumor Progression and Repression. Front Immunol **13**, 850856 (2022).

46. Guzman, G., Reed, M. R., Bielamowicz, K., Koss, B. & Rodriguez, A. CAR-T Therapies in Solid Tumors: Opportunities and Challenges. *Curr Oncol Rep* **25**, 479–489 (2023).

47. Majzner, R. G. et al. CD58 Aberrations Limit Durable Responses to CD19 CAR in Large B Cell Lymphoma Patients Treated with Axicabtagene Ciloleucel but Can be Overcome through Novel CAR Engineering. Blood **136**, 53–54 (2020).

48. Baldominos, P. et al. Quiescent cancer cells resist T cell attack by forming an immunosuppressive niche. Cell (2022) doi:10.1016/j.cell.2022.03.033.

49. Gorchs, L. & Kaipe, H. Interactions between Cancer-Associated Fibroblasts and T Cells in the Pancreatic Tumor Microenvironment and the Role of Chemokines. *Cancers* **13**, **29**95 (2021).

50. Sorkhabi, A. D. et al. The current landscape of CAR T-cell therapy for solid tumors: Mechanisms, research progress, challenges, and counterstrategies. Front Immunol **14**, 11**138**82 (2023).

51. Bompaire, F. et al. Advances in treatments of patients with classical and emergent neurological toxicities of anticancer agents. *Rev Neurol* **179**, 405–416 (2023).

52. Genoud, V. & Migliorini, D. Novel pathophysiological insights into CAR-T cell associated neurotoxicity. *Front Neurol* **14**, 1108297 (2023).

53. Schmidts, A., Wehrli, M. & Maus, M. V. Toward Better Understanding and Management of CAR-T

Cell–Associated Toxicity. *Annu Rev Med* **72**, 1–18 (2020).

54. Mahdi, J. et al. Tumor inflammation-associated neurotoxicity. *Nat Med* **29**, 803–810 (2023).

55. Shalabi, H., Nellan, A., Shah, N. N. & Gust, J. Immunotherapy Associated Neurotoxicity in Pediatric Oncology. Frontiers Oncol 12, 836452 (2022).

56. Ribas, A. Abstract IA10: The interferon receptor pathway's role in response and resistance to PD-1 blockade. Cancer Immunol Res 5, IA10–IA10 (2017).

57. Torrejon, D. Y. et al. Overcoming genetically based resistance mechanisms to PD-1 blockade. J Clin Oncol 37, 2584–2584 (2019).

58. Martínez-Sabadell, A. et al. Abstract 3970: Acquired cancer cell resistance to T cell bispecific antibodies and CAR T targeting HER2 through JAK2 down-modulation. Cancer Res 82, 3970–3970 (2022).

59. Arenas, E. J. et al. Acquired cancer cell resistance to T cell bispecific antibodies and CAR T targeting HER2 through JAK2 down-modulation. Nat Commun 12, 1237 (2021).

60. Jonsson, V. D. et al. CAR T cell therapy drives endogenous locoregional T cell dynamics in a responding patient with glioblastoma. Biorxiv 2021.09.22.460392 (2021) doi:10.1101/2021.09.22.460392.

61. E., B. C. et al. Regression of Glioblastoma after Chimeric Antigen Receptor T-Cell Therapy. New Engl J Med 375, 2561–2569 (2016).

62. Aykan, N. F. & Özatlı, T. Objective response rate assessment in oncology: Current situation and future expectations. *World J Clin Oncol* **11**, 53–73 (2020).

63. Yang, J., Chen, Y., Jing, Y., Green, M. R. & Han, L. Advancing CAR T cell therapy through the use of multidimensional omics data. *Nat Rev Clin Oncol* **20**, 211–228 (2023).

64. Jung, I.-Y. et al. BLIMP1 and NR4A3 transcription factors reciprocally regulate antitumor CAR T

cell stemness and exhaustion. Sci Transl Med 14, eabn7336 (2022).

65. Zebley, C. C. et al. CD19-CAR T Cells Develop Exhaustion Epigenetic Programs During a Clinical Response. *J Immunol* **208**, 122.04-122.04 (2022).

66. Chen, G. M. et al. Integrative Bulk and Single-Cell Profiling of Premanufacture T-cell Populations Reveals Factors Mediating Long-Term Persistence of CAR T-cell Therapy. Cancer Discov 11, 2186–2199 (2021).

67. Zebley, C. C. et al. CD19-CAR T Cells Develop Exhaustion Epigenetic Programs during a Clinical Response. Blood 138, 2782–2782 (2021).
68. Alvanou, M. et al. Empowering the Potential of CAR-T Cell Immunotherapies by Epigenetic Reprogramming. Cancers **15**, 1935 (2023).

69. Daubon, T., Hemadou, A., Garmendia, I. R. & Saleh, M. Glioblastoma Immune Landscape and the Potential of New Immunotherapies. Front Immunol 11, 585616 (2020).

70. Sharma, V., Aggarwal, A., Jacob, J. & Sahni, D. Myeloid-derived suppressor cells: Bridging the gap between inflammation and pancreatic adenocarcinoma. *Scand J Immunol* **93**, e13021 (2021).

71. Groth, C. et al. Immunosuppression mediated by myeloid-derived suppressor cells (MDSCs) during tumour progression. *Brit J Cancer* **120**, 16–25 (2019).

72. Ponomarev, A. Myeloid-Derived Suppressor Cells in Some Oncohematological Diseases. *Clin Oncohematology* **10**, 29–38 (2017).

73. Jojic, V. et al. Identification of transcriptional regulators in the mouse immune system. *Nat Immunol* **14**, 633–643 (2013).

74. Jain, S. et al. Single-cell RNA sequencing and spatial transcriptomics reveal cancer-associated fibroblasts in glioblastoma with protumoral effects. *J Clin Investigation* **133**, e147087 (2023).

75. Tarullo, S. E. et al. Receptor for Hyaluronan-Mediated Motility (RHAMM) defines an invasive niche associated with tumor progression and predicts poor outcomes in breast cancer patients. Biorxiv

2022.06.13.495375 (2022) doi:10.1101/2022.06.13.495375.

76. Malik, S., Westcott, J. M., Brekken, R. A. & Burrows, F. J. CXCL12 in Pancreatic Cancer: Its Function and Potential as a Therapeutic Drug Target. Cancers 14, 86 (2021).

77. Smit, M. J. et al. The CXCL12/CXCR4/ACKR3 Axis in the Tumor Microenvironment: Signaling, Crosstalk, and Therapeutic Targeting. *Annu Rev Pharmacol* **61**, 1–23 (2020).

78. Gunaydin, G. CAFs Interacting With TAMs in Tumor Microenvironment to Enhance Tumorigenesis and Immune Evasion. Frontiers Oncol 11, 668349 (2021).

79. Sipos, F. & Műzes, G. Cancer Stem Cell Relationship with Pro-Tumoral Inflammatory Microenvironment. *Biomed* **11**, 189 (2023).

80. Alkasalias, T., Moyano-Galceran, L., Arsenian-Henriksson, M. & Lehti, K. Fibroblasts in the Tumor Microenvironment: Shield or Spear? Int J Mol Sci 19, 1532 (2018).

81. Turley, S. J., Cremasco, V. & Astarita, J. L. Immunological hallmarks of stromal cells in the tumour microenvironment. Nat Rev Immunol 15, 669–682 (2015).

82. Wang, A. R. et al. Abstract B038: Remodeling the extracellular matrix environment and establishing distinct immune cell profiles enables the formation of brain metastasis in non-small cell lung cancer adenocarcinoma. Cancer Res 83, B038–B038 (2023).

83. Sathe, A. et al. Colorectal cancer metastases in the liver establish immunosuppressive spatial networking between tumor associated SPP1+ macrophages and fibroblasts. Clin Cancer Res 29, 244–260 (2022).

84. Hoeft, K. et al. Platelet-instructed SPP1+ macrophages drive myofibroblast activation in fibrosis in a CXCL4-dependent manner. *Cell Reports* **42**, 112131 (2023).

85. Qi, J. et al. Single-cell and spatial analysis reveal interaction of FAP+ fibroblasts and SPP1+ macrophages in colorectal cancer. Nat Commun 13, 1742 (2022).

86. Alshehri, S. et al. Extracellular Matrix Modulates Outgrowth Dynamics in Ovarian Cancer. *Adv Biology* **6**, 2200197 (2022).

87. Zhang, J. et al. Identifying cancer-associated fibroblasts as emerging targets for hepatocellular carcinoma. *Cell Biosci* **10**, 127 (2020).

88. Zhu, S., Wang, Y., Tang, J. & Cao, M. Radiotherapy induced immunogenic cell death by remodeling tumor immune microenvironment. Front Immunol 13, 1074477 (2022).

89. Grout, J. A. et al. Supplementary Table from Spatial Positioning and Matrix Programs of Cancer-Associated Fibroblasts Promote T-cell Exclusion in Human Lung Tumors. (2023) doi:10.1158/2159-8290.22541751.

90. Shurin, M. R. Osteopontin controls immunosuppression in the tumor microenvironment. J Clin Investigation **128**, 5209–5212 (2018).

91. Wei, J. et al. Osteopontin mediates glioblastoma-associated macrophage infiltration and is a therapeutic target. J Clin Invest **129**, 137–149 (2018).

92. Klement, J. D. et al. An osteopontin/CD44 immune checkpoint controls CD8+ T cell activation and tumor immune evasion. J Clin Invest 128, 5549–5560 (2018).
93. Klement, J. D. et al. Osteopontin Blockade Immunotherapy Increases Cytotoxic T Lymphocyte Lytic Activity and Suppresses Colon Tumor Progression. Cancers 13, 1006 (2021).

94. Li, H.-J. et al. Identification of metabolism-associated genes and pathways involved in different stages of clear cell renal cell carcinoma. *Oncol Lett* **15**, 2316–2322 (2018).

95. Bian, X. et al. Lipid metabolism and cancer. *J Exp Medicine* **218**, e20201606 (2020).

96. Hoy, A. J., Nagarajan, S. R. & Butler, L. M. Tumour fatty acid metabolism in the context of therapy resistance and obesity. Nat Rev Cancer 21, 753–766 (2021).

97. Xu, S. et al. Uptake of oxidized lipids by the scavenger receptor CD36 promotes lipid peroxidation and dysfunction in CD8+ T cells in tumors. Immunity 54, 1561-1577.e7 (2021).

98. Tan, Y. et al. Metabolic reprogramming from glycolysis to fatty acid uptake and beta-oxidation in platinum-resistant cancer cells. Nat Commun 13, 4554 (2022).

99. Yeh, Y.-H., Yang, Y.-C., Hsieh, M.-Y., Yeh, Y.-C. & Li, T.-K. A Negative Feedback of the HIF-1α Pathway via Interferon-Stimulated Gene 15 and ISGylation. Clin Cancer Res 19, 5927–5939 (2013).

100. Iglesias-Guimarais, V. et al. IFN-Stimulated Gene 15 Is an Alarmin that Boosts the CTL Response via an Innate, NK Cell–Dependent Route. J Immunol **204**, ji1901410 (2020).

101. Fan, J.-B. et al. Type I Interferon Regulates a Coordinated Gene Network to Enhance Cytotoxic T Cell–Mediated Tumor Killing. Cancer Discov 10, 382–393 (2020).

102. Kang, J. A., Kim, Y. J. & Jeon, Y. J. The diverse repertoire of ISG15: more intricate than initially thought. *Exp Mol Medicine* **54**, 1779–1792 (2022).

103. Villarreal, D. O. et al. Ubiquitin-like Molecule ISG15 Acts as an Immune Adjuvant to Enhance Antigen-specific CD8 T-cell Tumor Immunity. *Mol Ther* **23**, 1653–1662 (2015).